Deliverable 15.9 Integration of the findings on the impact of irradiation, dry density and particle size on the microbial community

Work Package 15 ConCorD

This project has received funding from the European Union's Horizon 2020 research and innovation programme 2014-2018 under grant agreement N°847593.

Document information

Project Acronym	**EURAD**
Project Title	**European Joint Programme on Radioactive Waste Management**
Project Type	**European Joint Programme (EJP)**
EC grant agreement No.	**847593**
Project starting / end date	**1st June 2019 – 30 May 2024**
Work Package No.	**15**
Work Package Title	**CONtainer CORrosion under Disposal conditions**
Work Package Acronym	**ConCorD**
Deliverable No.	**15.9**
Deliverable Title	**Integration of the findings on the impact of irradiation, dry density and particle size on the microbial community**
Lead Beneficiary	**TUL & HZDR**
Contractual Delivery Date	**29/02/2024**
Actual Delivery Date	**04/04/2024**
Type	**Document**
Dissemination level	**Public**
Authors	Mar Morales Hidalgo, Cristina Povedano Priego, Marcos F. Martinez Moreno, Fadwa Jroundi, Mohamed L. Merroun (UGR), Ursula Alonso, Ana María Fernández, Miguel García-Gutiérrez, Manuel Mingarro, Tiziana Missana Jesus Morejón, Paula Nieto, Pedro P. Valdivieso (CIEMAT) , Deepa Shree Bartak, Jakub Říha, Kateřina Černá (TUL), Šárka Šachlová, Vlastislav Kašpar, David Dobrev, Petr Večerník (UJV), Natalia Jakus, Eliot Jermann, Pierre Bena, Christina Zarkali, Rizlan Bernier-Latmani (EPFL), Ting-Shyang Wei, Vladyslav Sushko, Andrea Cherkouk (HZDR), Carla Smolders, Bruno Kursten, Kristel Mijnendonckx (SCK-CEN)

To be cited as:

Mar Morales Hidalgo, Cristina Povedano Priego, Marcos F. Martinez Moreno, Fadwa Jroundi, Mohamed L. Merroun, Ursula Alonso, Ana María Fernández, Miguel García-Gutiérrez, Manuel Mingarro, Tiziana Missana Jesus Morejón, Paula Nieto, Pedro P. Valdivieso, Deepa Shree Bartak, Jakub Říha, Kateřina Černá, Šárka Šachlová, Vlastislav Kašpar, David Dobrev, Petr Večerník, Natalia Jakus, Eliot Jermann, Pierre Bena, Christina Zarkali, Rizlan Bernier-Latmani, Ting-Shyang Wei, Vladyslav Sushko, Andrea Cherkouk, Carla Smolders, Bruno Kursten, Kristel Mijnendonckx (2024): Integration of the findings on the impact of irradiation, dry density and particle size on the microbial

community. Final version as of 04/04/2024 of deliverable D15.9 of the HORIZON 2020 project EURAD. EC Grant agreement no: 847593.

Disclaimer

Acknowledgement

This document is a deliverable of the European Joint Programme on Radioactive Waste Management (EURAD). EURAD has received funding from the European Union's Horizon 2020 research and innovation programme under grant agreement No 847593.

Status of deliverable		
	By	Date
Delivered (Lead Beneficiary)	TUL & HZDR	15.02.2024
Verified (WP Leader)	N. Diomidis	04.04.2024
Reviewed (Reviewers)	F. King, B. Kalinowski, C. Lilja, V. Maillot	01.03.2024
Approved (PMO)	B. Grambow	
Submitted to EC (Coordinator)	Andra (Coordinator)	05/04/2024

Executive Summary

The work performed in WP ConCorD's Subtask 4.1 focused on the effect of irradiation and other repository-relevant stressors on indigenous microorganisms in bentonite. The experiment of UGR + CIEMAT aimed to explore the impact of gamma radiation on the survival of microbial communities within compacted bentonites. To achieve this objective, FEBEX bentonite was compacted at a dry density of 1.6 g/cm^3 and fully saturated with artificial bentonite pore water. One group of samples underwent gamma irradiation at a dose rate 66 Gy/h, accumulating either a total dose of 14 kGy or 28 kGy. Additionally, certain samples were enriched with a sulphate-reducing bacteria (SRB) consortium to stimulate bacterial activity. Following 6-months and 1-year anaerobic incubation periods, DNA extraction, amplification and sequencing of the 16S rRNA gene were conducted along with quantitative PCR (qPCR) to analyse the microbial diversity across various treatments. The Most Probable Number of SRB was determined using anoxic Postgate's Medium. Furthermore, heterotrophic aerobic colony-forming units were computed to evaluate bacterial viability. The effect of gamma radiation on bacterial communities in bentonite depended on the cumulative radiation dose (14 or 28 kGy). The diversity data revealed that an incubation period before and after the radiation dose allowed the microbial communities to adapt and recover since the results were quite similar to those control treatments that had not been irradiated. The corrosion analyses of the copper coupons over the 6-month study period aligned with the microbial diversity results. The coupons from control treatments, where greater diversity and bacterial viability were observed, exhibited increased corrosion in the form of copper oxides and possible copper sulphides. Moreover, the addition of the SRB consortium may have played a role in the corrosion of the coupons, as a sulphide signal, potentially associated with copper sulphide precipitates, was detected only in the treatments enriched in SRB.

The experiment performed by TUL + UJV in Subtask 4.1 focused on the combined effect of irradiation (dose rate of 0.4 Gy/h) and heat (90 °C and 150 °C), where the values of both parameters were set as expected during the early phase of repository evolution. Long-term experiments (up to 18 months) with varying bentonite state (compacted bentonites BCV and MX-80 -1600 kg/m^3, powder, suspension) and saturation level were conducted. A combination of molecular-genetic approaches (sequencing, quantitative PCR), cultivation techniques, and microscopic analyses was used to estimate microbial survivability in the studied samples. The experiment demonstrated that the high temperature represents a crucial factor and long exposure to elevated temperatures significantly reduced the viability of bentonite microorganisms including spore-formers, with consistent effects observed in both BCV and MX-80 bentonite. The effect of irradiation and additional factors such as bentonite state and water availability proved to be insignificant (although their isolated effect could not be determined due to the major effect of temperature). The study also emphasized the critical role of exposure duration in understanding microbial responses to heat treatment. The results implied, that if the bentonite in the DGR is exposed to temperatures of 90°C or higher for the long-term, it could result in a reduction of microbial viability so severe that the creation of an abiotic zone around the canister during the early repository stages might be expected. However, the formation and spatial distribution of this zone will depend upon overall temperature conditions within the deep geological repository. Potential for microbially induced corrosion during the initial hot phase is thus very limited. In future long-term experiments microbial survivability at additional nearly limiting temperature ranges should be studied and combined with mathematical modelling of the temperature evolution in the DGR over its lifetime. This will refine predictions of microbial effects in the repository over time.

The work performed in Subtask 4.2 focused on the effect of dry density on microbial activity and microbially influenced corrosion. For this purpose, EPFL adaptated a diffusion reactor to microbial applications. The reactor design was optimized regarding its tubing (tubing failure and connection between plastic and stainless-steel tubing) and filter. The reactor setup is now structured in such a way that the microorganisms can only grow where the electron donor and acceptor gradients meet, that is, within the bentonite. Within the first experimental phase, compacted bentonite was saturated with APW (artificial porewater) and gypsum was dissolved by pumping a sulphate- and bromide-free anoxic APW past the bentonite on both sides of the reactor and measuring the sulphate concentration in the effluent.

It took approximately 95 days for sulphate to no longer be released from bentonite. Therefore, a batch treatment for gypsum dissolution was tested but it did not appear to be a better solution and the in-reactor dissolution will be used in future experiments despite its long duration. The next experimental phase entailed H_2 and sulphate amendment to the reactor and was tested for 12 reactors and a duration of 3 weeks. The first results showed that substantial microbial growth takes place within MX-80 bentonite during dissolution of gypsum and without any electron donor amendment in comparison to the reference bentonite. This finding suggests the importance of endogenous electron donors, such as organic carbon and the likelihood of microbial growth during the saturation phase, prior to the onset of anoxic steel corrosion and the associated H_2 production at a low dry density of 1.2 g/cm^3.

HZDR was involved in the modifications of the reactor design and built the same reactors and set up to investigate the Calcigel bentonite. During this project phase only the development and establishment of the diffusion reactor setup was possible including a first experimental phase. In addition, batch microcosms with Calcigel bentonite incubated under different conditions and different incubation times were performed. The results showed that the sulphate concentration decreased the most in the microcosms containing hydrogen in the atmosphere, Calcigel bentonite, and metal coupons. The hydrogen content in the atmosphere of these microcosms was also lower than that in the ones with sterilized bentonite. Therefore, the hydrogen and sulphate were microbially consumed in these microcosms. In the same microcosms, an enrichment of sulphate-reducing bacteria from the genus *Desulfotomaculum* was observed, indicating that Calcigel bentonite harbours sulphate-reducing bacteria that are active under the applied conditions. Regarding microbially influenced corrosion, a more pronounced morphological alteration was observed at lower incubation times because a layer of Ca-containing minerals was formed later that seemed to protect the surface of the coupons. In addition, sulfide minerals were found on the surface, which supports the activity of sulphate-reducing bacteria.

The aim of the experiments of SCK CEN was to investigate which bentonite dry density inhibits H_2 consumption originating from the anoxic corrosion of carbon steel by the indigenous community of the bentonite and if microbial activity would affect the corrosion of steel in compacted bentonite. Oedometers were used to tackle these questions. At this moment, final results are still pending but it seems that the setup is suitable. Hydrogen accumulation in the percolates was observed in abiotic conditions, while the first two data points were lower in the biotic conditions. Unfortunately, it seems that one abiotic control (with 1.5 bar H2) was contaminated. Currently it is not yet clear how long this microbial activity could persist during the percolation process. This will be examined when the cells are dismantled.

To sum up, microbial activity can be suppressed by compacted bentonite, but the threshold dry density depends on the bentonite (their physical-chemical properties and the indigenous microbial communities). Within ConCorD EPFL, HZDR further developed a diffusion reactor setup to study the effect of dry density on microbial activity and microbially influenced corrosion. Experiments with the two different bentonites MX-80 and Calcigel were started and are ongoing. Due to several reasons, we have not yet a full data set for these two bentonites and therefore no final conclusions can be drawn at present. SCK-CEN also started experiments with MX-80 by using oedometers but these experiments are also still ongoing.

One of the objectives of this project was to enable cross comparison between the obtained results. This is important as it is known that DNA extraction plays a crucial role in determining the variability of results obtained through 16S rRNA amplicon sequencing. Particularly, bentonite and other clay samples can impede the efficiency of standard cultivation-independent techniques. These samples often contain low biomass, further complicating the extraction process. To address these concerns, we conducted an inter-laboratory comparison study to thoroughly assess the efficacy of two published DNA extraction methods specifically designed for bentonite samples. Notably, our findings indicate that the selection of one or the other method is not critical, but rather dependent upon the specific analysis requirements. However, it is crucial to maintain consistency in the chosen method, as comparing results becomes challenging, particularly in the presence of bentonite. Additionally, we discovered that slight modifications to one of the extraction methods can enhance its efficiency. In summary, our study emphasizes the importance of standardized DNA extraction methods and underscores the importance

of validating these methods using appropriate controls when studying microbial communities with 16S rRNA amplicon sequencing, particularly in environments characterized by low biomass and clay-rich compositions.

Table of Contents

Executive Summary 4

1. Introduction 8

2. Impact of irradiation on microbial activity 10

2.1 UGR + CIEMAT 10

2.1.1. Materials and Methods 10

2.1.2. Results 13

2.1.3 Discussion 17

2.2 TUL + UJV 18

2.2.1 Materials and Methods 18

2.2.2 Results 21

2.2.3 Discussion 27

3 Impact of bentonite dry density on microbial activity 31

3.1 EPFL 31

3.1.1 Design and optimization of reactors 31

3.1.2 Experimental phase 1: Saturation and gypsum dissolution 33

3.1.3 Experimental phase 2: H_2 and sulphate amendment to the reactor 35

3.1.4. Experimental phase 3: microbial biomass analysis 36

3.2 HZDR 38

3.2.1 Set up of diffusion reactors to study the impact of Calcigel bentonite dry density on microbial activity 38

3.2.2 Batch experiments with Calcigel bentonite to study metal corrosion and activity of sulfate-reducing bacteria 41

3.3 SCK CEN 48

3.3.1 DNA extraction in bentonite: a comprehensive inter-laboratory investigation 48

3.3.2 Microbial consumption of hydrogen originating from the corrosion of carbon steel in compacted bentonite 53

4 Conclusions 59

4.1 Impact of irradiation on microbial activity 59

4.2 Impact of bentonite dry density on microbial activity 60

4.3 Keynotes 61

5 Outlook 62

References 63

1. Introduction

Within this task, remaining uncertainties associated with the impact of microbial activity in buffer materials on corrosion are investigated. Microbially influenced corrosion (MIC) can accelerate anoxic corrosion due to microbial metabolism. MIC can also play a role in the high-level waste (HLW) and spent fuel (SF) repository environment, even if biofilm formation on the surface of canisters is not expected (owing to the high initial thermal load and radiation field), nor yet observed in relevant experiments. However, it is well established that H_2 will be produced via anoxic corrosion of some container materials (e.g. steel). The H_2 produced could drive microbial processes such as sulphate reduction and methanogenesis. The associated sulphide production in the former could affect the corrosion rate, particularly for copper but potentially also for steel containers.

It has already been demonstrated that sulphate-reducing bacteria (SRB) are present in the host rock at most repository locations considered (Bagnoud et al., 2016; Bell et al., 2020), as well as in potential backfill materials (e.g., in bentonite as shown in Matschiavelli et al., 2019; Martinez-Moreno et al., 2023; and Povedano-Priego et al., 2023). Thus, the question is not whether sulphate reduction can occur in the repository, but whether it can be inhibited or controlled in a way that minimizes the impact on the corrosion rate of the container materials in the repository. The bentonite buffer is expected to play a key role in precluding microbial activity to limit any negative microbial impact on corrosion rates. Thus, it is critical to optimally select and design the bentonite buffer to inhibit or control microbial activity.

In the multi-barrier concept, it is important to understand the effect of radiation on the mineralogy and performance of the barrier material (i.e., bentonite), as well as the effect of radiation on the microbial communities within the barrier material. Within the EU-project Microbiology in Nuclear waste Disposal (MIND), deliverable D2.15 reported the results of a study of the effect of gamma radiation and pressure on the indigenous microbial community in bentonite (type BaM, Keramost, Czech Republic) that was enriched with a granitic porewater (VITA from the Josef Underground Research Center, Czech Republic). The latter was a natural source of sulphate-reducing bacteria. It was found that the microorganisms that adapted to the harsh conditions and survived were subjected to further selection by the effects of gamma radiation. In particular, the application of 19,656 Gy absorbed dose at a constant dose rate 13 Gy h^{-1} did not eliminate bacteria in a bentonite suspension. A decrease in total microbial biomass, but not species richness, was observed, as well as small changes in microbial community structure (Černá et al., 2019). The results suggest that some of the bacteria that are naturally present in bentonite are radiation resistant. Therefore, Subtask 4.1 of ConCorD investigates the evolution of microbial communities in bentonite under long-term irradiation. In addition, the effect of the bacterial communities in bentonite on the corrosion of metals, such as copper, were also studied.

Except for radiation, the effect of high temperatures during the initial hot phase of DGR on microbial survivability and future recovery needs to be evaluated. Early phase of the repository characterized by elevated temperatures, peak irradiation levels and a low water saturation state is considered to create physicochemical conditions that are considered unfavourable for microbial activity and evolution of the abiotic zone around the canister was predicted (Stroes-Gascoyne and West, 1997). However, long term experiments under realistic repository conditions are missing and past long-term experiments indicated that bentonite microorganisms can survive long-term extreme heat treatment (Kašpar et al., 2021), but these data needed further confirmation. In Subtask 4.1 of ConCorD, the long-term experiments were conducted under simulated repository conditions combining the effect of irradiation, temperature, water saturation and the level of bentonite compaction.

In the past, a few studies have attempted to determine the dry density threshold that would reliably inhibit microbial activity (e.g., Bengtsson et al., 2016 and 2017, 2017a; Stroes-Gascoyne, 2010). The data compilation shown in Taborowski et al., 2019 reflects the extreme scatter in the data, which is likely due to the variety of experiment approaches utilized. In the study of Povedano-Priego et al. (2021), the bacterial community did not differ for two compaction dry densities (1.5 and 1.7 g cm^{-3}). However, microbial growth within compacted bentonite is difficult to investigate due to the potential for experimental artifacts. For growth to be studied in compacted bentonite, there needs to be a time-

dependent quantification of the amount of biomass contained within the bentonite. Additionally, the electron donor and acceptor combination must be relevant to repository environments and only indigenous microorganisms should be considered. In addition, a high enough resolution of dry density must be achieved to obtain a clear estimation of the targeted dry density that could ensure no (or very limited) microbial growth under repository relevant conditions. Finally, to obtain statistically tractable results, the experiment should be designed to allow for several replicates. Many experiments include tedious set-ups for which replication is extremely challenging and, as a result, data points often do not include error bars that would allow the extraction of more conclusive findings. To date, no such experiments have been conducted as either lactate or acetate were used as electron donors, microorganisms were amended to the bentonite, artifacts related to growth on the filters holding the bentonite at the appropriate density occurred, or there were no experimental replicates.

Microbial activity need not rely solely on the presence of organic carbon, since autotrophic growth, with H_2 as the electron donor, sulphate as the electron acceptor, and CO_2 as the carbon source, is also conceivable. In fact, such a potential exists in specific host rocks, such as Opalinus Clay, and in the backfill material bentonite (Matschiavelli et al., 2019). An *in-situ* experiment that was conducted in the Mont Terri underground laboratory in Switzerland showed that SRB growth was stimulated by the addition of H_2. These organisms served as primary producers and were the origin of a microbial food web that developed in the borehole (Bagnoud et al., 2016). However, the absence of bentonite was a major limitation in this experiment, and it would be more relevant to measure H_2 consumption in bentonite as a function of dry density and swelling pressure. Therefore, Subtask 4.2 examines the fundamental variables influencing the bentonite dry density threshold at which microbial activity is inhibited for two different bentonite types (MX-80 and Calcigel).

2. Impact of irradiation on microbial activity

The work in the subtask 4.1 aimed to evaluate the effect of irradiation under anaerobic conditions on microbial activity in bentonite with special emphasis on microbial survivability and corrosion processes (including microbially induced corrosion (MIC)) of metal canister. The Spanish team investigated the effect of gamma radiation on the survival of microbial populations, mainly sulphate reducing bacteria (SRB), in compacted bentonites at ambient temperature. High doses of irradiation (up to 28 kGy) were applied. On the other hand, the Czech team (TUL + UJV) focused on the simulation of the conditions expected during the early stage of the repository, where highest dose rates of irradiation as well as high temperatures are expected. The major question here was, whether the microorganisms naturally present in bentonite can survive long-term exposures to such conditions and are able to resume their metabolic activity after the conditions become more favourable.

2.1 UGR + CIEMAT

2.1.1. Materials and Methods

Sample preparation

FEBEX bentonite, a Ca-Mg bentonite from Cortijo de Archidona (Spain) (Huertas et al, 2000), was compacted in cylindrical blocks of 38 mm in diameter and 25 mm height (Figure 1) at a dry density of 1.6 g·cm^{-3}.

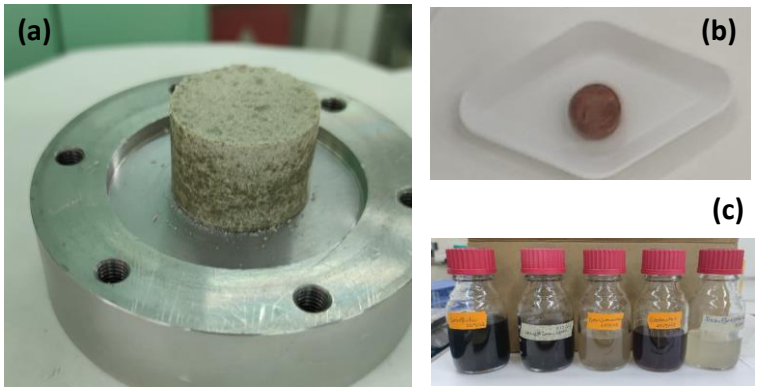

Figure 1: (a) Example of compacted bentonite sample including a (b) Cu-coupon in the centre and (c) inoculated with a custom-made bacteria consortium for gamma-irradiation experiments

Small pure-copper coupons (Figure 1b) from *GoodFellow* (UK) were used as representative of metal canisters. Coupons have diameter of 10 mm, a thickness of 4 mm and an average weight of 2.8 g and were included in the core of each bentonite block to analyse their corrosion. Acetate (1.5 mM) was added as energy and carbon source for the enhancement of microbial growth.

A custom consortium of sulphate-reducing bacteria (*Desulfovibrio*, *Desulfotomaculum*, *Desulfuromonas*, *Desulfosporosinus*) and *Geobacter* (Figure 1c) was used to inoculate the bentonite samples prior to compaction. The genera included represent the SRB group previously identified in FEBEX bentonite diversity studies (Martinez-Moreno, et al., 2023; Povedano-Priego et al., 2019, 2021, 2022). In addition, controls without spiked bacteria were also prepared for comparison.

All the samples were 100% saturated with FEBEX bentonite pore water obtained for saturated conditions at a dry density of 1.6 g.cm$^{-3.}$ FEBEX pore water recipe was prepared as is indicated in Fernandez & Rivas, 2005.

Irradiation experiments

For gamma-irradiation, bentonite samples were introduced in specific metal containers at the CIEMAT Nayade ^{60}Co gamma irradiation pool facility. Samples were initially irradiated for 9 days at a dose rate of 66 Gy/h, accumulating a total dose of 14 kGy (designated R). Some samples were irradiated after 6

months of incubation for the second time, at the same dose rate of 66 Gy/h, to an accumulated a total dose of 28 kGy (designated 2R).

Summary of experimental conditions

The whole study took 1 year with the sampling times at 0, 6 months and 1 year of incubation. All the samples were incubated at 28 ºC in anaerobic conditions. The experimental design and data are summarized in (Table **1**).

For the study of 6-months and 1-year incubation (12 months), natural FEBEX bentonite was compacted and then, irradiated. So, the treatments under study were as follows: (1) Blocks irradiated at a dose of 14 kGy at the beginning of the experiment and then incubated for 6 months (R6). Some of these blocks were irradiated again with the same dose and then incubated for another 6 months; thus, they are a new different treatment which have received a double dose of gamma radiation (28 kGy) (represented as a 2R); (2) Blocks irradiated for the first time after six months' incubation and then incubated for another 6 months. These samples only have received 1 dose of irradiation (represented as R12).

All these treatments were elaborated with and without the bacterial consortium (which is represented as B) and in triplicates except for double-irradiated treatments (2R) for the capacity reason.

Controls, which consist of unirradiated bentonite prepared and treated similarly to the irradiated samples, were included and represented as a C. There are controls after 6 and 12 months of incubation.

Microbial analyses

For microbiological analyses, both culture-independent and culture-dependent techniques have been employed. In the case of culture-independent techniques, bentonite samples were examined through the Illumina sequencing of the 16S rRNA gene to assess microbial diversity, Sanger sequencing was used for identifying isolated strains, and qPCR to quantify microbial activity.

DNA extractions from the bentonite samples followed the phenol-chloroform-based protocol detailed in Povedano-Priego et al. (2021). Mechanical lysis involved mixing glass beads. This was followed by chemical lysis, including 0.12 M pH 8 NaH_2PO_4 solution, lysis buffer, freshly lysozyme and proteinase K. The subsequent phenol-chloroform steps were employed to separate the DNA from other cellular compounds. Following this, isopropanol and sodium acetate steps were utilized to precipitate the DNA, which was then purified from impurities using 80% ethanol. The concentration of the obtained DNA was measured using the Qubit 3.0 Fluorometer (Life Technology, Invitrogen™). The NGS and qPCR analyses were conducted in collaboration with the Technical University of Liberec (Czech Republic). The details of these analyses are described in Section 2.2.1. Regarding Sanger sequencing of isolates, DNA extraction from individual colonies was achieved by resuspending a single, pure colony in MilliQ water and subjecting it to heating at 100 ºC for 10 minutes. The 16S rRNA gene in the extracted DNA underwent sequencing using the primers 1492R (5'-TACGGYTACCTTGTTACGACTT-3') and 27F (5'-AAGAGTTTGATYMTGGCTCAG-3') through bidirectional Sanger sequencing. PCRs were conducted using the M.B.L. Recombinant Taq Polymerase kit (Material Blanco de Laboratorio, S.L., Spain). Before sequencing, PCR products were purified using the Clean-Easy™ PCR Purification Kit (Canvax Biotech, Spain). Subsequently, sequences were compiled and aligned using BioEdit and the comparative analysis was carried out by matching these sequences with those in the GenBank database.

Concerning culture-dependent techniques, the cell viability of aerobic heterotrophs was analysed by counting the colony-forming units (CFU). The experimental conditions were 28 ºC for 3 days under aerobic conditions. The R2A medium was selected for the growth and isolation of heterotrophic microorganisms. The survival of SRB was determined using the Most Probable Number method in Postgate culture media. The ratio 1:10 was chosen for the mixture of bentonite and degassed Phosphate-Buffered Saline (PBS). Then, serum bottles were filled with 4.5 mL of anoxic Postgate's Medium (DSMZ 2022; https://www.dsmz.de/). Decimal dilutions were elaborated in triplicates from 10^{-1} to 10^{-5}. The incubation conditions were at rest in darkness for 30 days at 28 ºC. After that time, the DNA extraction from the positive wells was carried out using the DNeasy PowerSoil Pro Kit (Qiagen).

Table 1: Summary table of the experimental conditions for each treatment.

Label	Bacterial Consortium (B)	Copper Disk	Radiation prior to incubation (dose rate: 66 Gy/h)	Late radiation (R) [at 6 months] (dose: rate 66 Gy/h)	Double radiation dose (2R)	Total cumulative dose (kGy)	Powdered bentonite weight (g)	Cu disk weight (g)	Final weight (g)	Pore water volume (mL)	Total volume inoculated culture media / filtered culture media	Sodium acetate 1.5 mM (µL)	Total volume (mL)	Purpose (Treatment)
T.0 N														Non-incubated natural powdered FEBEX bentonite
T.0 N			✔			14								Non-incubated irradiated powdered FEBEX bentonite
C6		✔					51.28	2.83	54.11	3.2	1.8	150	5	6-month incubation control
CB6	✔	✔					51.28	2.77	54.05	3.2	1.8	150	5	6-month incubation control + B
C12		✔					51.28	2.77	54.06	3.2	1.8	150	5	12-month incubation control
CB12	✔	✔					51.28	2.79	54.08	3.2	1.8	150	5	12-month incubation control + B
R6		✔	✔			14	51.28	2.82	54.10	3.2	1.8	150	5	1 dose R prior incubation + 6-month incubation
RB6	✔	✔	✔			14	51.28	2.81	54.09	3.2	1.8	150	5	1 dose R prior incubation + B + 6-month incubation
R12		✔		✔		14	51.28	2.81	54.09	3.2	1.8	150	5	1 dose R at 6-months incubation + another 6-month incubation
RB12	✔	✔		✔		14	51.28	2.82	54.10	3.2	1.8	150	5	1 dose R at 6-months incubation + B + another 6-month incubation
2R12		✔	✔	✔	✔	28	51.28	2.77	54.05	3.2	1.8	150	5	1 dose R prior incubation + 1 dose at 6-months (total 28 kGy) (total 12-month incubation)
2RB12	✔	✔	✔	✔	✔	28	51.28	2.81	54.09	3.2	1.8	150	5	1 dose R prior incubation + 1 dose at 6-months (total 28 kGy) + B (total 12-month incubation)

Corrosion analyses

For the analysis of the metal corrosion products, a combination of techniques based on Environmental Scanning Electron Microscopy (ESEM), X-ray Photoelectron Spectroscopy (XPS) and Micro-Fourier Transform Infrared Spectroscopy (micro-FTIR) was used. For the preparation of copper samples for ESEM, each disc was fixed in a 2.5% glutaraldehyde solution in cacodylate buffer. Subsequently, it was metalized with a carbon layer and subjected to critical point drying. The copper samples intended for

XPS and micro-FTIR analyses did not require prior preparation. They were covered with aluminum foil until their analysis.

Bentonite mineralogical analyses

The bentonite was characterized by XRD (total and <2 µm fraction) and FTIR techniques. Other physico-chemical properties, such as cation exchange capacity (CEC), soluble salts and exchangeable cations were also analysed.

2.1.2. Results

The 16S rRNA gene sequencing results showed that at time 0, there was no difference between natural powdered bentonite and the irradiated one (14 kGy). The sequencing of the samples from the 6-months study period failed and is pending being repeated. Regarding the results after one year of incubation, similar results were observed for the control samples (C) and those that were irradiated with only one dose (14 kGy) in the middle of the incubation time (treatments R). Results of the two-times irradiated (2R) treatments (28 kGy) differed from the rest (Figure 2). Some genera of the inoculated consortium, such as *Desulfovibrio* and *Desulfotomaculum*, were still detectable after one year of anaerobic incubation in all consortium treatments. In general, the most abundant genera both at time 0 and after one year were *Saccharopolyspora, Pseudomonas, Streptomyces, Acinetobacter* and *Bacillus* (Figure 2).

The qPCR analyses have only been carried out on the 1-year samples. These results have been developed during a research stay in collaboration with Dr. Kateřina Černá at the Technical University of Liberec. qPCR results of 16S gene corroborated the NGS data and the one time-irradiated treatments (R) exhibited a remarkable similarity to non-irradiated controls (C12). On the other hand, a double radiation dose of 14 kGy (28 kGy in total) was enough to barely obtain a signal. Thus, when the total irradiation dose is reduced to 14 kGy, accompanied by a pre- and post-incubation period of six months each, a remarkable resilience in the survival of microbial communities was observed.

Two specific sulphate-reducing genes, *apsA* (adenosine-5′-phosphosulfate) and *dsrA* (dissimilatory sulfite reductase), have been studied for the quantification of sulphate reducing bacteria. The abundance of FEBEX autochthonous SRB was very low as it was corroborated in the control without consortium (C). A dose of 14 kGy (R) was already enough to not be able to detect signal for either of the two genes *apsA* or *dsrA*. With double dose of irradiation (2R), no signal was observed either. On the other hand, the SRB consortium (B) seemed to withstand the conditions of 14 kGy since there was signal in the one-time irradiated treatment (R). Although in very low relative quantification, both genes were also still detected in the two-times irradiated treatments (28 kGy + SRB treatment – 2R).

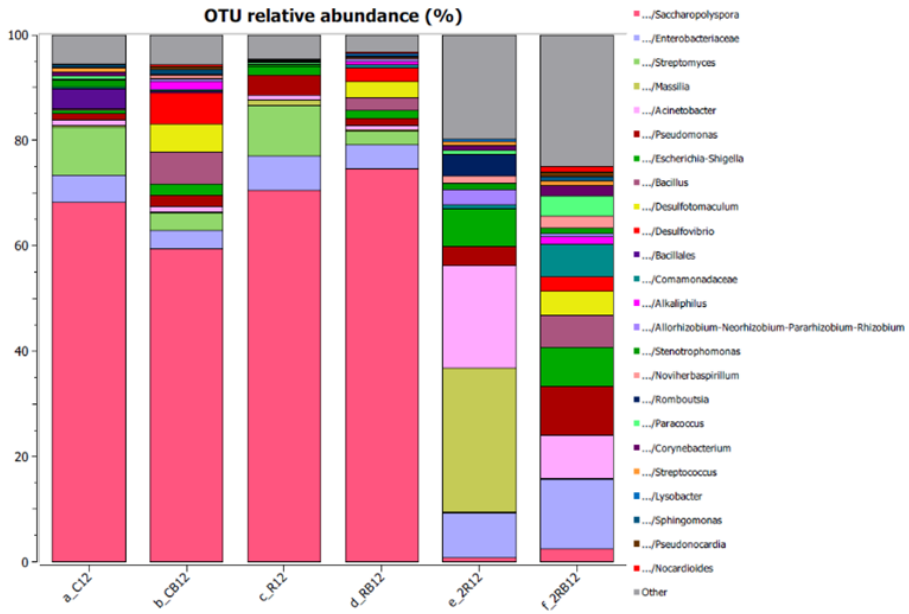

Figure 2: OTU relative abundances at genus level of the microbial communities in compacted bentonite after 1 year of anaerobic incubation. Cut off: 0.25% of relative abundance. Stacked bars represent the mean values of biological triplicates (except 2R12 and 2RB12 in duplicate). C: non-irradiated controls; B: SRB consortium; R: one-time irradiated treatments in the middle of the incubation time (14 kGy); 2R: two-times irradiated treatments (28 kGy).

The impact of irradiation on the microbial viability has also been studied by determining the aerobic colony-forming units (CFU). Time 0 results showed that 14 kGy of gamma irradiation was enough to kill all the viable bacterial cells. After 6 months of anaerobic incubation, there was a lack of growth observed in the irradiated treatments too (14 kGy at the beginning of the incubation). However, a few colonies were found in the irradiated treatment with the SRB consortium on the plates inoculated directly without any dilution. In relation to 1-year samples, there was a lack of growth observed in the two times irradiated treatments (28 kGy). However, in the one-time irradiated treatment in the middle of the incubation time, growth was detected. Cultivable aerobic heterotrophs have been isolated from the 6-months samples. Strains such as *Lysinibacillus* sp., *Lysinibacillus fusiformis, Peribacillus frigoritolerans, Paenibacillus elgii, Bacillus* sp., *Bacillus thuringensis* and *Neobacillus* sp. were isolated and identified.

On the other hand, the survival of SRB was also estimated by determining the Most Probable Number (MPN) in the different treatments under study. To assess the presence of SRB, the studied bentonite was inoculated into a Postgate's medium using decimal dilutions. A statistical algorithm was then used to estimate the number of SRB based on its growth across different dilutions. Control treatments with non-irradiated bentonite were positive for the presence of this group at time 0, 6 months and 1 year. However, no evidence of SRB growth was found in the irradiated treatments at time 0 (14 kGy), 6 months (14 kGy) and 1 year (14 kGy in the middle of the incubation and 28 kGy). Only a few bottles tested positive in the irradiated treatment with the SRB consortium at 6 months. The results of 16S rRNA gene sequencing for one of the positive bottles revealed the presence of *Desulfosporosinus* and *Bacillus*. Therefore, both strains would have survived such an irradiation dose.

Each bentonite block contained a pure copper disc inside for corrosion analysis. After 6 months of incubation, the discs from each treatment were collected for their analysis by ESEM, XPS and micro-FTIR. The same procedure has been repeated for the blocks corresponding to 1 year which are in the process of analysis. Regarding the results of the 6-month discs (Figure 3), greater corrosion was generally observed in the non-irradiated controls, and this corrosion was even more pronounced in the control spiked with the SRB consortium. Microscopy results revealed that this sample with greater corrosion exhibited a surface that was entirely oxidized, displaying copper oxide precipitates with various morphologies. Additionally, small precipitates of copper sulphides were detected, along with precipitates of copper chlorides. The pore water added to the bentonite blocks contained chlorine compounds such

as $CaCl_2$, $MgCl_2$, KCl, NaCl. The other unspiked control sample also presented a similar corrosion behaviour showing a completely oxidized surface with copper oxide precipitates. However, no copper sulphides were found in this sample. With respect to the irradiated treatments (14 kGy), corrosion was much lower, with localized areas with copper oxide precipitates. In the irradiated treatment with SRB consortium, small deposits with sulphur and copper signals were found. Therefore, signals of copper sulphides were only found in the two treatments with the SRB consortium added.

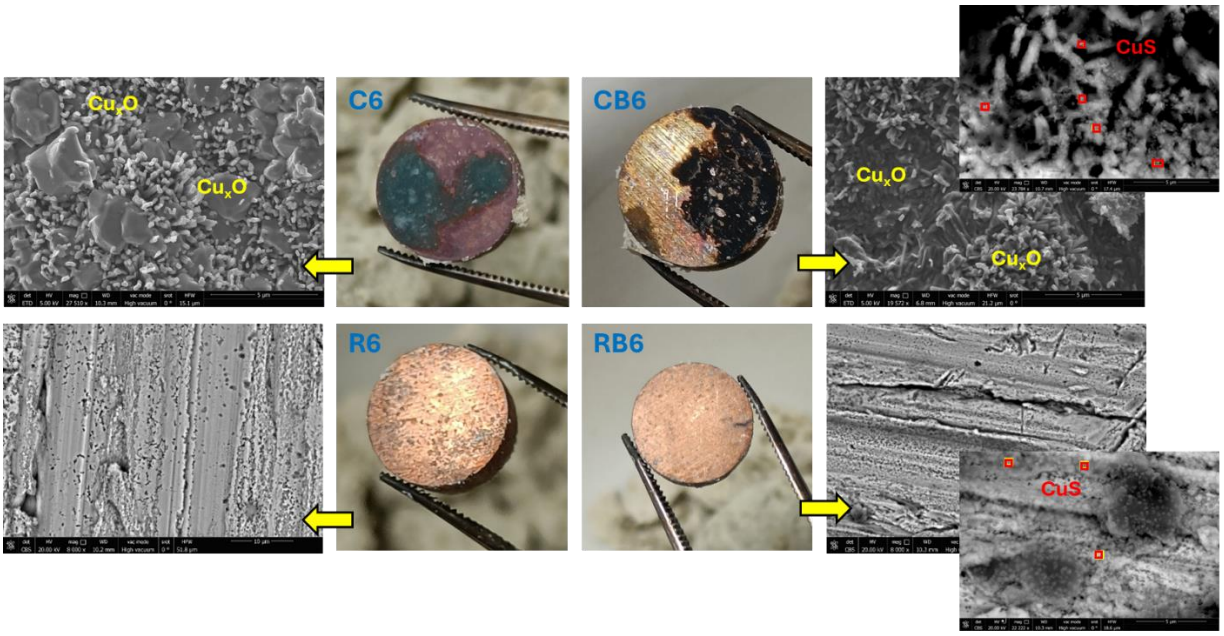

Figure 3: Copper discs from different treatments (C6, CB6, R6, RB6) after 6 months of anaerobic incubation. Microscopic images from scanning electron microscopy of the surface of the Cu discs with yellow markedthe areas of copper oxide deposits and red marked the areas of S signal (possible copper sulphides).

From a mineralogical point of view, no significant changes were observed in the bentonite samples after irradiation (R and 2R) during 6 and 12 months of incubation and/or with the addition of bacteria, maintaining the main character of a dioctahedral two-layer hydrated Ca-Mg-montmorillonite (Figure 4), with typical vibrational bands (Figure 5), and their expansibility or swelling behaviour, with no signs of illitization (Figure 6). In addition, no modifications are observed in the cation exchange properties and ion inventories of the analysed samples with respect the untreated FEBEX bentonite (Table 2).

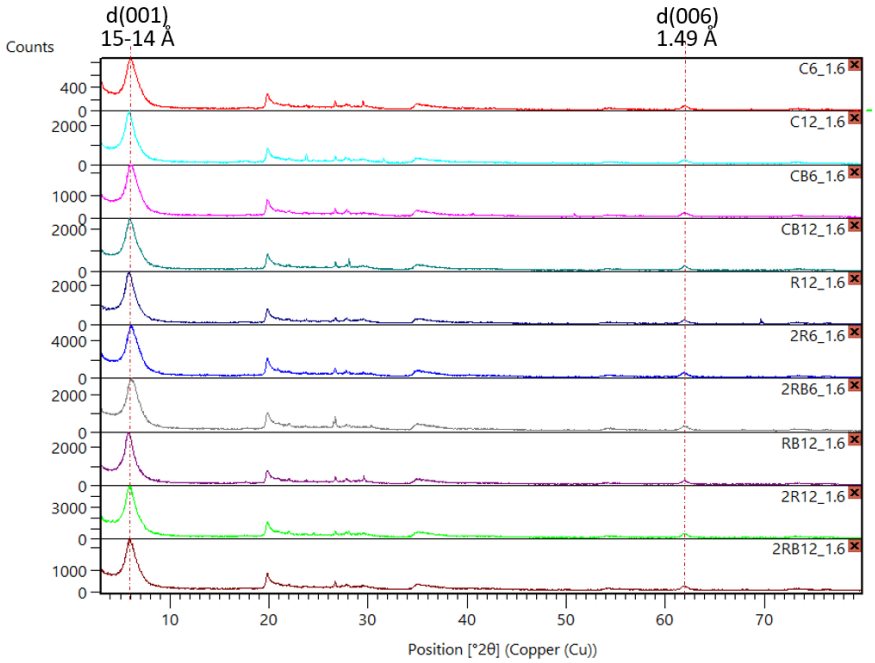

Figure 4: XRD patterns of randomly oriented bulk bentonite samples after 6 months and 1 year of anaerobic incubation (C: non-irradiated controls; B: SRB consortium; R: one-time irradiated treatments in the middle of the incubation time (14 kGy); 2R: two-times irradiated treatments (28 kGy)).

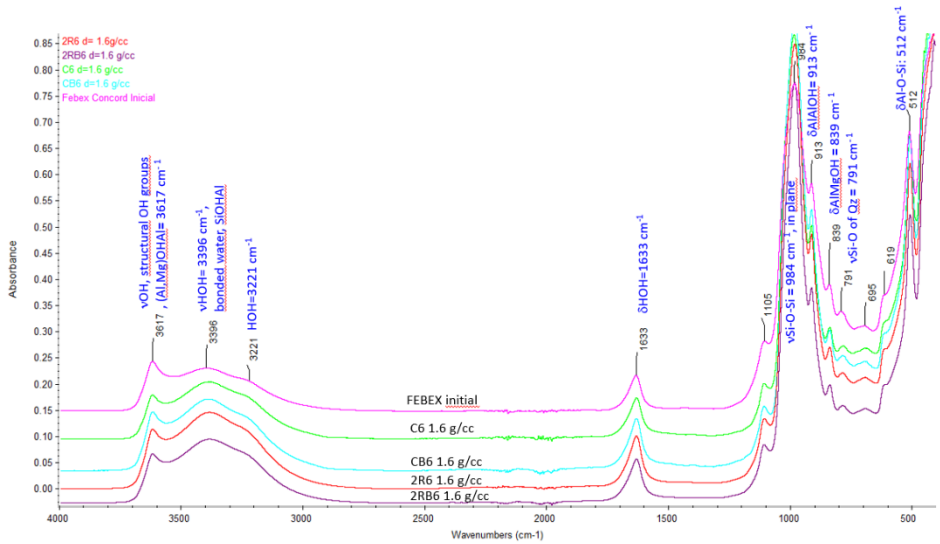

Figure 5: FTIR spectra of powdered samples from bentonite samples after 6 months of anaerobic incubation (C: non-irradiated controls; B: SRB consortium; 2R: two-times irradiated treatments (28 kGy)).

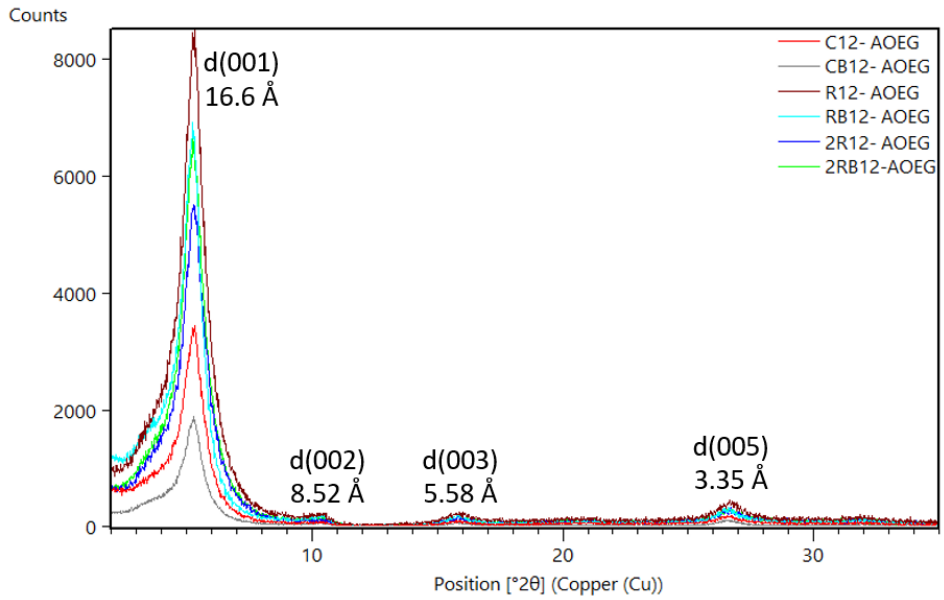

Figure 6: XRD patterns of oriented aggregate samples after ethylene glycol treatment of the bentonite samples after 1 year of anaerobic incubation (C: non-irradiated controls; B: SRB consortium; R: one-time irradiated treatments in the middle of the incubation time (14 kGy); 2R: two-times irradiated treatments (28 kGy)).

Table 2: Cation exchange properties and ion inventories of the bentonite samples after 6 months of anaerobic incubation, in meq/100g. (C: non-irradiated controls; B: SRB consortium; 2R: two-times irradiated treatments (28 kGy)).

				Cation exchange				Aqueous leaching			
Sample	Na meq/100 g	K meq/100 g	Mg meq/100 g	Ca meq/100 g	Sr meq/100 g	Ba meq/100 g	Sum meq/100 g	CEC meq/100 g	pH	Cl mmol/kg	SO_4^{2-} mmol/kg
C6 1.6	28.78	3.06	31.23	36.05	0.19	0.003	99.31	100.8	8.1	27.55	15.19
CB61.6	31.28	3.71	34.19	39.68	0.30	0.005	109.16	104.7	8.1	28.85	15.00
2R6 1.6	28.33	2.96	30.35	35.45	0.24	0.004	97.34	97.5	8.1	26.27	14.20
2RB6 1.6	29.54	3.00	30.53	35.96	0.27	0.004	99.30	97.9	8.1	26.48	13.85

2.1.3 Discussion

In the present work, the impact of gamma radiation on the microbiology of FEBEX bentonite has been studied combining microbiological, microscopic, and spectroscopic techniques.

At time 0, in non-incubated powdered bentonite, no difference in the diversity between the irradiated and non-irradiated samples was observed. The presence of some DNA does not necessarily imply the survival of the genera identified. In addition, there wouldn't be enough time for the damaged DNA to degrade, and the effect would not be observed.

After one year of anaerobic incubation, those samples irradiated in the halfway of the incubation time (6 months, 14 kGy) behaved similarly to the non-irradiated controls. The incubation period before and after irradiation could have allowed the bacterial community to recover better from the radiation dose and therefore be similar to the controls. On the other hand, treatments with double irradiation (at the beginning and in the middle of the incubation period) showed a more shifted diversity. The most abundant genera both at time 0 and after one year are able to persist the hard conditions such as

desiccation. Sporulation or biofilm formation are the most well-known survival strategies (Laskowska and Kuczyńska-Wiśnik, 2020). In addition, spores exhibit approximately five times higher radiation tolerance, than vegetative cells (van Gerwen et al., 1999). The impact of irradiation on the microbial viability has also been studied by determining the aerobic colony-forming units. There was no growth observed in any of the treatments irradiated with 14 kGy, corresponding to both time 0 and 6 months (irradiation at the beginning of the incubation). However, in the treatment after one year, where the 14 kGy radiation was applied in the middle of the incubation period, growth was observed. Therefore, gamma irradiation would affect cell viability differently, depending on the stage in which the bacterial community is found. These results align with Pitonzo et al., (2019) who observed that irradiated bacteria (up to a total dose of 9.34 kGy) could potentially be reactivated to a completely cultivable state over time as environmental conditions become more favourable.

In relation to the survival of sulphate-reducing bacteria based on the most probable number (MPN) in Postgate medium, all irradiated treatments at time 0, 6 months, and 1 year were negative, except for the treatment at 6 months with the added SRB consortium. Sequencing results of such exception agreed with Haynes et al. (2018) who using FEBEX bentonite, subjected to 1 kGy gamma dose, detected *Desulfosporosinus* and *Bacillus* in the MPN enrichments. However, the rest of the irradiated experiments remained negative for the growth of this bacterial group. So, it can be concluded that gamma irradiation at a total cumulative dose of 14 kGy or 28 kGy seems to negatively affect the viability of sulphate-reducing bacteria.

The copper corrosion results indicated that the coupons showing biggest signs of corrosion corresponded to the non-irradiated controls resulting in mainly copper oxides and possible copper sulphides as the main corrosion products. As mentioned in results section (2.2.2), gamma irradiation has a negative impact on bacterial communities, including sulphate-reducing bacteria. Therefore, biotic corrosion was significantly reduced in irradiated treatments. The SRB consortium was added to enhance the effect of this group of bacteria, which is primarily involved in copper corrosion through the production of sulphide (Martínez-Moreno et al., 2023). This effect is supported by the fact that only in coppers from treatments with the SRB consortium showed signs of copper sulphide precipitates in microscopic analysis, although this was not confirmed by the mineralogy studies probably due to their trace content.

2.2 TUL + UJV

For the reliable prediction of long-term microbial effects in the DGR, it is crucial to assess changes in microbial survivability of bentonite microorganisms during the initial hot phase. In Subtask 4.1 of the WP ConCorD, our investigation focused on the microbial response to the combined long-term effects of gamma radiation (≈ 0.4 Gy/h dose rate) and heat (90 °C or 150 °C) in bentonite (BCV and MX80) under anaerobic conditions, emphasizing the microbial potential to regenerate from dormant stages post-treatment.

2.2.1 Materials and Methods

Materials

Czech Ca-Mg bentonite BCV calcium-magnesium bentonite (BCV) from the Czech Republic provided by KERAMOST, Plc., Czech Republic and the reference sodium bentonite (MX-80) provided by CIEMAT were used for the experiments. Synthetic granitic water (SGW3, (Červinka et al., 2018)) was used for saturation of experimental sets A and B, while sterile deionized water was used for pre-wetting of compacted bentonites in sets A, B and C and suspension preparation in D. Carbon steel coupons from a reference material for Czech canister concept (S355J2H) (Forman et al., 2021) supplied by Škoda company, were used as corrosion material in sets A and B.

Experimental set up

Four sets of experiments were conducted to analyse the microbial survivability in bentonite labelled A, B, C, and D, using two types of bentonites, BCV and MX80. These four sets are also referred to as the main experiment. During the course of the project, two more additional experimental sets with only BCV were included to obtain additional information, their design is described below. The conditions used in each set are summarized in

Table **3** together with the major results.

In the main experiment, the first two experimental sets, A (temperature 150 °C) and B (90 °C), consisted of bentonites BCV and MX-80. Samples were compacted to a dry density of 1600 kg/m^3 with embedded carbon steel coupons and partially pre-saturated by distilled water (DW) (15 % saturation for samples heated by 150 °C and 20 % for samples heated by 90 °C). The sample preparation and pre-saturation was performed in an anaerobic box. As these two sample sets were shared with UJV for Tasks 3 and 5, the detailed description of the sample preparation and treatment is included in DL 15.7 (Bevas et al., 2024). Prepared samples were then closed in Ar-filled steel vessels to maintain anaerobic atmosphere and continuously saturated by SGW3 (Figure 7) and exposed to heat (90 or 150 °C) or a combination of heat and irradiation (^{60}Co source) at an approximate dose rate of 0.4 Gy/h. The exposure time was 6, 9, 12, and 18 months for 150 °C and 9, 12, and 18 months for 90 °C in the case of BCV. For MX-80, the exposure was only limited to 18 months. Experimental sets A+B target to mimic the saturated compacted bentonite system during the DGR hot phase and to estimate the microbial survivability and corrosion rate at the studied conditions (corrosion data are included in another WP Concord deliverables DL 15.7 (Bevas et al., 2024), DL 15.8 and DL 15.12).

Another two sets (C and D) were not shared with Tasks 3 and 5 and did not include metal coupons. Set (C) comprised of pre-saturated (15% moisture content) compacted bentonite (BCV/MX-80) in metal canisters similarly to the previous sets but was not continuously saturated during the experiment duration. The samples were exposed to either heat or a combination of heat and irradiation similarly to the set A+B for a duration of 12 months (MX-80 only temperature 90 °C). Furthermore, half of the BCV samples were resaturated for a further 6 months in DW following the treatment. This experimental set was included to see the effect of low water saturation level on microbial survivability in compacted bentonite.

The final set (D) included bentonite (BCV/MX-80) as a dry powder or 1:3(BCV)/1:6(MX-80) w/w suspension in sterile DW representing two possible extremes in terms of water availability in bentonite environment. These samples were prepared in sealed glass ampoules and exposed to similar conditions as sets A, B and C for 12 months. The only exception was suspension samples which were kept in metal cells similarly to compacted bentonite and heated to 150 °C for only 1 month. Here the longer-term exposure was not possible due to technical issues.

Furthermore, within each of these experimental sets, laboratory controls were included. These controls were not exposed to either heating or irradiation. They were either saturated (by immersing into the DW in plastic saturation reservoir) or not similarly to corresponding treated samples and placed inside the anaerobic box at the laboratory temperature to facilitate a comparison between the treated and non-treated samples.

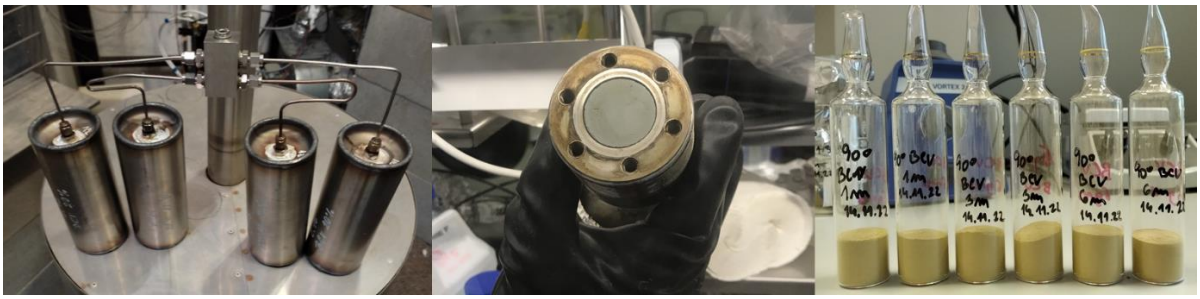

Figure 7: Steel vessels containing steel cells connected by metal capillaries with saturation medium situated in the irradiation area, steel cell with compacted bentonite and glass ampoules with bentonite powder.

As the main experiment clearly demonstrated the major effect of temperature exposure on bentonite survivability, the additional experiment including BCV powder heated to either 90 or 150 °C for shorter periods of 1, 3, and 6 months was included to better distinguish the time effect of heat exposure on BCV powder in its natural dry state, where the highest survivability chance was expected based on our previous experimental data. The samples were sealed in glass ampoules and exposed to the desired temperature in an oven.

Furthermore, 2-year-old samples of BCV powder and suspension heated to 150 °C within Eurad WP HITEC were also taken during the scheduled sampling to check the microbial survivability. These samples were considered as additional to the main experimental set D.

Sample processing

The disassembly of the compacted bentonite samples from the first two sets (A and B) shared with the Tasks 3 and 5 was performed within a glove box under Ar atmosphere. Here the maintaining of fully sterile conditions during the sampling was not possible, because the priority was to maintain the samples under anaerobic condition the whole time for the subsequent corrosion analyses in Tasks 3 and 5. On the other hand, the samples from sets C, D and also additional experiments were sampled in sterile laminar box. Here the priority was the sterility of the sampling.

In sets A+B, the compacted bentonite samples were sliced using a sterile knife from the side, where the saturation ports were positioned. In general, three distinct types of loaded material were obtained from each cell: 1) bentonite for microbiological analyses (Gen1, Gen2) including sample from the corrosion layers in the proximity of metal coupons (CorrP), 2) bentonite for geochemical and mineralogical analyses, and 3) steel specimens (corrosion coupon). In Task 4.1, only microbiological analyses were performed, the remaining analyses were conducted within Task 3 and 5 by UJV (see DL 15.7 (Bevas et al., 2024), DL 15.8 and 15.12). In set C without corrosion coupons, two samples were taken for microbiological analyses from the central part of each cell and the rest of the sample was used to estimate the moisture content. In the case of set D and additional experiment, the glass ampoules were delicately broken in a laminar flow box after the glass surface sterilization and samples were carefully transferred to sterile plastic tubes for further analyses.

For cultivation analyses, all the samples (compacted bentonite, powder, and suspension) were first suspended in sterile deionized water to obtain approximately a 1:5 ratio w/w (bentonite to water) for BCV and 1:8 for MX-80. From this suspension, 0.5 ml in duplicate was cultivated in 14 ml of R2A broth (M1687; Himedia, India) for culturing aerobic and anaerobic heterotrophic microorganisms and Sulphate reducing medium (M803; Himedia, India) for culturing anaerobic sulphate-reducing bacteria. The cultivations were performed for 1 week (R2A - aerobic), 3 weeks (R2A - anaerobic) and 5 weeks (PGM) respectively. 10 ml of the suspension was further used for 30 days (30D) natural incubation in anaerobic chamber containing atmosphere of 6% H_2 + 94% Ar. This natural incubation was done to simulate more realistic culture conditions and aimed to overcome the primary limitation (high selectivity) of culture-based methods.

After the incubation, all media cultures and natural incubations were first checked microscopically for the presence of living cells at the end if incubation period (see 0), and all the samples were centrifuged at 11.000 x g for 10 min and resulting pellets stored in the freezer (-20 °C) for subsequent DNA extraction and genetic analyses. In case of saturated control samples, water from saturation reservoirs (boxwater) was filtered by 0.22 µm Sterivex filters and used for subsequent DNA extraction and genetic analyses.

DNA extraction

Two different extraction methods were used for our samples. Bentonite samples (fresh samples and 30D incubations) were extracted (approximately 5 g of wet weight) using the DNeasy PowerMax Soil Kit (Qiagen, Germany), following the manufacturer's protocol. The resulting DNA extract (1 mL) was subsequently purified and concentrated to a final volume of 50 µL using the Genomic DNA Clean & Concentrator kit (Zymo Research, USA). The DNA from culture samples and Sterivex filters was extracted using the DNAeasy PowerWater kit (Qiagen, Germany) following the manufacturer's protocol.

Kit (negative) control sample without the input matrix was processed in the same way as the real samples together with each extraction batch to uncover contamination arising during DNA isolation, either from the environment (laboratory background) or from the kits (kit contaminations).

Relative quantification by qPCR

Quantitative PCR (qPCR) on a LightCycler® 480 system (Roche, Switzerland) was used to monitor changes in the relative abundance of total bacterial biomass, using the universal primers U16SRT-F and U16SRT-R to target all bacteria encoding the V3 region of the 16S rRNA gene (Clifford et al., 2012). Preparation of the qPCR reaction mix and PCR cycler conditions were as described by (Bartak et al., 2023). To distinguish bentonite and culture samples with possible ongoing proliferation, Cq positivity threshold was estimated for each matrix separately based on the mean Cq values of samples negative for all the cultivations as Cq_{Avg} - $3xSD_{Avg}$ for each bentonite and matrix. All the Cq values lower than this threshold were considered positive.

Next generation sequencing (NGS)

All the bentonite samples together with all the positive culture samples and reservoir waters were sequenced on Ion Torrent Genexus platform using the universal primers 515F (Dowd et al., 2008) and 802R (Claesson et al., 2010). The procedure of library preparation and subsequent bioinformatical processing was similar as described in (Bartak et al., 2023). Statistical identification and removal of contaminant sequences was done using the Decontam package (v1.20.0; (Davis et al., 2018)) based on the signal in sequenced kit control sample. Taxonomy bubble plots were created using the same relative abundances, but only including bacteria with a mean relative abundance greater than 0.005.

Cell Extraction and microscopic analysis

Cell extraction followed by LIVE/DEAD (L/D) staining was performed on 30D natural incubations using 1 mL of suspension, as described by (Hlavackova et al., 2023). Similarly, L/D staining was applied to detect the presence of living and dead cells in culture samples, using 8 µL from each culture sample mixed with 4 µL of L/D BacLight ™ Bacterial Viability Kit fluorescent dye (Thermo Fischer Scientific, USA). The stained sample was incubated in the dark for 15 min before observing under a Zeiss Axio Imager M2 epifluorescence microscope (Carl Zeiss, Germany), using the AxioVision (AxioVs40x69V v.4.9.1.0) imaging software program (Carl Zeiss, Germany).

2.2.2 Results

Main experiment

In all the culture samples, microscopic analyses as well as genetic analyses were performed. The qPCR results obtained for enrichment cultures generally aligned well with microscopic observations, with only a few discrepancies. In cases of such disparities, the qPCR results were considered more relevant as the microscopy can easily indicate false negative results in bentonite environment.

The cultivations obtained from heat/IR treated BCV and MX-80 samples from main experiments A, B, C, and D showed microbial proliferation in only a few culture samples across all three cultivation conditions regardless of the temperature (150 °C or 90 °C) and the presence of radiation (

Table **3**). The positive BCV cultures were mostly dominated by single dominant genera such as *Kocuria*, *Enhydrobacter* or *Nocardioides* (Figure 8). However, only one positive culture sample was detected in case of MX-80 bentonite, but sequencing was not performed on this sample due to technical issue.

On the other hand, almost all the BCV and MX-80 control samples from the main experiment resulted in positive culture results (

Table **3**) with diverse microbial composition. In BCV samples, in the R2A (aerobic and anaerobic) medium growth of common bentonite genera belonging to the family Bacillaceae, family Clostridiaceae, and genus *Pelosinus*. Additionally, some rare genera, including *Sedimentibacter, Sporomusa,*

Sporacetigenium, Fonticella, and *Anaerosporomusa*, were also identified (Figure 8). In PGM cultivations genera like *Pelosinus* and *Sporacetigenium* were most abundant, followed by genus *Desulfosporosinus*, *Bacillus*, a range of *Clostridium* spp. along with rarer genera like *Sporomusa* and *Anaerosporomusa*.

In the control MX-80 samples, the overall diversity was much lower in the culture samples. In the R2A enrichments (aerobic and anaerobic) were primarily dominated by genera belonging to the order Bacillales, particularly the genus *Paenibacillus*. Additionally, the occurrence of the genera *Clostridium* or *Lysinibacillus* was noticed in the R2A anaerobic cultivation. In case of PGM, genera such as *Sporacetigenium*, *Desulfosporosinus*, *Anaerospora, Sedimentbacter,* and *Pelosinus* or members of the order Bacillales dominated the culture samples (Figure 9).

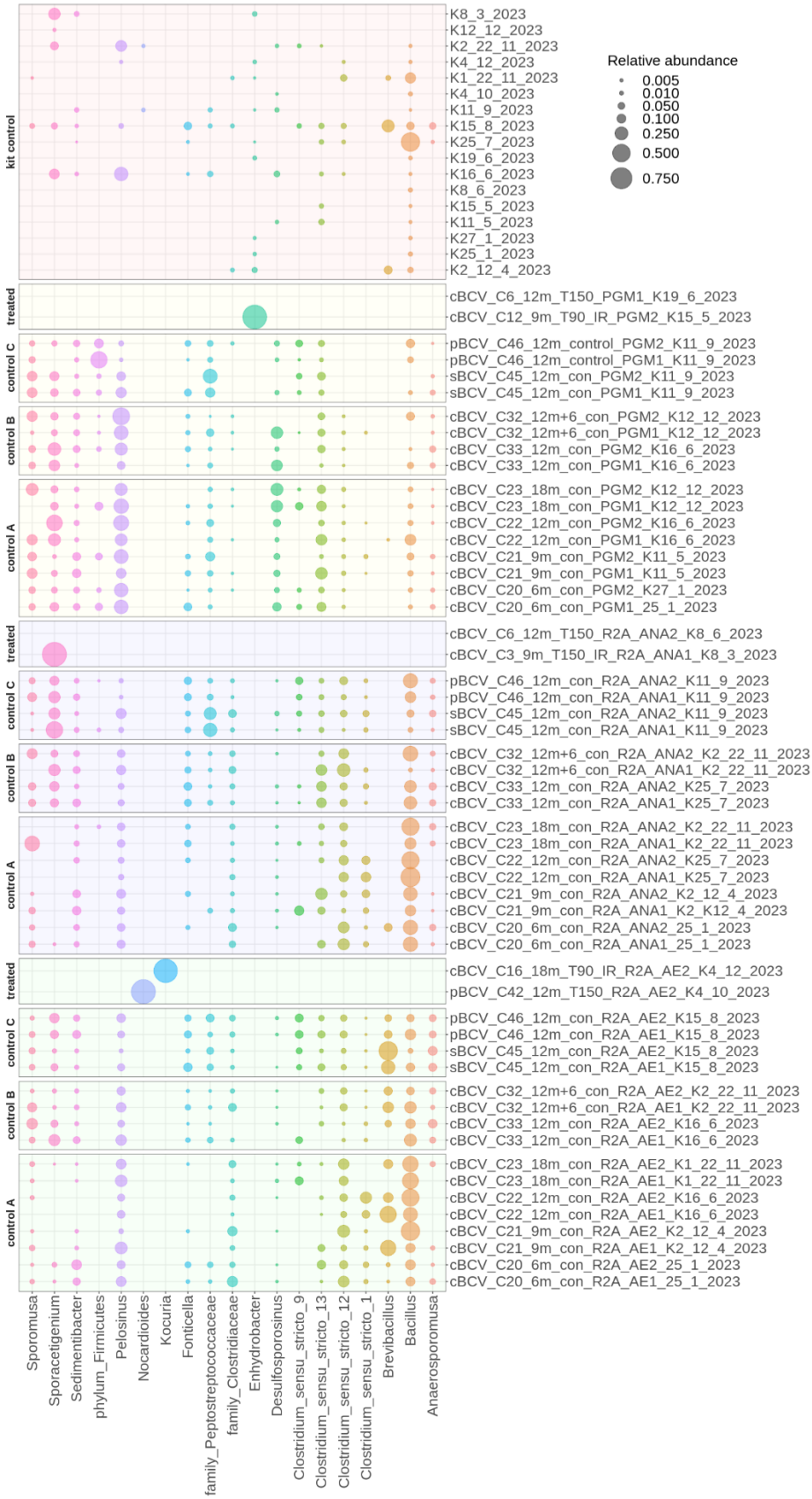

Figure 8: Microbial composition of positive enrichment cultures from the BCV samples of the main experiment. CX - sample number, con - control sample, 6-18m - exposure time, R2A_ANA/AE/PGM - media used for cultivations, K - kit controls.

Table 3: Summary result table of the main experiment (sets A, B, C and D). 30D - 30-days natural incubations, CorrP - bentonite corrosion layer, Water - saturation water, R2A AE/ANA/PGM - media cultivations, LD/qPCR - result of microscopic/qPCR analysis (+ positive/- negative).

Sample name	Experiment	Metal coupons	Continuous saturation	Dry density (kg/m3)	Start w	Final w	Exposure (m)	Temperature (°C)	Radiation dose (Gy/h)	Fresh Gen1 (qPCR)	Fresh Gen2 (qPCR)	30D (LD)	30D (qPCR)	CorrP (qPCR)	Water (qPCR)	R2A AE1 (LD)	R2A AE1 (qPCR)	R2A AE2 (LD)	R2A AE2 (qPCR)	R2A ANA1 (LD)	R2A ANA1 (qPCR)	R2A ANA2 (LD)	R2A ANA2 (qPCR)	PGM1 (LD)	PGM1 (qPCR)	PGM2 (LD)	PGM2 (qPCR)
cBCV_C20_6m_con	A +B	yes	yes	1600	0.200	0.226	6	RT	0	-	-	-	+	+	+	+	+	+	+	+	+	+	+	+	+	+	+
cBCV_C21_9m_con	A +B	yes	yes	1600	0.200	0.245	9	RT	0	-	NA	+	+	-	+	+	+	+	+	+	+	+	+	+	+	+	+
cBCV_C22_12m_con	A +B	yes	yes	1600	0.200	0.238	12	RT	0	+	-	+	+	NA	+	+	+	+	+	+	+	+	+	+	+	+	+
cBCV_C23_18m_con	A +B	yes	yes	1600	0.200	0.239	18	RT	0	+	NA	+	+	+	NA	+	+	+	+	+	+	+	+	+	+	+	+
cBCV_C12_9m_T90_IR	B	yes	yes	1600	0.200	0.209	9	90	0.4	-	NA	-	-	-	NA	-	-	-	+	-	-	-	-	-	+	+	+
cBCV_C14_12m_T90_IR	B	yes	yes	1600	0.200	0.232	12	90	0.4	-	-	-	-	NA	NA	-	-	-	-	-	-	-	-	-	-	-	-
cBCV_C16_18m_T90_IR	B	yes	yes	1600	0.200	0.183	18	90	0.4	-	NA	-	-	-	NA	-	-	+	+	-	+	-	-	-	-	-	-
cBCV_C13_9m_T90	B	yes	yes	1600	0.200	0.246	9	90	0	-	-	-	-	-	NA	-	-	-	-	-	-	-	-	-	-	-	-
cBCV_C15_12m_T90	B	yes	yes	1600	0.200	0.239	12	90	0	-	-	-	-	NA	NA	-	-	-	-	-	-	-	-	-	-	-	-
cBCV_C17_18m_T90	B	yes	yes	1600	0.200	0.218	18	90	0	-	NA	-	-	-	NA	-	-	-	-	-	-	-	-	-	-	-	-
cBCV_C1_6m_T150_IR	A	yes	yes	1600	0.150	0.211	6	150	0.4	-	-	-	-	-	NA	-	-	-	-	-	-	-	-	-	-	-	-
cBCV_C3_9m_T150_IR	A	yes	yes	1600	0.150	0.251	9	150	0.4	-	NA	-	-	-	NA	-	-	-	-	+	+	-	-	-	-	-	-
cBCV_C5_12m_T150_IR	A	yes	yes	1600	0.150	0.205	12	150	0.4	-	-	-	-	NA	NA	-	-	-	-	-	-	-	-	-	-	-	-
cBCV_C7_18m_T150_IR	A	yes	yes	1600	0.150	0.226	18	150	0.4	-	NA	-	-	-	NA	-	-	-	-	-	-	-	-	-	-	-	-
cBCV_C2_6m_T150	A	yes	yes	1600	0.150	0.213	6	150	0	-	NA	-	-	-	NA	-	-	-	-	-	-	-	-	-	-	-	-
cBCV_C4_9m_T150	A	yes	yes	1600	0.150	0.220	9	150	0	-	NA	-	-	-	NA	+	+	-	-	-	-	-	-	+	+	-	-
cBCV_C6_12m_T150	A	yes	yes	1600	0.150	0.093	12	150	0	-	-	-	-	NA	NA	-	-	-	-	-	-	+	+	+	+	-	-
cBCV_C8_18m_T150	A	yes	yes	1600	0.150	0.223	18	150	0	-	NA	-	-	-	NA	-	-	-	-	-	-	-	-	-	-	-	-
cMX80_C11_18m_con	A	yes	yes	1600	0.150	0.196	18	RT	0	-	NA	-	-	+	NA	+	+	+	+	+	+	+	+	+	+	+	+
cMX80_C18_18m_T90_IR	A	yes	yes	1600	0.200	0.206	18	90	0.4	-	NA	-	-	-	NA	-	-	-	-	-	-	-	-	-	+	-	-
cMX80_C19_18m_T90	A	yes	yes	1600	0.200	0.204	18	90	0	-	NA	-	-	-	NA	-	-	-	-	-	-	-	-	-	-	-	-
cMX80_C9_18m_T150_IR	A	yes	yes	1600	0.150	0.166	18	150	0.4	-	NA	-	-	-	NA	-	-	-	-	-	-	-	-	-	-	-	-
cMX80_C10_18m_T150	A	yes	yes	1600	0.150	0.200	18	150	0	-	NA	-	-	-	NA	-	-	-	-	-	-	-	-	-	-	-	-
cBCV_C33_12m_con	C	no	no	1600	0.150	0.118	12	RT	0	+	-	+	+	NA	NA	+	+	+	+	+	+	+	+	+	+	+	+
cBCV_C32_12m+6_con	C	no	no+R	1600	0.150	0.243	12+6	RT	0	-	-	+	+	NA	+	+	+	+	+	+	+	+	+	+	+	+	+
cBCV_C29_12m_T90_IR	C	no	no	1600	0.150	0.125	12	90	0.4	-	-	-	-	NA	NA	-	-	-	-	-	-	-	-	-	-	-	-
cBCV_C28_12+6m_T90_IR	C	no	no+R	1600	0.150	0.243	12+6	90	0.4	-	-	-	-	NA	-	-	-	-	-	-	+	-	-	-	-	-	-
cBCV_C31_12m_T90	C	no	no	1600	0.150	0.141	12	90	0	-	-	-	-	NA	NA	-	-	-	-	-	-	-	-	-	-	-	-
cBCV_C30_12m+6_T90	C	no	no+R	1600	0.150	0.242	12+6	90	0	-	-	-	-	NA	-	-	-	-	-	-	-	-	-	-	-	-	-
cBCV_C25_12m_T150_IR	C	no	no	1600	0.150	0.101	12	150	0.4	-	-	-	-	NA	NA	-	-	-	-	-	-	-	-	-	-	-	-
cBCV_C24_12m+6_T150_IR	C	no	no+R	1600	0.150	0.237	12+6	150	0.4	-	-	-	-	NA	-	-	-	-	-	-	-	-	-	-	-	-	-
cBCV_C27_12m_T150	C	no	no	1600	0.150	0.099	12	150	0	-	-	-	-	NA	NA	-	-	-	-	-	-	-	-	-	-	-	-
cBCV_C26_12m+6_T150	C	no	no+R	1600	0.150	0.232	12+6	150	0	-	-	-	-	NA	-	-	-	-	-	-	-	-	-	-	-	-	-
cMX80_C36_12m_con	C	no	no	1600	0.150	0.132	12	RT	0	-	-	+	+	NA	NA	+	+	+	+	+	+	+	+	+	+	+	+
cMX80_C34_12m_T90_IR	C	no	no	1600	0.150	0.125	12	90	0.4	-	-	-	-	NA	NA	-	-	-	-	-	-	-	-	-	-	-	-
cMX80_C35_12m_T90	C	no	no	1600	0.150	0.125	12	90	0	-	-	-	-	NA	NA	-	-	-	-	-	-	-	-	-	-	-	-
sBCV_C45_12m_con	D	no	NA	suspension 1:3		NA	12	RT	0	+	NA	NA	NA	NA	NA	+	+	+	+	+	+	+	+	+	+	+	+
sBCV_C39_12m_T90_IR	D	no	NA	suspension 1:3		NA	12	90	0.4	-	NA	-	-	NA	NA	-	-	-	-	-	-	-	-	-	-	-	-
sBCV_C40_12m_T90	D	no	NA	suspension 1:3		NA	12	90	0	-	NA	-	-	NA	NA	-	-	-	-	-	-	-	-	-	-	-	-
sBCV_C37_1m_T150_IR	D	no	NA	suspension 1:3		NA	1	150	0.4	-	NA	-	-	NA	NA	-	-	-	-	-	-	-	-	-	-	-	-
sBCV_C38_1m_T150	D	no	NA	suspension 1:3		NA	1	150	0	-	NA	-	-	NA	NA	-	-	-	-	-	-	-	-	-	-	-	-
pBCV_C46_12m_con	D	no	NA	powder	0.114	NA	12	RT	0	-	NA	+	+	NA	NA	+	+	+	+	+	+	+	+	+	-	+	+
pBCV_C43_12m_T90_IR	D	no	NA	powder	0.114	NA	12	90	0.4	-	NA	-	-	NA	NA	-	-	-	-	-	-	-	-	-	-	-	-
pBCV_C44_12m_T90	D	no	NA	powder	0.114	NA	12	90	0	-	NA	-	-	NA	NA	-	-	-	-	-	-	-	-	-	-	-	-
pBCV_C41_12m_T150_IR	D	no	NA	powder	0.114	NA	12	150	0.4	-	NA	-	-	NA	NA	-	-	-	-	-	-	-	-	-	-	-	-
pBCV_C42_12m_T150	D	no	NA	powder	0.114	NA	12	150	0	-	NA	-	-	NA	NA	-	-	+	+	-	-	-	-	-	-	-	-
sMX80_C55_12m_con	D	no	NA	suspension 1:6		NA	12	RT	0	+	NA	NA	NA	NA	NA	+	+	-	-	+	+	+	+	+	+	+	+
sMX80_C49_12m_T90_IR	D	no	NA	suspension 1:6		NA	12	90	0.4	-	NA	-	-	NA	NA	-	-	-	-	-	-	-	-	-	-	-	-
sMX80_C50_12m_T90	D	no	NA	suspension 1:6		NA	12	90	0	-	NA	-	-	NA	NA	-	-	-	-	-	-	-	-	-	-	-	-
sMX80_C47_1m_T150_IR	D	no	NA	suspension 1:6		NA	1	150	0.4	-	NA	-	-	NA	NA	-	-	-	-	-	-	-	-	-	-	-	-
sMX80_C48_1m_T150	D	no	NA	suspension 1:6		NA	1	150	0	-	NA	-	-	NA	NA	-	-	-	-	-	-	-	-	-	-	-	-
pMX80_C56_12m_con	D	no	NA	powder	0.074	NA	12	RT	0	-	NA	+	+	NA	NA	+	+	+	+	+	+	+	+	+	+	+	+
pMX80_C53_12m_T90_IR	D	no	NA	powder	0.074	NA	12	90	0.4	-	NA	-	-	NA	NA	-	-	-	-	-	-	-	-	-	-	-	-
pMX80_C54_12m_T90	D	no	NA	powder	0.074	NA	12	90	0	-	NA	-	-	NA	NA	-	-	-	-	-	-	-	NA	-	-	-	-
pMX80_C51_12m_T150_IR	D	no	NA	powder	0.074	NA	12	150	0.4	-	NA	-	-	NA	NA	-	-	-	-	-	-	-	-	-	-	-	-
pMX80_C52_12m_T150	D	no	NA	powder	0.074	NA	12	150	0	-	NA	-	-	NA	NA	-	-	-	-	-	-	-	-	-	-	-	-

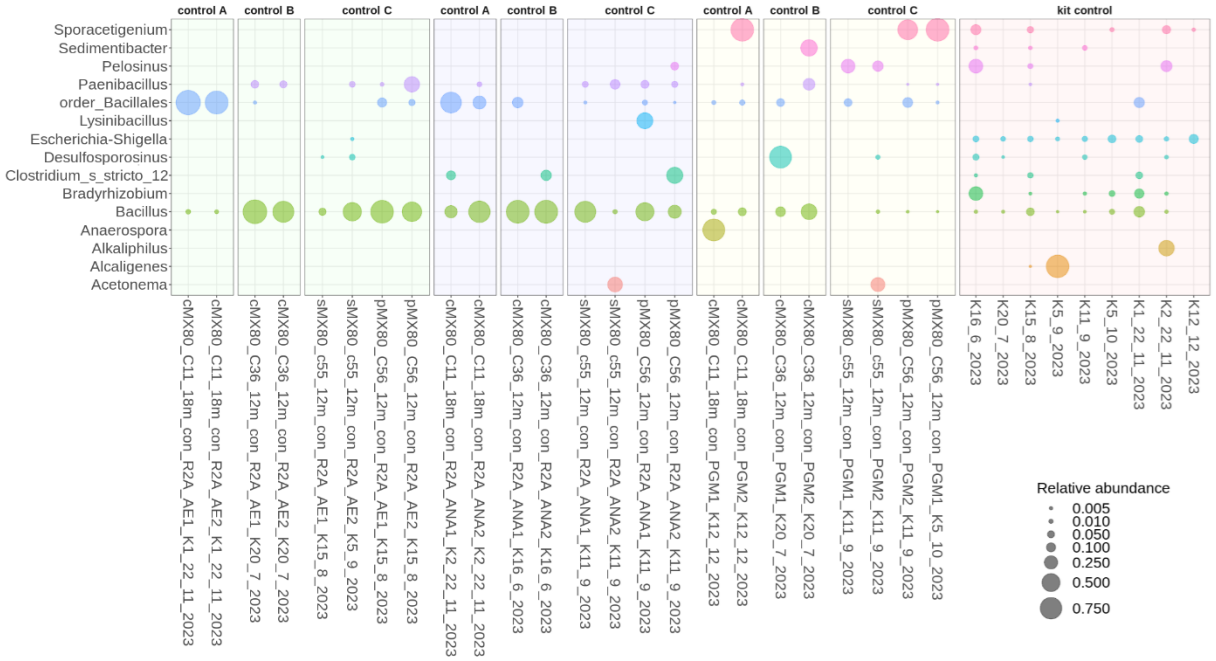

Figure 9: Microbial composition of positive enrichment cultures from MX-80 samples of the main experiment. C - sample number, con - control sample, 12-18m - exposure time, R2A_ANA/AE/PGM - media used for cultivations, K - kit controls.

Relative quantification of 16S rRNA gene copies in fresh BCV and MX80 bentonite samples from the main experiment (A, B, C and D) did not reveal noticeable growth in total microbial biomass in any of the fresh bentonite samples subjected to continuous heating or a combination of heat and irradiation (

Table **3**). The same result was also obtained from the 30D natural incubations of these samples. None of the incubated suspension was positive either for the qPCR or microscopic observations (cell extraction). Furthermore, no microbial proliferation was observed in treated compacted bentonite samples from set C even after their 6m saturation at laboratory temperature after the heat treatment. These long-term incubated and re-saturated samples also did not show microbial recovery even after further 30D natural incubation in suspended form. Similarly, the water used for long-term saturation (Water) did not show any signs of microbiological growth (

Table **3**). In accordance with the qPCR/microscopic results, the microbial composition detected in all the treated bentonite samples was similar to the co-extracted kit controls verifying lack of the true genetic signal (data not shown). Because of the overall lack of the microbial proliferation in all the treated bentonite samples, no difference between the experimental sets, both temperatures (90 °C and 150 °C) or effect of irradiation could be detected. All the treated bentonite samples showed lack of proliferation.

Control fresh BCV and MX-80 samples showed signs of microbial proliferation (based on 16S rRNA qPCR) in some of the control samples. The positive Cq values were detected in compacted bentonite samples after at least 12m exposure in controls to the set A, B and C and in 12m incubated suspension samples in set D. The 30D incubations of control samples were positive in all the samples as well as analysed water samples (Water) from saturation reservoirs (

Table **3**). The bentonite from the corrosion layer was positive only after 6m and 18m incubations from the BCV controls and after 18m incubations from the MX-80 control to the sets A and B.

The NGS analysis revealed that most of the compacted bentonite samples shared a similar microbial composition pattern (Figure 10). In the BCV samples, members of the orders Vicinamibacterales, Gaiellales or Bacillales together with taxons MB-A2-108 and KD4-96 were most abundant. On the other hand, very week signal was detected in MX-80, where the pattern was very similar to the kit controls. In 12m incubated bentonite suspensions family Oxalobacteraceae dominated the sample. In 30D

incubated BCV control samples genera Streptomyces, Micromonospora, Bacillus or members from the family Oxalobacteraceae and Peptococcaceae dominated the samples, while in 30D incubated MX-80 control samples genera Streptomyces or family Oxalobacteraceae dominated the samples. In the saturated BCV samples, genera Desulfosporosinus, Anaerospora and Ralstonia were detected as dominants in the water used for saturation (Figure 10). The samples from the control sample corrosion layers were mostly similar to other bentonite samples in case of BCV and proliferation of any particular genus could not be clearly distinguished. In MX-80, nonspecified member of the order Bacillales was enriched in the corrosion layer sample (Figure 10).

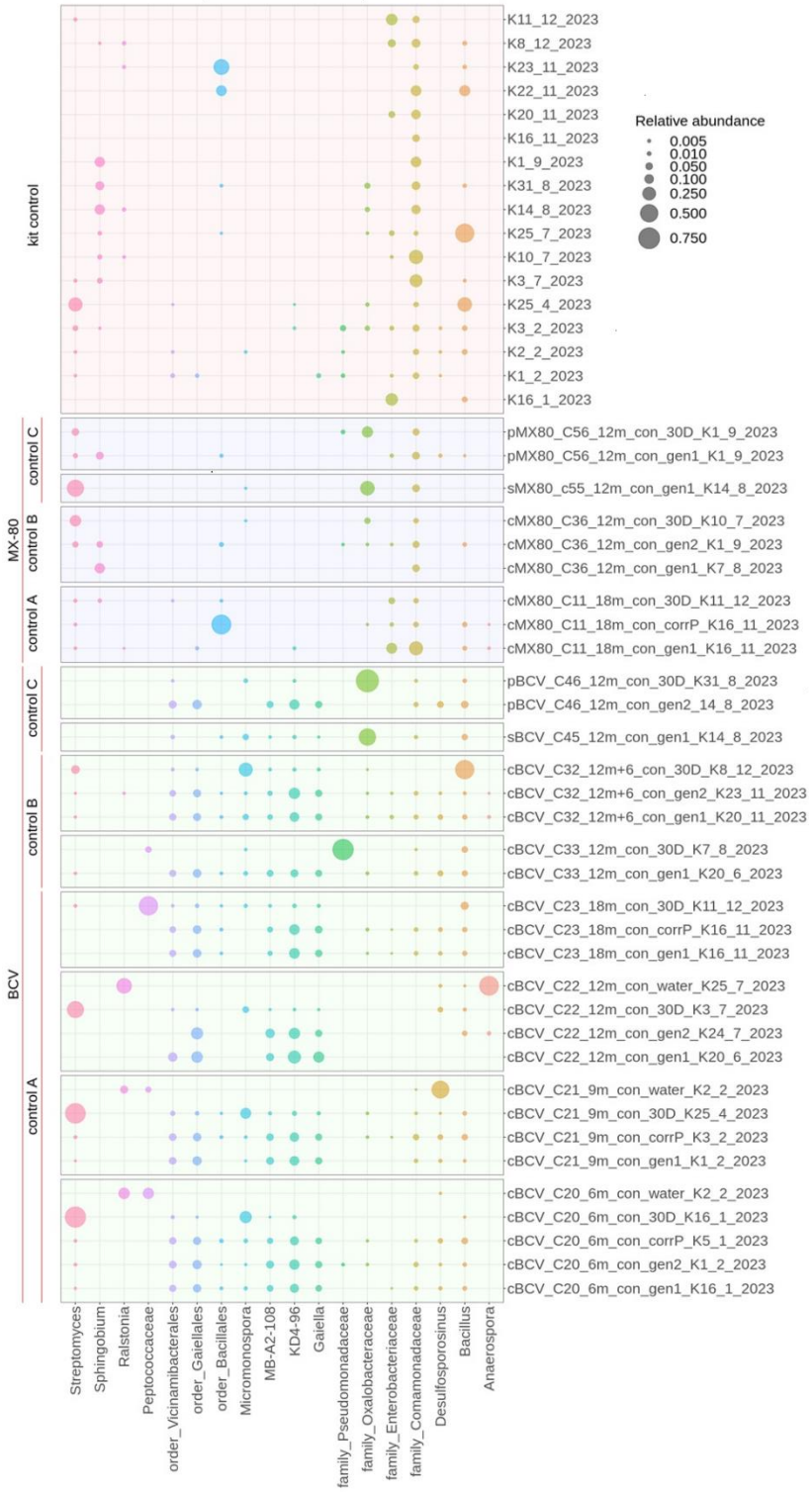

Figure 10: Microbial composition of the control bentonite samples (BCV/MX-80) from the main experiment. C - sample number, con - control sample, 30D - 30-days natural incubations, 6-18m - exposure time, K - kit controls.

Additional experiments

In additional experiments with heated BCV powder, microbial proliferation was detected in several culture samples mainly from samples exposed to 90 °C over 1-6 months duration. On the other hand, samples loaded to 150 °C exhibited cultivability in only one culture sample (Table 4).

In positive culture samples, the genus *Bacillus* was predominantly identified both in R2A (both aerobic and anaerobic) as well as in PGM medium. The PGM medium further exhibited the presence of genus *Brevibacillus* and class *Negativicutes* as significant communities after 1m of exposure to a thermal load of 90 °C. Interestingly, a shift in microbial composition became apparent after 3 months exposure to the same thermal conditions, with different genera such as *Exiguobacterium* (R2A aerobic), *Sphingomonas* (R2A anaerobic), and *Gordonia* (PGM) dominating particular media. Moreover, except for the presence of genus *Brevibacillus* in PGM medium, none of the heterotrophic aerobe and anaerobe remained cultivable after 6 months of exposure to 90 °C tested by R2A. In samples heated at 150 °C only one positive culture sample dominated by the genus *Micrococcus* was detected (Figure 11). BCV suspension and powder samples exposed to 150 °C for 2 years from the HITEC experiment showed no cultivability in any of the treated samples (Table 4).

Table 4: Summary result table of the additional experiments. 30D - 30-days natural incubations, AE/ANA/PGM - media cultivations, LD/qPCR - result of microscopic/qPCR analysis (+ positive/- negative).

Sample name	Temperature (°C)	Exposure (m)	Sample form	Fresh Gen (qPCR)	30D (LD)	30D (qPCR)	R2A AE1 (LD)	R2A AE1 (qPCR)	R2A AE2 (LD)	R2A AE2 (qPCR)	R2A ANA1 (LD)	R2A ANA1 (qPCR)	R2A ANA2 (LD)	R2A ANA2 (qPCR)	PGM1 (LD)	PGM1 (qPCR)	PGM2 (LD)	PGM2 (qPCR)
BCV_P1_1m_T90	90	1	powder	-	-	-	+	+	+	+	+	+	+	+	+	+	+	+
BCV_P2_1m_T90	90	1	powder	-	-	-	-	-	-	-	-	-	-	-	-	-	-	-
BCV_P1_3m_T90	90	3	powder	-	-	-	+	+	-	-	-	-	-	-	-	-	-	-
BCV_P2_3m_T90	90	3	powder	-	-	+	-	-	-	-	-	+	-	-	-	-	-	-
BCV_P1_6m_T90	90	6	powder	-	-	-	-	-	-	-	-	-	-	-	-	-	-	-
BCV_P2_6m_T90	90	6	powder	-	-	-	-	-	-	-	-	-	-	-	-	+	-	+
BCV_P1_1m_T150	150	1	powder	-	-	-	-	-	-	-	-	-	-	-	-	-	-	-
BCV_P2_1m_T150	150	1	powder	-	-	-	-	-	-	-	-	-	-	-	-	-	-	-
BCV_P1_3m_T150	150	3	powder	-	-	-	-	-	-	-	-	-	-	-	+	+	-	-
BCV_P2_3m_T150	150	3	powder	-	-	-	-	-	-	-	-	-	-	-	-	-	-	-
BCV_P1_6m_T150	150	6	powder	-	-	-	-	-	-	-	-	-	-	-	-	-	-	-
BCV_P2_6m_T150	150	6	powder	-	-	-	-	-	-	-	-	-	-	-	-	-	-	-
HITEC_S1_UP	150	24	suspension	-	-	NA	-	NA	-	NA	-	NA	-	NA	-	NA	-	NA
HITEC_S1_D	150	24	suspension	-	-	NA	-	NA	-	NA	-	NA	-	NA	-	NA	-	NA
HITEC_S1_CorrP	150	24	suspension	-	NA	NA	NA	NA	NA	NA	NA	NA	NA	NA	NA	NA	NA	NA
HITEC_S2_UP	150	24	suspension	-	-	NA	-	NA	-	NA	-	NA	-	NA	-	NA	-	NA
HITEC_S2_D	150	24	suspension	-	-	NA	-	NA	-	NA	-	NA	-	NA	-	NA	-	NA
HITEC_S2_ CorrP	150	24	suspension	-	NA	NA	NA	NA	NA	NA	NA	NA	NA	NA	NA	NA	NA	NA
HITEC_P1	150	24	powder	NA	-	NA	-	NA	-	NA	-	NA	-	NA	-	NA	-	NA
HITEC_P2	150	24	powder	NA	-	NA	-	NA	-	NA	-	NA	-	NA	-	NA	-	NA

Corresponding to the culture results, heated BCV powder samples and their subsequent 30D incubations did not show microbial proliferation except for the samples heated at 90 °C for 3 months. Similar observation was detected in the HITEC samples for both bentonite powder and suspension. The detected microbial composition of these samples was similar to the extraction kit controls indicating lack of true signal of these samples similarly to the main experiment (Figure 11). Due to the lack of positive bentonite samples, Decontam was not applied for the additional experiment sample set.

2.2.3 Discussion

Our work within Task 4.1 primarily focused on examining the impact of multiple repository-relevant stressors on the viability of indigenous microorganisms in bentonite. We benefited from the workload planned in Concord Tasks 3 and 5 to unravel the effects of high temperatures (90 °C or 150 °C) and high temperatures plus irradiation (from a ^{60}Co source) on the corrosion of carbon steel in the compacted bentonite environment (see DL 15.7 (Bevas et al., 2024), 15.8 and 15.12). Using UJV samples from Tasks 3 and 5 extended by a few other sample sets, we aimed to simulate the conditions in the proximity of the canister during the hot phase of the repository to estimate response of indigenous bentonite microorganisms to these conditions. Additionally, the water content and bentonite state

(compacted/noncompacted) was varied to see the effect of these factors on microbial survivability. To estimate the effect of exposure duration, multiple time points were included.

Our data demonstrated a strong effect of long-term exposure to both the temperatures tested (90 and 150 °C) leading to dramatic loss of viability and cultivability of indigenous bentonite microorganisms with similar effects observed in both BCV and MX-80 bentonites. The single effect of temperature detected in the current experiment was actually so strong, that no effect of irradiation or additional factors such as bentonite state or water availability could be clearly distinguished in our data, although both and water availability are known factors influencing viability and survivability of bacteria in bentonite (Stroes-Gascoyne et al., 1995; Motamedi et al., 1996; Brown et al., 2015).

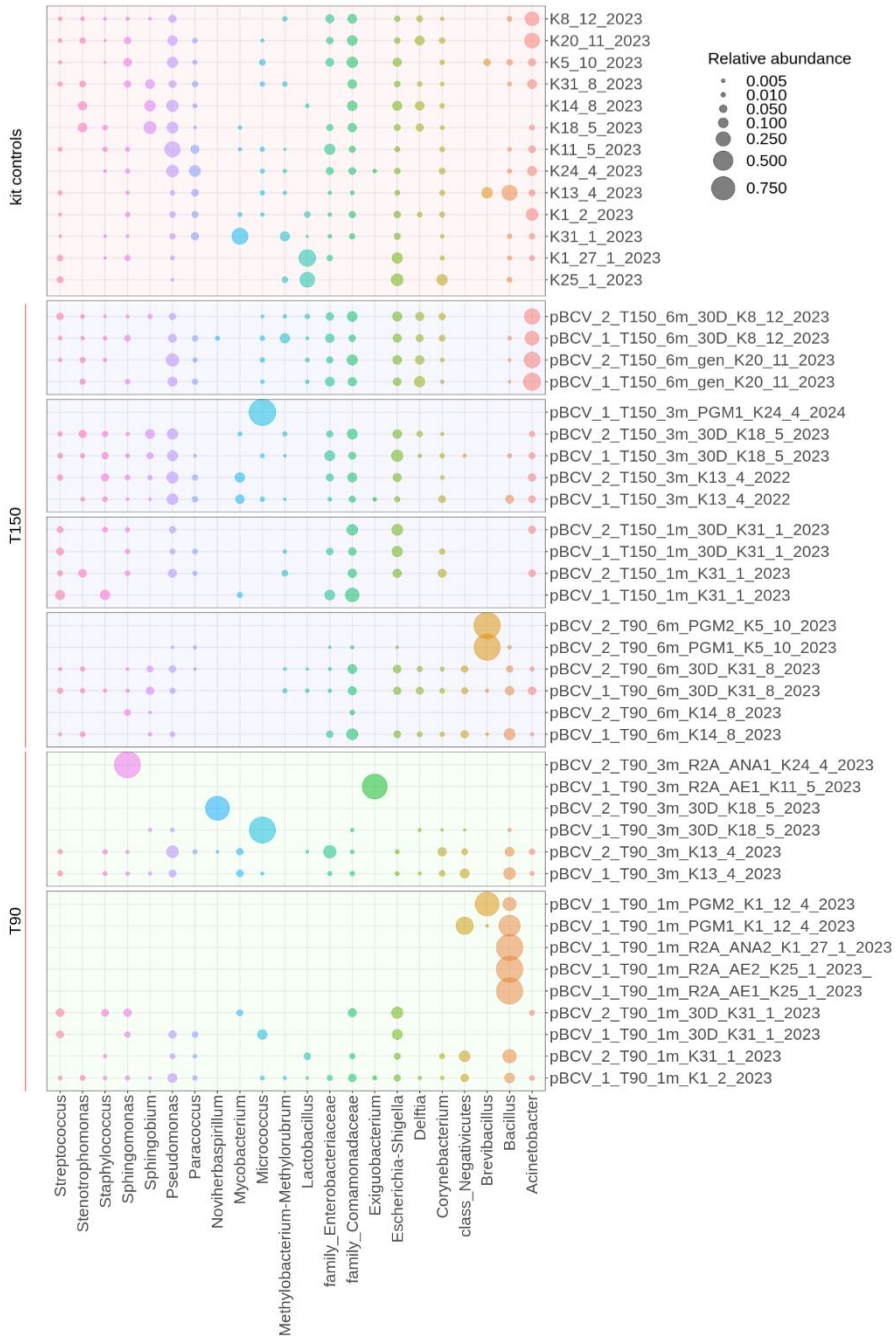

Figure 11: Microbial composition detected in the powder BCV samples (pBCV) from the additional experiment and powder (P) and suspension (S) samples from WP HITEC (2y exposure to 150 °C). C - sample number, con - control

sample, 30D - 30 days long natural incubations, 6-18m - exposure time, R2A_ANA/AE/PGM - media used for cultivations, K - kit controls. Decotam was not applied for this sample set.

Additional experiment with heated BCV powder enabled us to detect effect of the exposure duration. The samples heated at 90 °C showed cultivability even after 6m exposure. However, after 12m exposure the cultivability dramatically decreased in bentonite powder. In case of heating BCV powder at 150 °C, single month exposure resulted in (probably complete) bentonite sterilization. These results are contradictory to the previous data on BCV powder heated at 150 °C for 6 and 12m performed on the samples from Eurad project HITEC (Kašpar et al., 2021). Here the possible microbial proliferation was detected after 6m exposure and possibly also after 12m exposure. However, these data relied only upon natural incubation of heated bentonite in suspended form and no enrichment cultures or microscopic analyses were performed to independently confirm these findings. Additionally, the microbiological analyses were performed on the obtained material and we did not perform the sampling, so we cannot rule out, that the detected positive growth could result from unintentional sample contamination during the sampling or sample storage post sampling.

In our experiment, both enrichment cultures in different media as well as natural incubations in form of bentonite suspension were included to test; what cultivation conditions will be more suitable to demonstrate studied effects on microbial survivability. The natural incubations were successfully used in our previous experiments (Kašpar et al., 2021; Bartak et al., 2023), where it helped us to detect reaction of bentonite microorganisms to elevated pressure or temperature. In the recent ConCord experiment, the superiority of the enrichment culture approach over natural incubations to detect microbial survivability was clearly visible. This finding agrees well with the previous data, where excess of available nutrients promoted microbial recovery after harsh treatments, such as irradiation (Nicholson et al., 2000; Gilmour et al., 2021). On the other hand, enriched cultures are more susceptible to contaminations as they represent suitable environment for many contaminant species. This revealed to be a major drawback of sharing samples among Concord tasks especially for microbial applications. The compacted bentonite samples, that were shared with UJV (Tasks 3 and 5) had to be dismantled in the anaerobic glove box, where the completely sterile conditions could not be maintained, although several precautions were taken to minimize this risk. As a result, several positive cultures originating from the treated samples in sets A+B were detected. On the other hand, much less positive culture samples were obtained in sets C and D, where samples were dismantled under controlled sterile conditions. As a result, we evaluated the positive culture results detected in sets A+B as likely contaminations occurring during the shared sample processing in anaerobic glove box.

Our study has shown that untreated bentonites (BCV and MX80) host a diverse range of indigenous bentonite microbial communities, many of which are known to be very resistant and capable of germination to a metabolically active state when the conditions became favourable again (Gilmour et al., 2021; Masurat et al., 2010b; Stroes-Gascoyne et al., 2002). In accordance with this, we observed, that cultivability of bentonite bacteria remained unaffected even after 18m in the bentonite samples compacted to 1600 kg/m3 dry density. Compaction itself thus proved to be an insufficient factor to eradicate bentonite microorganisms, and these microorganisms might pose a risk to the canister's stability. On the other hand, bentonite compaction clearly limited ongoing microbial activity. Although qPCR analysis indicated possible ongoing microbial proliferation in the corrosion layers near the corrosion coupons in control samples, the proliferation of any particular genera could be detected by NGS. Furthermore, only minimal corrosion rate was found in steel samples embedded in saturated compacted bentonite samples (BCV/MX80) stored under laboratory temperature without irradiation (DL 15.7 (Bevas et al., 2024)), Thus, our data cannot confirm the ongoing MIC in the control samples, possibly due to the severe slowdown of all the biological and chemical processes in compacted bentonite due to its high dry density.

It was predicted that during the initial hot phase of the DGR evolution, when temperature and irradiation reach their peak, prevailing conditions will cause a dramatic loss in microbial survivability, resulting in the possible creation of abiotic zones around the canister (Aoki et al., 2010; Stroes-Gascoyne and West,

1997). The results obtained on the treated samples are in good accordance with this hypothesis, and we showed that microbial activity (including spore-forming microorganisms) in bentonite and, therefore, the risk of MIC is strongly suppressed when the bentonite temperature is long term 90 °C or higher, which are the conditions expected near the canister surface. . However, formation and spatial distribution of such presumable abiotic zone will depend upon overall temperature conditions within the deep geological repository. The presence of highly resistant bentonite microorganisms capable of germination to a metabolically active state when the conditions became favorable again was clearly demonstrated in the heated samples (up to 6m exposure to 90 °C), where some bacteria still showed cultivability in enriched media. Long-term experiments testing the microbial response to nearly limiting temperatures are needed to see the possible effect of temperature gradients on microbial survivability in the bentonite sealing layer. Another non-resolved question is the microbial mobility through the compacted bentonite, as this can lead to reinfestation of the abiotic zone from the surrounding environment. Combining microbial survivability data with mathematical modelling of the evolution of environmental conditions in DGR across its lifetime has excellent potential to increase the accuracy of long-term predictions of microbial effects in the DGR.

3 Impact of bentonite dry density on microbial activity

3.1 EPFL

3.1.1 Design and optimization of reactors

The original plan of the proposal was to run reactors at various dry densities and to obtain a clear dataset for MX-80 that is representative of the expected progressive decrease in biomass accumulation over a specific duration across dry densities. However, the development of a novel approach to investigate this point resulted in delays that precluded the generation of a detailed dataset. Therefore, instead, we spent the time to develop a unique, robust and statistically tractable approach that is applicable to all compacted clays.

The overall goal of this experiment was to quantify microbial growth in compacted bentonite as a function of dry density while avoiding the common pitfalls associated with this type of experiment. The main pitfall is that it is difficult to avoid growth on the filters (or any device) that hold the bentonite in place post-compaction. Therefore, we designed a system that fulfils the conditions necessary to be representative of repository conditions. The design relies on opposing diffusion gradients of electron donor and acceptor. Indeed, we borrowed the diffusion reactor design from Luc Van Loon (Van Loon et al., 2003) and adapted it to microbial applications. The reactor was designed at the Paul Scherrer Institute in Switzerland and consists of a stainless-steel cylinder and stainless-steel end plates with titanium filters at either end and is held closed by a set of screws (Figure 12A). The bentonite is placed between the two filter s and each end plate is connected to tubing connected to two ends of a groove etched into the end plate (Figure 12B). Thus, a solution can be circulated through this groove and solutes diffuse through the filter into the bentonite (Figure 12C). In this instance, two different solutions, one containing H_2 and no sulphate and the other containing sulphate and no H_2 are to be connected to the tubing at either end (Figure 12D). However, contrary to a standard diffusion experiment, the solution is not recirculated. This is to avoid microbial contamination. The solution therefore is flowed past the bentonite once and the effluent collected in a waste bottle.

The reactor design required extensive optimization: (a) to avoid tubing failure, various types of tubing were tested and the best found to be thick Norprene tubing (ID 1.6 mm and OD 4.8 mm); (b) to avoid filter corrosion, we ended up using titanium filters as stainless filters quickly corroded; (c) to prevent leakage from the plastic to stainless steel tubing, the stainless steel tubing was wrapped in Teflon tape, the Norprene tubing slid on top and a zip tie added to hold the plastic tubing in place.

With this set-up, the microorganisms can only grow where the electron donor and acceptor gradients meet, that is, within the bentonite. It is also possible to adjust the flow rate of one or the other solutions

as H_2 is expected to diffuse faster than sulphate. Finally, bromide (Br^-) is added to the sulphate-containing solution to serve as a conservative diffusion tracer. To ensure that oxygen does not enter the system and fuel microbial growth, dissolved oxygen (DO) in the APW reservoir and in the waste bottle are monitored continuously via an optical sensor (optode) system.

The solution that is flowed into the bentonite is artificial Opalinus Clay porewater, the composition of which is given in Table 5. There are two APW recipes to account for the fact that the influent entering the top of the reactor does not contain sulfate or bromide (but contains dissolved H_2), while the one entering the bottom of the reactor contains sulfate and bromide (but no dissolved H_2). The solution is brackish, which is why the filters used to keep the compacted bentonite in place were chosen to be titanium as the stainless steel used initially corroded rapidly.

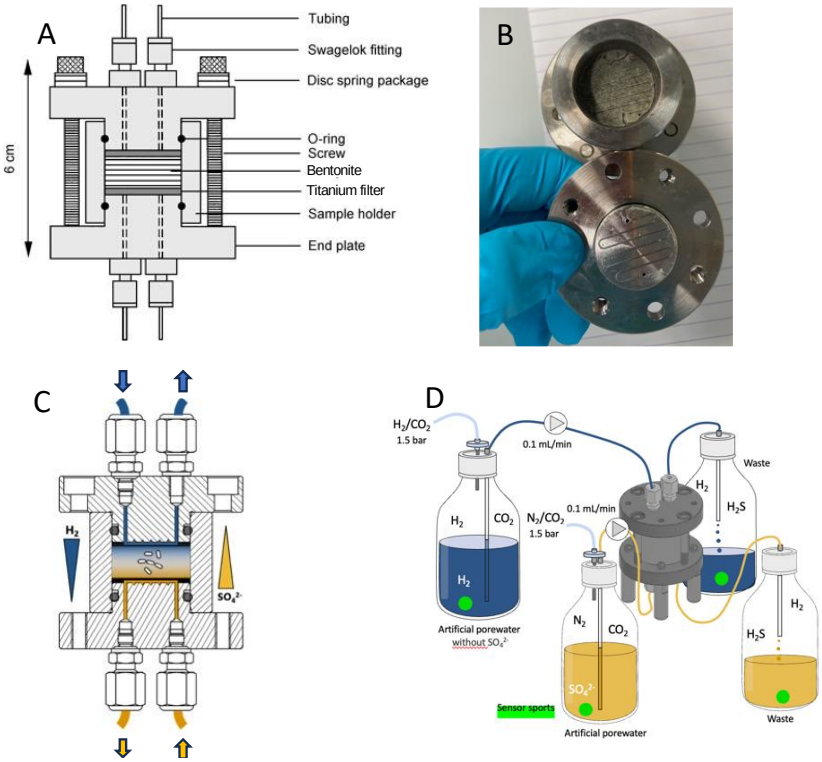

Figure 12: A. Diagram showing the reactor (modified from Van Loon et al., 2003). B. image of the recator showing the groove in the end plate with fingers for scale. C. Ilustration of the gradient of electron donor and acceptor. D. Solutions and waste vessel when connected to a reactor. The optode system sensor is shown with a green dot.

Table 5: Composition of artificial porewater (APW) based on Opalinus Clay porewater. The last two entries correspond to the optional inclusion of sulfate and bromide.

Compounds	mM	g/L	g for 5L
NaCl	212	12.6	63
$NaHCO_3$	0.47	0.04	0.2
$CaCl_2 * 2H_2O$	26	3.8	19
$SrCl_2 * 6H_2O$	0.51	0.13	0.65
KCl	1.6	0.12	0.6
$MgCl_2 * 6H_2O$	17	3.5	17.5
$(Na_2SO_4$	*14*	*2.0*	*10*)
$(NaBr$	*3*	*0.309*	*1.54*)

Table 6: As received MX-80 bentonite weight (containing 8.7% water) needed to reach the desired density in the reactor.

Dry density [g/cm^3]	Wet bentonite [g]
1.2	6.70
1.3	7.26
1.4	7.81
1.5	8.37
1.6	8.93

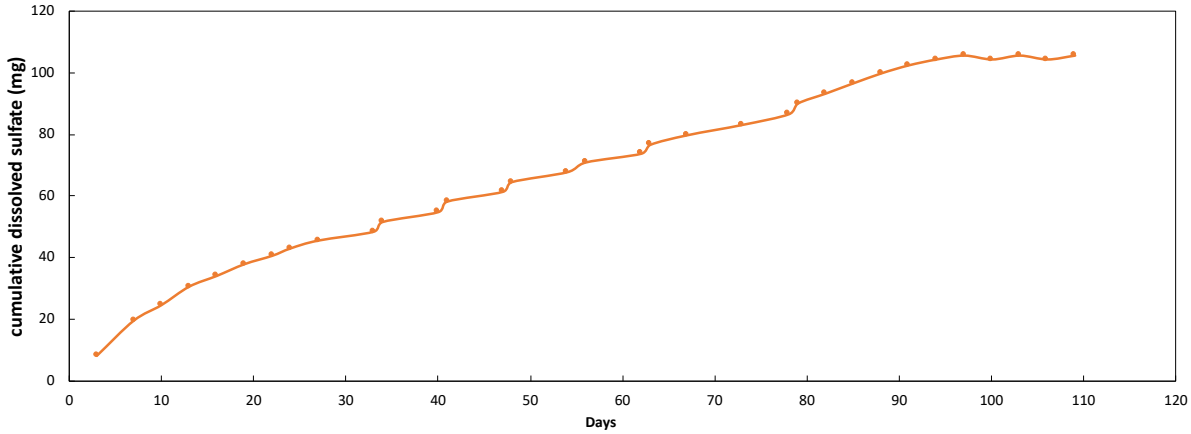

Figure 13: Cumulative release of sulfate from compacted MX-80 bentonite placed in the diffusive reactor at 1.2 g/cm^3 dry density.

3.1.2 Experimental phase 1: Saturation and gypsum dissolution

3.1.2.1 In-reactor bentonite preparation

The bentonite is first flushed with N_2/CO_2-equilibrated anoxic APW to remove the free or loosely bound O_2 only on one side of the reactor for one week.

Wyoming bentonite MX-80 contains gypsum ($CaSO_4.2H_2O$) at 0.2-0.3 mass % (Schneeberger et al. 2023). As clay is packed into the reactor, the mass of bentonite amended will depend on the dry density desired. Table 6 shows the mass of bentonite (as received at mass water content of 8.7 +/- 0.2%) needed to fill the reactor (volume of 5.095 cm^3) as a function of the desired dry density. Considering the mass of bentonite for a targeted dry density of 1.2 g/cm^3, we calculate a mass of 0.14g of gypsum in the corresponding reservoir, which is equivalent to ~80 mg of sulphate.

To start establishing opposing gradients of H_2 and sulphate (Figure 12), sulphate must be removed from the bentonite. This means that gypsum must be dissolved first. Therefore, the first phase of the experiment also involves the diffusion-controlled dissolution of gypsum. It entails pumping a sulphate- and bromide-free anoxic (equilibrated with 1.5 bar N_2/CO_2) APW past the bentonite on both sides of the reactor and measuring the sulphate concentration in the effluent (Figure 12). Thus, the clay is saturated through the recirculating flow of anoxic APW (sulphate-free) at both ends of the reactor while the effluent goes to a waste beaker. The APW is changed every week initially and every 3 days later in the experiment. The effluent sulphate concentration is monitored.

Analysis of the sulphate released from the bentonite placed in the diffusive reactor at 1.2 g/cm^3 dry density reveals that approximately 100 mg of sulphate are released from the bentonite through the slow dissolution of gypsum because of diffusion of sulphate out of the reactor. It took approximately 95 days to reach a plateau in sulphate release from bentonite. This process was much slower than expected

based on simple diffusion calculations that predicted that one week was needed. The total amount of sulphate released exceeds the expected average amount by 25%, which is reasonable considering that the 0.2-0.3 mass % gypsum content is based on an average composition.

At this stage, the bentonite is ready for the second phase, in which the electron donor and acceptor will be supplied in opposing directions.

3.1.2.2 Batch bentonite preparation

Because the in-reactor gypsum dissolution was very slow, we also attempted to dissolve gypsum from bentonite in a batch system. Bentonite was placed in oxic APW (2.4g of bentonite in 50 mL of APW) in triplicate serum bottle and placed on a horizontal shaker. Samples were collected every day and the solution exchanged with a fresh sulphate-free APW. The aqueous phase separated from the clay by centrifugation. The aqueous sulphate concentration was measured (Figure 14).

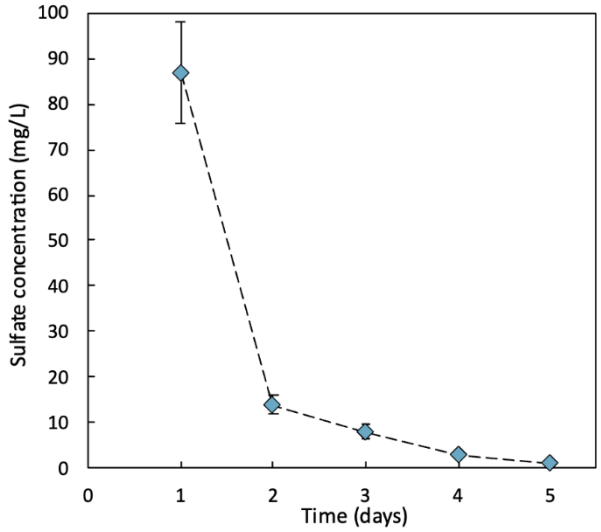

Figure 14: Sulphate concentration in equilibrium with bentonite in APW with daily changes of the solution.

In contrast to the *in-reactor* process and, as expected, the dissolution of gypsum is rapid in a batch system with sulphate being completely removed after 5 days. However, it is also important to consider whether this treatment of the bentonite results in changes in the activity of the microbial community that would introduce bias. After drying the bentonite (38º C for 24 hours), will the microbial activity remain the same as that in untreated bentonite? If the bentonite is then packed into the reactor, would the experimental results be representative of the bentonite for which sulphate is removed *in-reactor*? To test this potential bias, untreated and dried batch-treated bentonite was placed in APW (containing sulphate) with or without H_2 and the concentration of sulphate monitored. The results (Figure 15) show that a decrease in sulphate concentration is only observed in the untreated bentonite amended with H_2 (over a period of one month), but there is visual evidence for sulphide production in the treated bentonite with H_2 condition as well. Therefore, the batch treatment of bentonite negatively impacted sulphate-reduction activity. The underlying reason is unclear. We hypothesize that the oxic dissolution treatment decreased the number of viable anaerobic microorganisms.

As expected, there is evidence for gypsum dissolution in the untreated bentonite. The expected amount released (~ 100 mg/l) corresponds to ~ 1mM and it is observable that after 7 days, the concentration of sulphate in both untreated controls (with and without H_2) increases by approximately that amount.

Overall, the batch treatment for gypsum dissolution does not appear to be the optimal strategy and we will continue to use in-reactor dissolution in future experiments despite its long duration.

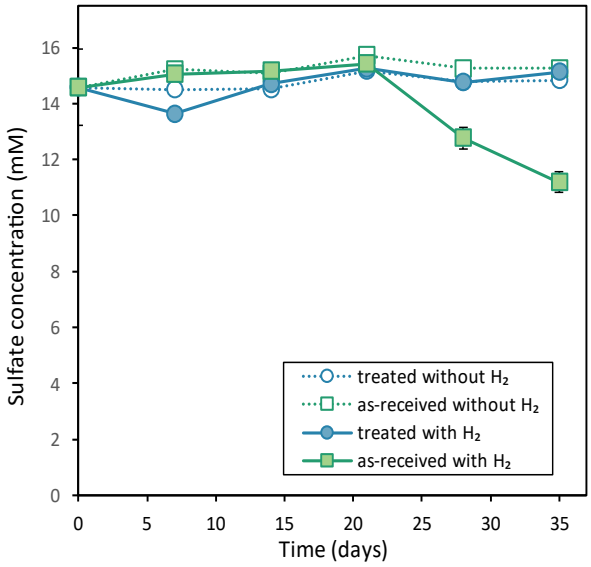

Figure 15: Sulphate concentration as a function of time in APW (with sulphate) containing either untreated bentonite with or without H_2 or batch-treated bentonite with or without H_2.

3.1.3 Experimental phase 2: H_2 and sulphate amendment to the reactor

The experiment was performed as follows: Twelve reactors were packed with bentonite MX-80, as described above. One end of the reactors was connected to a reservoir of APW that included sulphate and bromide (and under 1.5 bar of N_2/CO_2) while the other end received APW in equilibrium with 1.5 bar of H_2. For safety reasons, the experiment must be run in the fume hood. Running twelve replicate reactors at a time is the maximum that can be achieved Figure 16. Each reactor is connected to two reservoirs (one containing sulphate/bromide and the other, H_2) and to two waste containers, each collecting the waste from one of the reactor's ends.

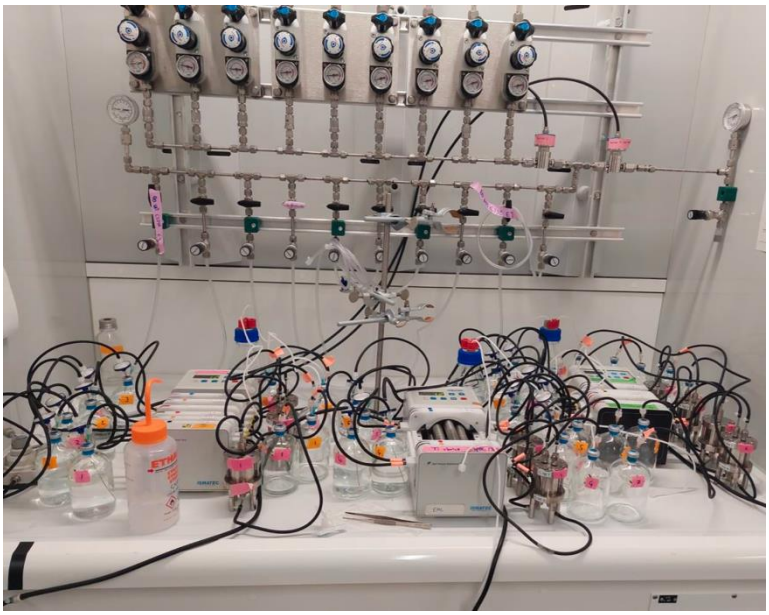

Figure 16: Experimental set-up showing the twelve reactors and the APW reservoirs during the experimental phase 2. Each reactor includes two APW reservoirs (used for either end) and two waste bottles.

The difficulty associated with this experiment is that the reservoir APW cannot be recirculated. This entails producing large volumes of anoxic APW in order to continuously run the experiment. Daily reservoir change is needed to keep the experiment running. The solution is pumped along the bentonite at either end of each reactor with a peristaltic pump at the lowest achievable flow rate of 0.1 mL/min. This set-up allows the collection of the effluent for characterization of its composition. In particular, we monitored the effluent at the end that did not receive sulfate and bromide in the hope of observing a "breakthrough". The experiment was performed for 3 weeks and three reactors were destructively sampled at time zero and after each week. Unfortunately, neither sulfate nor bromide was detected at the effluent for the three-weeks of the experiment.

The bentonite was removed from each reactor with a lever press under sterile conditions. Therefore, twelve bentonite plugs were recovered and stored in sterile petri dishes prior to DNA extraction (Figure 17).

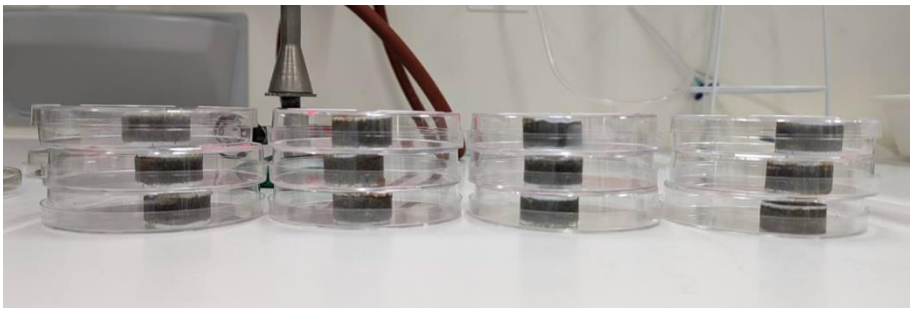

Figure 17: Twelve plugs of bentonite recovered from the twelve reactors.

3.1.4. Experimental phase 3: microbial biomass analysis

The bentonite plugs were sliced in quarters vertically and DNA extracted from one quarter. The quarters were weighed, and then transferred into sterile 50 mL Falcon tubes containing glass beads for DNA extraction.

The DNA extraction and purification was conducted based on the Qiagen DNeasy PowerMax Soil Kit protocol as previously used for DNA extractions from compacted clay used for iron corrosion (IC) experiments (Burzan et al., 2022) with several modifications:

1. Addition of 11.5 g of 2 mm-diameter glass beads to the PowerMax Bead Tubes and autoclave of the tubes. This step helped to break down compacted pieces of bentonite.

2. Addition of 3 ml of 15% hexametaphosphate solution after adding PowerBead solution and before the addition of the C1 solution from the kit. This step helps to disperse clay and liberate cells and DNA fragments.

3. Addition of 10 µl (instead of 8.4 µl) of co-precipitant LPA 5 mg/ml provided by Invitrogen Thermo Fisher (instead of GenElute; 25 mg of LPA/ml) during the purification step. This modification was necessary due to the delay in delivery of the GenElute used in the original protocol. Despite the lower concentration, the final DNA concentration did not differ from expected values when purifying DNA extracted from clays with GenElute.

4. Air-drying of the samples for 10 minutes and resuspension of the pellet by 45 µl of elution buffer C6 (instead of 125µl). A lower volume allows for higher concentration of DNA in the final product.

Quantitative PCR analyses of the bacterial 16S rRNA gene were prepared using the MYRA robotic system and conducted on a MIC qPCR Cycler (both BioMolecular Systems, Australia). Analysis was carried out in triplicate in 10 µl reactions as follows: 2.5 µl template DNA, 2.1 µl water, 0.2 µl of each primer (100mM stock) (see below) and 5 µl of 2× SensiFAST SYBR® No-ROX Kit (Meridian Bioscience,

UK). Samples were cycled (40 cycles) at 95 °C for 5 s, followed by an extension at 62 °C for 10 s and acquisition at 72 °C for 5 s. The final melting step was carried out from 72 °C to 95 °C, at a rate of 0.1 °C/s. Analysis of the results was carried out using the built-in analytical software (micPCR, BioMolecular Systems, ver. 2.12.6). In average, efficiency (0,943 – 1,003) and r^2 values (> 0,99) were determined from seven points of the serial dilutions (107–101 copies) of each target gene. Based on calibration curves, C_q values were used to calculate the gene copy numbers which were normalized against mass (ng) of the extracted DNA.

Primers for Bacteria:

338f: 5'-ACT CCT ACG GGA GGC AGC AG-3'

534r: 5'-ATT ACC GCG GCT GCT GGC A-3'

Primers used for Archaea

931f : 5' AGG AAT TGG CGG GGG AGC A 3'

M1100r: 5' BGG GTC TCG CTC GTT RCC 3'

The bacterial abundance results (Figure 18) reveal an unexpected trend. While the reference bentonite exhibits very low bacterial abundance (6.4E+03), as expected, the time zero samples, corresponding to the bentonite at the beginning of the H_2 and sulphate amendment (in opposite ends of the reactor), there is a large range of 16S rRNA copy number/g dry bentonite, with values from 5.0E+04 to 4.3E+05. Most intriguing, the values are orders of magnitude larger than those obtained for the original bentonite. Therefore, we conclude that growth occurred during phase 1 (gypsum dissolution phase). As no H_2 was being supplied at that time, another source of electrons must be present. Based on the literature (Maanoja et al., 2021), we hypothesize that the organic carbon contained within MX-80 bentonite supports microbial growth once water is provided. MX-80 has been reported to contain 2,032 mg/kg of TOC and 83 mg/kg of DOC (Maanoja et al., 2021). Therefore, at the low-density condition selected here (1.2 g/cm^3), the bentonite organic carbon is sufficient to support bacterial growth. The microbial community analysis (pending) will provide more insight into the specific microorganisms able to grow under these conditions.

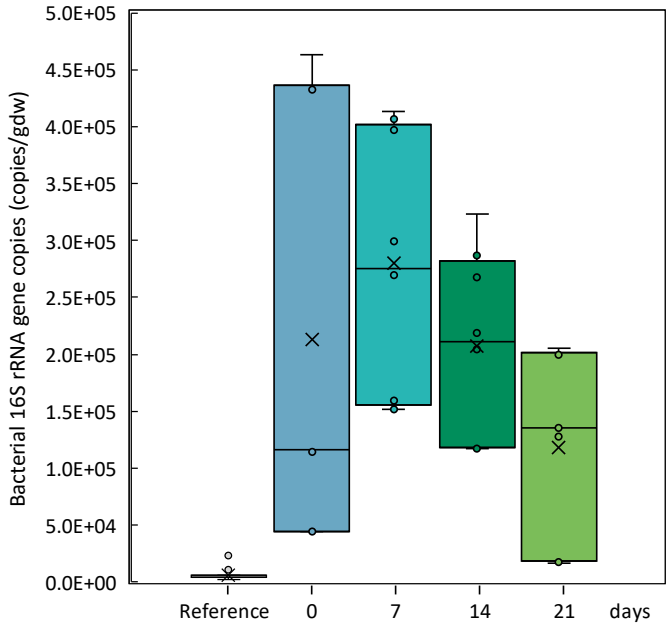

Figure 18: Bacterial abundance expressed as 16S rRNA gene copy numbers per gram of bentonite (dry weight) for the reference bentonite (as received) and the bentonite after treatment for dissolution (0 days) and subsequently after 7, 14 and 21 days. Data are presented in a box and whisker plot in which the median is indicated with a cross,

the mean with a line, each data point with a dot, the box shows the 25th to 75th percentile and the whiskers show the maximum and minimum values of the data. The bentonite had a dry density of 1.2 g/cm3.

The other surprise was the observation that subsequent time points did not show evidence of an increase in biomass but rather no statistically significant change between times 0, 7, 14, and 21 days despite the addition of H_2 as an electron donor starting at time zero. The most likely interpretation for this observation is that sulphate and H_2 have not yet diffused sufficiently to meet, and biomass no longer has an electron acceptor, therefore, there is no additional growth relative to time zero. It is also conceivable that an organic carbon source was limited but autotrophic growth could also take place as CO2 is provided.

The archaeal abundance data exhibited a similar trend (Figure 19). There was a large increase in archaeal abundance from the reference bentonite to time zero and no change in biomass subsequently.

We conclude that a much longer time is needed for biomass growth under diffusion limited conditions.

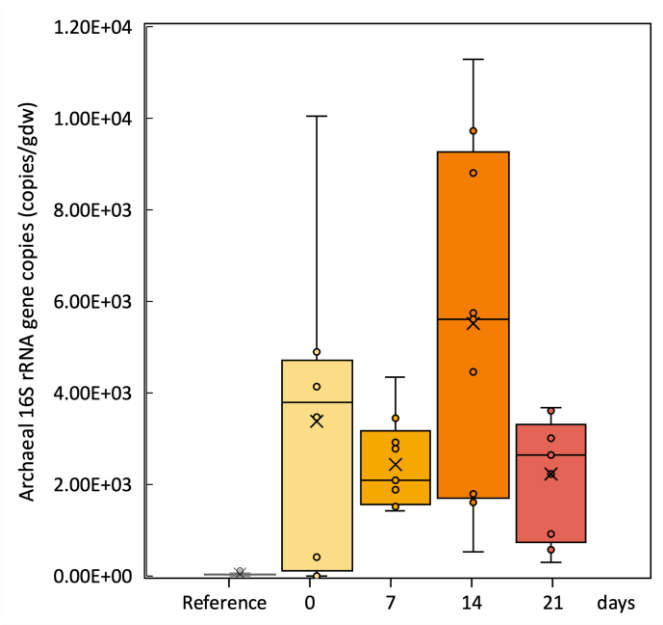

Figure 19: Archaeal abundance expressed as 16S rRNA gene copy numbers per gram of bentonite (dry weight) for the reference bentonite (as received) and the bentonite after treatment for dissolution (0 days) and subsequently after 7, 14, and 21 days. Data are presented in a box and whisker plot in which the median is indicated with a cross, the mean with a line, each data point with a dot, the box shows the 25th to 75th percentile and the whiskers show the maximum and minimum values of the data. The bentonite had a dry density of 1.2 g/cm3.

3.2 HZDR

3.2.1 Set up of diffusion reactors to study the impact of Calcigel bentonite dry density on microbial activity

Diffusion reactors were selected to study the impact of bentonite dry density on microbial activity. The design and development of the setup was already described in chapter 3.1. The focus at HZDR was to setup similar diffusion reactors in our labs and to investigate, in comparison to EPFL, the impact of Calcigel bentonite dry density on microbial activity.

Material and methods

Calcigel bentonite

The Calcigel® bentonite powders (Cal) were purchased from Clariant (Munich, Germany) and provided by Institut für Nukleare Entsorgung, Karlsruher Institut für Technologie (KIT). This bentonite is naturally occurring and mined in Bavaria, Germany. The main proportion (up to 90%) of particle size of Cal ranged from 0.5 to 90 µm, although particle size up to 150 µm was also observed (HELOS Series KF + Quixel, SYMPATEC, Clausthal-Zellerfeld, Germany). The mineral composition of Cal provided by the supplier was 60-70% montmorillonite, 6-9% quartz, 1-6% mica, 1-4% feldspar, 1-2% kaolinite, and 5-10% of others.

Design of diffusion reactor

The design of the diffusion reactors is the same as the one described by the colleagues from EPFL (see 3.1). It was decided to use the same design for a better comparability of the results.

Determination of water and sulphate content of raw Calcigel bentonite

The water content (w/w%) of raw Calcigel bentonites was calculated by mass loss on drying. The measured water content was applied for dry density calculation. Triplicates were conducted with the same batch of bentonites. For determination of the sulphate content, 1g of bentonite was saturated with 10.8 ml of artificial porewater (APW) containing no sulphate in 50 ml centrifuge tube and placed on an overhead shaker for 24 h. Supernatant was collected via centrifugation at 12,000 g before sulphate quantification via ion chromatography (IC). It was repeated 4 times, and the sulphate content was calculated based on the volume of bentonite and APW.

Diffusion reactors setup with peristaltic pump

For saturation and equilibration phase, 180 ml of anoxic APW without sulphate was prepared in 250 ml narrow-neck serum bottle in the glovebox workstation. The headspace was pure N_2 gas at 0.4 bar. Calcigel bentonite with selected dry density (1.2 g/cm^3) was compacted into the reactor and the entire system was flushed with N_2 gas to avoid oxygen. A peristaltic EVA-pump (Eppendorf, Germany) with speed parameter at 1 (~0.103 ml/min) was then used to connect the reservoir of APW to the topside of the reactor. The outflow of topside was then circulated back to the reservoir. Both outflow from the bottom side of reactor was attached to an anoxic narrow-neck serum bottle with N_2 gas also at 0.4 bar (Figure 20). The outflow was then collected for sulphate quantification via High-Pressure Ion Chromatography (HPIC, Dionex Integrion, Thermo Fisher Scientific, USA).

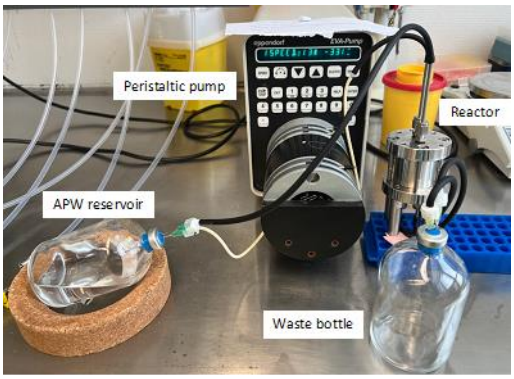

Figure 20: Trial reactor setup for saturation and equilibration phase. Both anoxic APW reservoir and waste bottle were pressured with N_2 gas at 0.4 bar.

Results and Discussion

Trial run for saturation and equilibration

The Calcigel bentonite has a water content of 4.96%±0.28 and at least 0.056 mg of sulphate per g bentonite. We expected that time needed for saturation and equilibration for Calcigel would be faster than MX-80 bentonites (see 3.1.) due to the lower content of sulphate. After 48 hours, we observed that Calcigel bentonite appeared to be saturated (Figure 21).

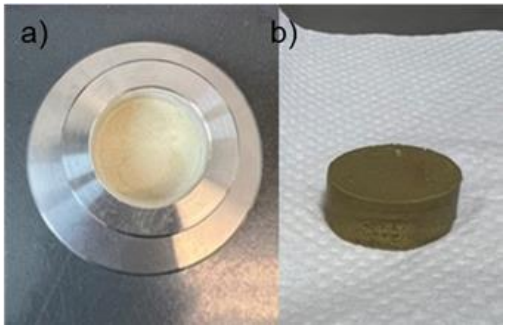

Figure 21: The compacted Calcigel bentonite (a) and saturated bentonite after 48 hours (b).

Then 6.5 ml of outflow was collected for sulphate quantification. However, a flow rate slower than 0.1 ml/min was also observed and this might result in pressure accumulation in the entire system. To adjust this, we set the speed parameter to 2 to maintain the flow rate at 0.1 ml/min. The relationship between detected flow rate and different speed parameter under the pressure is listed in Table 7.

Table 7: The detected flow rate with different speed parameters of the peristaltic pump under different pressures. *parameter set for ~0.1ml/min.

Speed setup	System pressure	Flow rate (ml/min.)
Speed 1	Open atmosphere	0.103
Speed 1	0.4 bar	0.03325
Speed 2*	0.4 bar	0.098
Speed 3	0.4 bar	0.165

The pressure may continuously increase during the equilibration phase due to the closed system. To overcome this, we adapted the setup from EPFL in which the pressure of waste bottle indirectly balanced with atmosphere but devoid of oxygen (Figure 22). The entire setup remained functioning but the actual flow rate with speed 1 parameter under this new condition may need to be measured. We are currently collecting outflow weekly to estimate the time needed for equilibrium (until the sulphate is under detection limit by IC). Other compacted bentonites with different dry densities (1.4 and 1.6 g/cm^3) will also be applied for the trial equilibration. In addition, an experimental trial run (supplying exogenous H_2 gas) with a dry density of 1.2 g/cm^3 will be conducted.

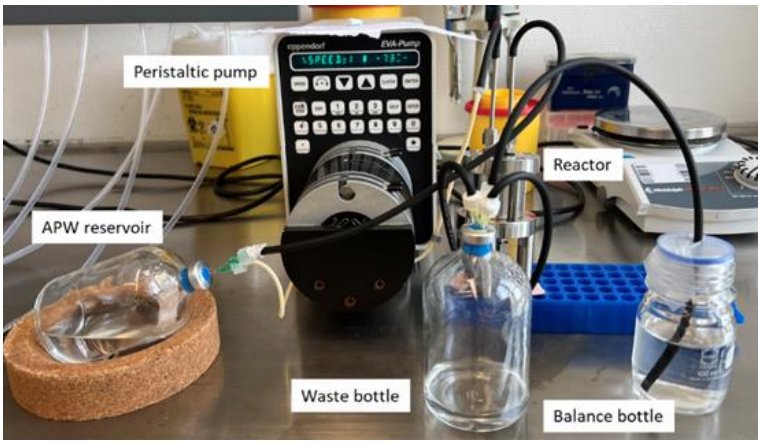

Figure 22: The final reactor setup for trial saturation and equilibration phase. The anoxic artificial Opalinus Clay porewater (APW) reservoir was pressured with N_2 gas at 1.5 bar, and the waste bottle was flushed with N_2 gas before closure.

3.2.2 Batch experiments with Calcigel bentonite to study metal corrosion and activity of sulfate-reducing bacteria

It was planned to study the metal corrosion in the compacted Calcigel bentonite. However, to date, it remains unclear whether Calcigel bentonite contains any sulphate-reducing bacteria and their potential to induce metal corrosion. While waiting for the construction of the diffusion reactors due to problems with material procurement (effects of Corona pandemic), we studied the metal corrosion in Calcigel bentonite using batch experiments with hydrogen as electron donor. The selected conditions are similar to the planned diffusion reactor experiments but without compaction.

Materials and methods

Metal coupons preparation

The metallic coupons (cast iron GGG40 in size of 1x1x0.5 cm) were subjected to a preparatory polishing process using fine-grit sandpaper. For coupons subjected to Scanning Electron Microscopy with Energy Dispersive X-ray Spectroscopy (SEM-EDX), a sputtering process with a gold layer was applied before the cleaning. Subsequently, they were cleaned in an ultrasonic bath using acetone as following. Firstly, five beakers (100 ml) were filled with 100 ml of acetone, and in each beaker, 10 coupons were immersed. Secondly, these beakers were then placed in an ultrasonic bath containing deionized (DI) water. The sonification of these coupons was performed for 15 minutes.

The cleaned coupons were weighed using a precision balance (Quantos QB5/QD206, Mettler Toledo) to obtain the mass with high accuracy. Sterilization of coupons was achieved using isopropanol (99.5%) under laminar flow conditions (HERAsafe KS15, ThermoScientific, USA) and placed into sterile 24-well plates before transferring into an anaerobic glovebox workstation (MB200MOD, MBraun, Germany).

Calcigel bentonite

The Calcigel® bentonite powders (Cal) were also used for the microcosm set ups (see details under 3.2.1.).

Preparation of anoxic artificial Opalinus clay porewater

The artificial Opalinus clay porewater (APW) solution, (212 mM NaCl, 26 mM $CaCl_2$, 14 mM Na_2SO_4, 1.6 mM KCl, 17 mM $MgCl_2$, 0.51 mM $SrCl_2$, and 0.47 mM $NaHCO_3$) (Pearson, 1998) was prepared anaerobically as previously described (Matschiavelli et al., 2019). After the de-gassing by N_2, the solution was immediately transferred into the glovebox workstation. After autoclaving, 30 ml of APW solution was distributed into a 100 ml narrow-neck serum bottle for microcosm setup.

Microcosm setup

In total, five conditions of anaerobic microcosms containing 30 ml of APW were prepared in the glovebox. In general, 15 g of raw Cal were added into each autoclaved serum bottle. Two cast iron coupons (one with gold sputtering and one without) were placed into the bottle. The gas phase was defined by purging a mixture of N_2:CO_2:H_2/80:10:10 at 0.5 bar. The condition of this microcosm was denoted HCalC (Hydrogen+Calcigel+Coupons). For microcosms with same component but without hydrogen gas, the gas phase was defined by a mixture of N_2:CO_2/90:10 at 0.5 bar and this condition was denoted CalC (Calcigel+Coupons). On the other hand, microcosms containing hydrogen gas and Calcigel bentonite but no metal coupons were denoted HCal (Hydrogen+Calcigel). Two conditions of microcosms with sterilized Calcigel bentonite were also set up, these conditions were denoted SC (Sterilized Calcigel+Coupons) and HSC (Hydrogen+Sterilized Calcigel+Coupons). The sterilization of the bentonites was achieved by two times of autoclaving in serum bottles with APW before addition of metal coupons or hydrogen gas. All the conditions of microcosms were performed in triplicates at 37°C in the dark for one day, 3, 6 and 9 months.

Determination of the H_2 gas via gas chromatography (GC)

To measure H_2 gas changes, 50 µl gas samples were extracted with a syringe and needle from headspace of each microcosm and injected into a gas chromatograph for analysis. The GC conditions included a temperature of 200 °C, pressure at 126 kPa, flow rate of 136.2 ml/min, and a split ratio of 1:50. An Agilent CP7551 PoraPLOT Q column was used for gas separation, operated under a specific temperature program. A Helium Ionization Detector, set at 250 °C, was used to quantify the gas concentration.

Geochemical analyses of APW from microcosms

The geochemistry of APW was analysed for sulphate by High-Pressure Ion Chromatography (HPIC, Dionex Integrion, Thermo Fisher Scientific, USA) and for total organic carbon (TOC) and total inorganic carbon (TIC) by Multi N/C 2100S (Analytik Jena, Germany). Additional volume of water samples was subjected to Inductively Coupled Plasma Mass Spectrometry (ICP-MS, ELAN 9000, PerkinElmer, Germany)) for quantifying cations (Fe, Ca, Mg, Na and K for example).

Microbial diversity analysis

The DNA of raw Calcigel bentonites (n=2), CalC microcosms (n=2) at 3 months and 9 months (n=1), HCalC microcosms at 3 months (n=2), 6 months (n=2) and 9 months (n=2) was extracted using PowerMax Soil Kit (QIAGEN, Germany) as previously described (Engel et al., 2019). Only slight modifications of the protocol were done: the elution volume for the kit was 2.5 ml and the final concentration of linear polyacrylamide (ThermoScientific, USA) for precipitation step was 10 µg/ml. The DNA was quantified using Qubit 1X dsDNA HS Assay kit (Thermo Scientific), and subjected to PCR to amplify the V4 region of 16S rRNA genes using modified bacterial V4 primer set (Walters et al., 2016). Blank extraction of PowerMax kit was also conducted as negative control. Microbial diversity was analysed using 16S amplicon sequencing on a next-generation sequencer, MiSeq platform, at Eurofins Genomics (Germany), DADA2 (Callahan et al., 2016) was applied to generate amplicon sequence variants (ASVs), and assignment of ASVs to bacterial taxonomy was based on Silva SSU database (Quast et al., 2013). The contamination ASVs from blank extraction of the kit were removed using Decontam with “prevalence” parameter (Davis et al., 2018). The true microbial diversity data was normalized and visualized using phyloseq (McMurdie & Holmes, 2013). The microbial diversity analysis of bentonites from different conditions and replicates is still in process.

SEM-EDX for surface of metal coupons

SEM characterization of metal coupon surfaces was performed using a Carl Zeiss AG - EVO® 50 microscope, and EDS analysis was employed using a Bruker QUANTAX system, with an acceleration voltage of 15.0 kV. The samples, consisting of GGG40 spheroidal graphite cast iron were rinsed with MilliQ water to remove bentonite while preserving surface depositions and potential microorganisms.

Coupons were transferred from an anaerobic glovebox to the SEM chamber in an airtight container, minimizing oxygen exposure. They were mounted on stubs that allowed fixation from four sides without acrylic glue and scanned uncoated.

Determination of the corrosion rate

The procedures for cleaning and determining the corrosion rate by measuring weight loss in our study were conducted in accordance with the guidelines specified in the ASTM G1-03(2017)e1 International document "Standard Guide for Conducting Corrosion Tests in Field Applications" (2017).

Results and Discussion

Evolution of sulphate concentration and hydrogen gas content in microcosms

The sulphate concentration in APW of the microcosms under each condition on day 1 was approximate 13 mM. A minor decrease of sulphate concentration was observed in microcosms under conditions of CalC, SC, HSC and HCal at all time points (down to ~10 mM at 9 months). On the other hand, in HCalC microcosms the sulphate concentration was 13.05±0.18 mM on day 1 but decreased to 8.18 ±0.28 mM and 6.47±0.16 mM at 6 and 9 months, respectively (Figure 23). Other geochemical data of APW, including Na, Mg, Al, Si, K, Ca, Fe, Sr concentrations, TOC and TIC were also quantified (data not shown). No greater changes were observed for these values.

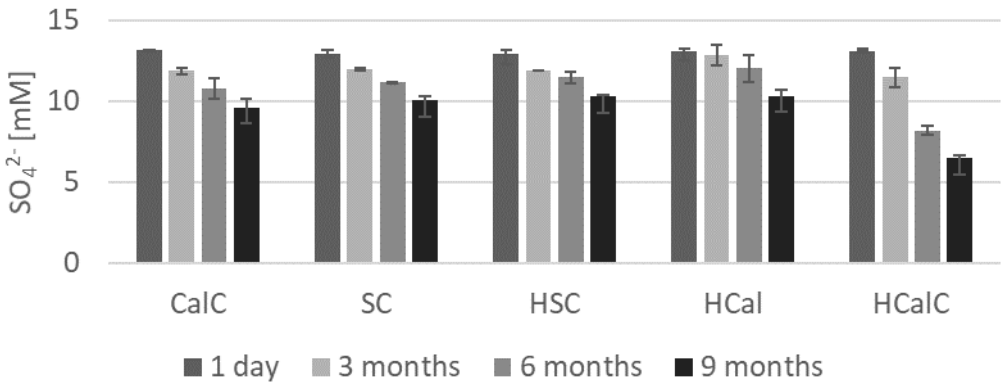

Figure 23: The changes of sulphate concentration in microcosms under five different conditions. CalC: Calcigel bentonite + metal coupons; SC: sterilized Calcigel bentonite + metal coupons; HSC: hydrogen gas + sterilized Calcigel bentonite + metal coupons; HCal: hydrogen gas + Calcigel bentonite; HCalC: hydrogen gas + Calcigel bentonite + cast iron coupons.

The GC analysis of hydrogen content in the gas phase showed variations in each condition of microcosms (Figure 24). In HCal microcosms, the hydrogen gas content decreased from 3.16±0.16 mM at day 1 to 0.66±0.10 mM at 6 months. However, in microcosms containing cast iron coupons an increase of hydrogen gas content was observed. The hydrogen gas content in HCal and SC microcosms (without exogenous hydrogen gas) increased up to 6.13±3.19 mg and 13.63±1.18 mg at 9 months, respectively. In both HSC and HCalC microcosms, the initial gas content was ~3mg on day 1 but largely increased up to 19.41±0.88 mg and 15.91±0.53 mg at 9 months, respectively. It is worth mentioning that in microcosm with sterilized bentonites (SC and HSC conditions), the increase of hydrogen gas was greater than that in microcosms with raw bentonites (CalC and HCalC conditions) (Figure 24). This can be an indication for microbial consumption of hydrogen in combination of reduction of sulphate in the HCalC samples.

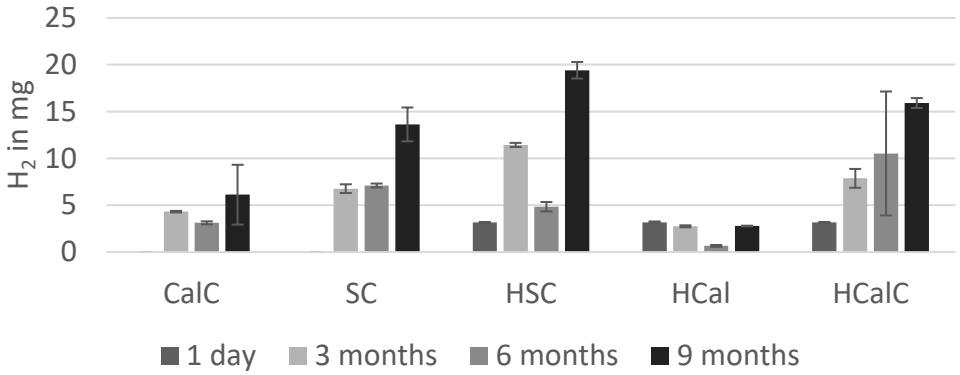

Figure 24: The changes in the hydrogen content of gas phase in microcosms under five different conditions. CalC: Calcigel bentonite + metal coupons; SC: sterilized Calcigel bentonite + metal coupons; HSC: hydrogen gas + sterilized Calcigel bentonite + metal coupons; HCal: hydrogen gas + Calcigel bentonite; HCalC: hydrogen gas + Calcigel bentonite + metal coupons.

Microbial diversity in bentonites from microcosms

The microbial community structure of raw Calcigel bentonites were highly diverse, comprising 41 phyla with Acidobacteria, Actinobacteria, Chloroflexi, Firmicutes, Methylomirabilota, and Proteobacteria as majority (Figure 25). Notably their relative abundance varied among the replicates, suggesting that the microbial biomass might not be homogenous in raw Calcigel bentonite.

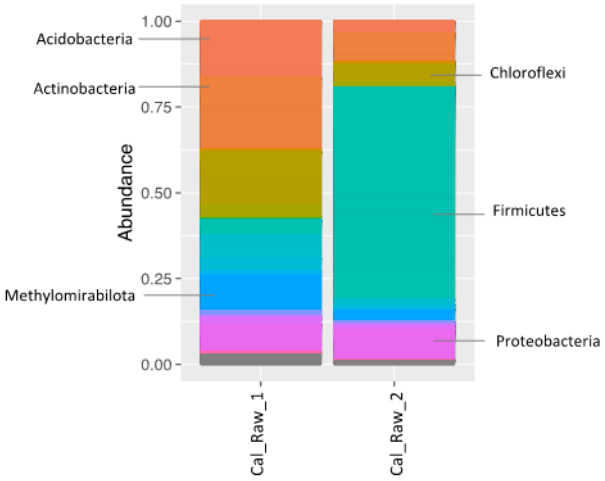

Figure 25: The microbial diversity in two biological replicates of raw Calcigel bentonite

When comparing the microbial diversity in different microcosms, we observed an enrichment of certain bacterial classes of Firmicutes in bentonites from CalC and HCal microcosms (Figure 26). At 3 months, Bacilli were the dominant taxa in CalC microcosms, whereas Desulfotomaculia was largely enriched (relative abundance up to 91.7%) at 9 months. Similar observation was made in HCalC microcosms where Desulfotomaculia dominated the bentonite communities at 3 months (except for sample Cal_3M_1) and 6 months. However, the abundance of Desulfotomaculia was relatively low in HCalC microcosms at 9 months. Notably, *Desulfotomaculum* was the only enriched genus of *Desulfotomaculia* in these microcosms. The enrichment of *Desulfotomaculum* by H_2 gas was also observed in borehole water of Opalinus clay rock (Bagnoud et al., 2016). These microorganisms are able to use H_2 gas as electron donor and sulfate as electron acceptor (Aüllo et al., 2013).

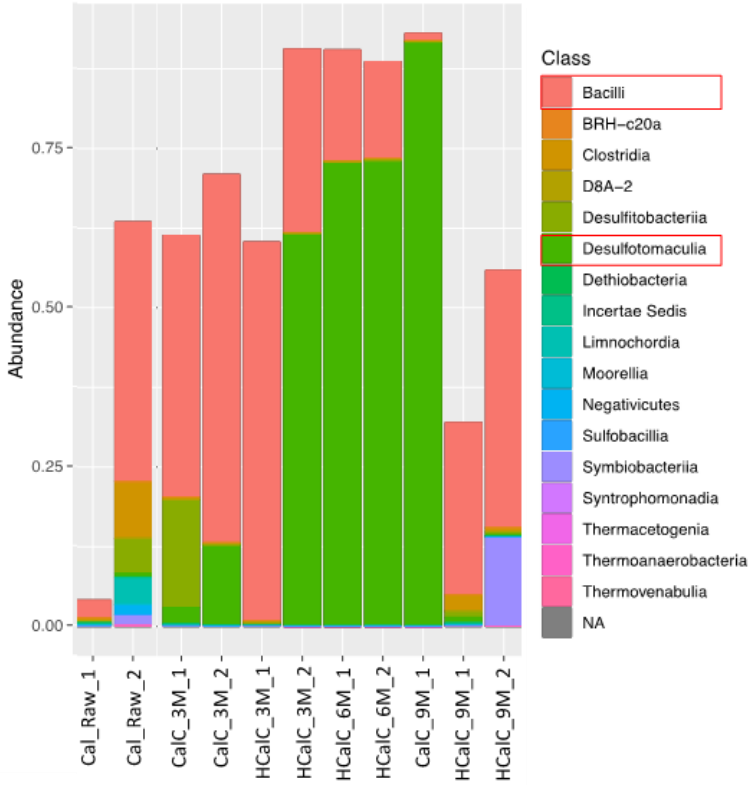

Figure 26: Changes at class level of Firmicutes in raw bentonite (Cal_Raw), bentonite from HCal (hydrogen gas + Calcigel bentonite) and HCalC (hydrogen + Calcigel bentonite + metal coupons) microcosms. Red blocks highlight the dominant taxa. M: months.

Surface analysis of the metal coupons via SEM-EDX

The surface of the coupons incubated in different bentonite slurry microcosm conditions for different periods were analysed with SEM coupled with EDX to get some information about the formation of secondary phases and the corrosion of the surface. The results from the coupons of HCalC (hydrogen + Calcigel bentonite + cast iron coupons) are shown because in these microcosms the highest decrease in sulfate concentration was observed (Figure 23). In addition, an increase in hydrogen gas content was observed but not as strong as in the microcosms with sterilized bentonite.

In this analysis, cast iron coupons were subjected to incubation with hydrogen and Calcigel bentonite, leading to observable variations in surface morphology attributed to corrosion, as demonstrated by the SEM micrographs in Figure 27. Intriguingly, coupons incubated for three months exhibited more pronounced morphological alterationsindicative of corrosion, surpassing those observed in those incubated for six months. The corrosion layer on the six-month incubated coupons is notably enriched with calcium. The augmented presence of this calcium-containing layer implies a potential protective or stabilizing effect over the course of the incubation. Further examination of SEM micrographs of coupons incubated for nine months revealed a trend in which the extent of corrosion-induced morphological surfaces changes either matches or in certain cases exceeded the three-month incubation period, as shown in Fig. 27.

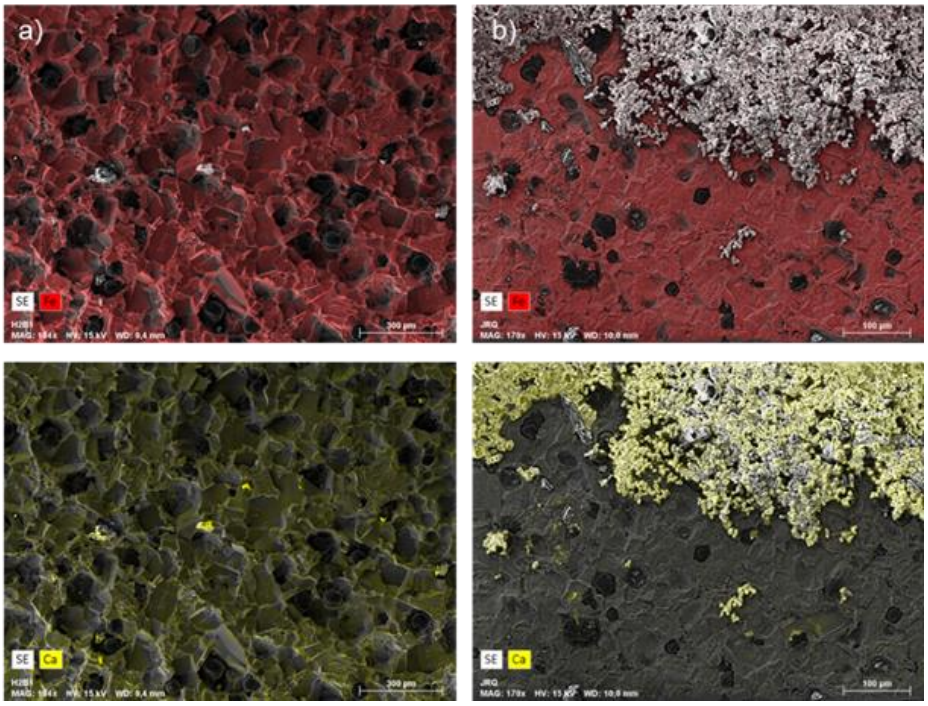

Figure 27: Scanning electron microscopic images from the surface of cast iron coupons incubated for a) 3 and b) 6 months in HCalC (hydrogen + Calcigel bentonite + metal coupons) microcosms. On the top is showing the EDX mapping of iron (Fe) and below of calcium (Ca).

Further adding to the complexity of the findings, a notable difference was observed when comparing the coupons incubated with hydrogen and non-sterilized Calcigel bentonite (HCalC) for 9 months with those incubated with sterilized Calcigel (HSC) or incubated with only in APW with hydrogen in the atmosphere (HC) for nine months (Figure 27). The SEM micrographs clearly show that the surface of the HSC-incubated coupon appears more damaged.

Intriguingly, the calcium-containing corrosion layer, which seemed to play a protective role in the HCalC samples, especially noticeable in the six-month incubation period, is only minimally present on the surface of the HSC-incubated coupon. This minimal presence is akin to what was observed in the coupons incubated for three and nine months with non-sterilized Calcigel.

In stark contrast, SEM micrographs of the nine-month incubated coupons, which were exposed to hydrogen and artificial porewater (APW) without Calcigel addition (HC), reveal a distinctly different calcium-rich corrosion layer (Figure 28). Despite the visual differences, this layer also appears to possess similar protective properties. Underneath this layer, the surfaces remain largely intact and demonstrate minimal damage, a stark contrast to the surfaces of coupons exposed to both hydrogen and Calcigel. This disparity strongly suggests that Calcigel's presence in the incubation environment significantly influences the corrosion process and, consequently, the structural integrity of the cast iron coupons.

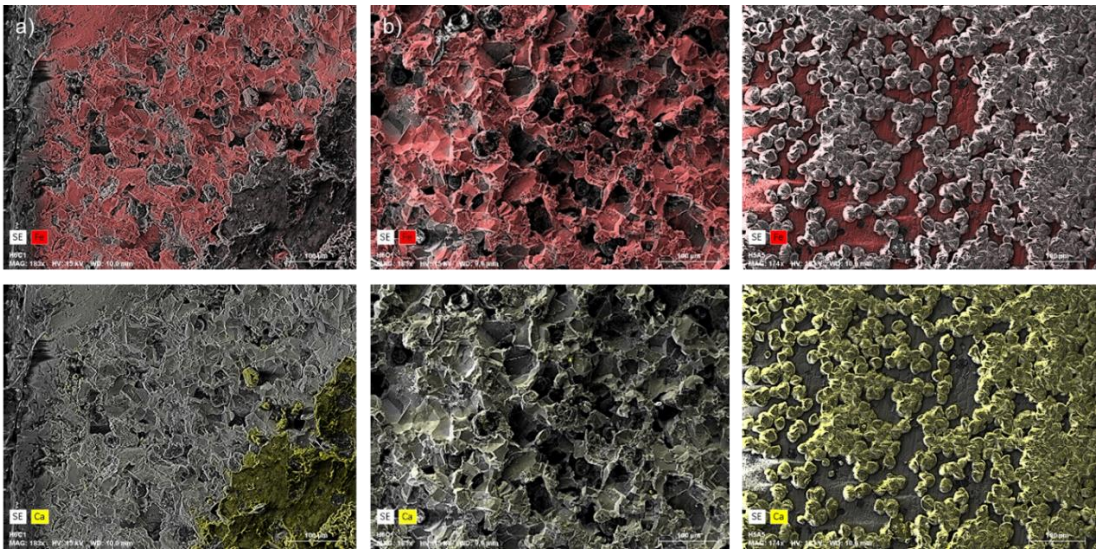

Figure 28: Scanning electron microscopic images from the surface of cast iron coupons incubated for 9 months in a) HCalC (hydrogen + Calcigel bentonite + metal coupons), b) HSC (hydrogen + sterilized Calcigel + metal coupons) and c) HC (hydrogen + metal coupons) microcosms. On the top is showing the EDX mapping of iron (Fe) and below of calcium (Ca).

EDX analysis conducted on the surface layers of HC (Figure 29) coupons revealed the presence of iron, calcium, oxygen, and carbon. These elemental compositions suggest that the corrosion layer is likely a composite matrix of calcium and iron carbonates. This finding is significant as it indicates a complex chemical interaction at the surface, influenced by the incubation conditions and these secondary phases were already observed by the corrosion of carbon steel in CO_2-containing environments (Metamoros-Veloza et al., 2020). Furthermore, the EDX analysis of HCalC coupons (Figure 29) highlighted trace amounts of sulphur, predominantly localized in regions where the calcium-containing corrosion layer is present. The detection of sulphur, particularly in these specific areas, raises the possibility of sulphide formations. This observation is of particular interest as it indicates the activity of sulphate-reducing bacteria (Tamisier et al., 2023) that were detected via microbial diversity analysis in this bentonite sample (see above). Their presence could be a contributing factor to the distinct corrosion patterns observed on these coupons.

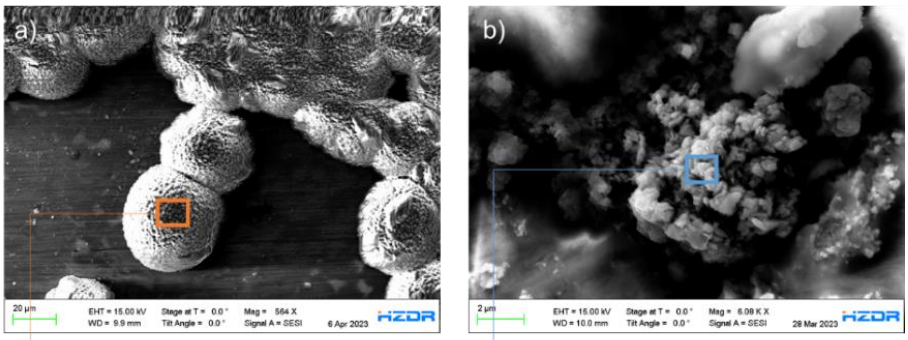

Element	Mass Norm. [%]
Carbon	9,31518932
Oxygen	**63,1341273**
Calcium	3,64375867
Iron	**23,9069247**

Element	Mass Norm. [%]
Carbon	6.488998
Oxygen	11.15734
Fluorine	4.708624
Aluminium	0.281647
Silicon	0.143848
Sulfur	**21.00347**
Calcium	1.136645
Iron	**55.07943**

Figure 29: Scanning electron microscopic images from the surfaces of cast iron coupons incubated for 6 months in a) HC (hydrogen + metal coupons) and in b) HCalC (hydrogen + Calcigel bentonite + metal coupons) microcosms. On the top is showing the iron mapping and below the Ca mapping. The colored rectangle marked the area that was analysed via EDX. The corresponding elemental composition of marked area is given in table below.

Corrosion rate

The corrosion rate of the coupons incubated under different conditions in microcosms for different incubation times were determined (Figure 30). Only slight changes in the corrosion rate were observed at different incubations times. The lowest corrosion rates were determined when the coupons were incubated with Calcigel bentonite and APW (CalC) or hydrogen gas in the atmosphere and APW (HC). The corrosion rate of the coupons incubated with sterilized Calcigel bentonite and APW (SC) was slightly higher (4.33 to 4.5 µm/year) than the ones in CalC and HC. The highest corrosion rates of the coupons showed the incubations with hydrogen in the atmosphere and sterilized Calcigel bentonite or Calcigel bentonite (HSC and HCalC). The corrosion rates of different carbon steel materials that incubated in compacted MX-80 bentonite during the *in situ* corrosion experiment (IC-A) in the Mont Terri Underground Research Laboratory in Switzerland was mostly below 3 µm per year (Smart et al., 2021).

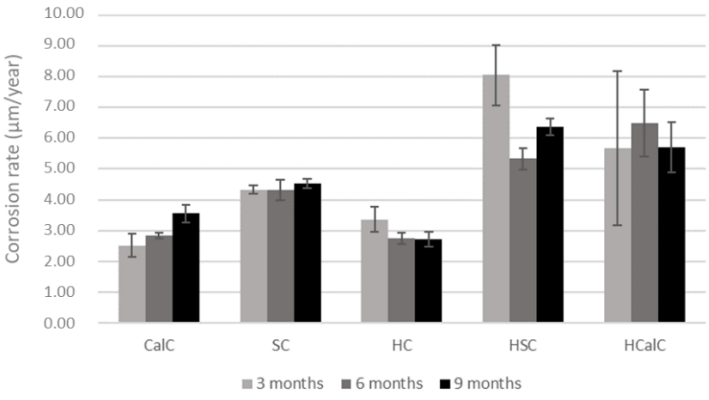

Figure 30: Corrosion rates of coupons incubated in microcosms under five different conditions. CalC: Calcigel bentonite + cast iron coupons; SC: sterilized Calcigel bentonite + cast iron coupons; HC: hydrogen gas + cast iron coupons, HSC: hydrogen gas + sterilized Calcigel bentonite + cast iron coupons; HCalC: hydrogen gas + Calcigel bentonite + cast iron coupons.

3.3 SCK CEN

3.3.1 DNA extraction in bentonite: a comprehensive inter-laboratory investigation

A known challenge of clay-rich samples is that they hamper the efficiency of several standard cultivation-independent methods. Clay particles are known to tightly adsorb organic and inorganic phosphorous compounds (Cai *et al.* 2007), significantly hindering the efficiency of DNA extraction (Frostegård *et al.* 1999). Although a few DNA extraction methods have been published for clay, they have either been validated with spiking of a single strain or not validated at all (Chi Fru and Athar 2008, Engel *et al.* 2019, Povedano-Priego *et al.* 2021). Validation using a mock community is essential, as applying different DNA extraction methods to clay samples has resulted in significant variation in the outcomes of 16S rRNA amplicon sequencing (Mijnendonckx *et al.* 2021). Thus, a more standardized research methodology is needed to study microbial communities in low biomass, clay-rich environments. This is especially important if cross-comparison of the results obtained through 16S rRNA amplicon sequencing is needed. Therefore, within the ConCorD project, we compared two distinct DNA extraction methods (Engel *et al.* 2019, Povedano-Priego *et al.* 2021) that have shown suitability for clay samples (Mijnendonckx *et al.* 2021).

Materials and Methods

Experimental setup

We used two commercial microbial community standards consisting of DNA or intact cells of three Gram-negative bacteria, five Gram-positive bacteria and two yeast species with varying size and cell wall recalcitrance (ZymoBIOMICS Mock Community standards, Zymo Research Corporation, Irvine, USA). Mock 1 contains a total cell concentration of ca. 1.4 x 10^{10} cells/ml and a linear distribution of each of the species, while Mock 2 contains ca. 1.5 x 10^{9} cells/ml with a logarithmic distribution of the different strains. Two grams of sterile MX-80 bentonite (sterilized by gamma irradiation with a total dose of 50 kGy) was supplemented with 12.5 ml Phosphate-buffered saline (PBS), and either 75 µl of Mock 1 or Mock 2 or nothing (control). All experiments were performed in triplicate. Samples were thoroughly mixed by vortexing and incubated for 3 days at 4°C to enable water absorption into and cell interaction with bentonite. After the incubation step, samples were centrifuged at 11,000 rpm for 10 min. The supernatant was discarded and the pellet used for DNA extraction. To elucidate the possible bias introduced by the presence of bentonite on DNA recovery, extractions were also performed on 75 µl of both mock communities.

TUL (Lab 1) and SCK CEN (Lab 3) used the method described by Engel *et al.* (2019) with some modifications as described in detail in the manuscript (currently in revision). This method is a kit-based approach involving a combination of sodium dodecyl sulfate (SDS)-based and mechanical lysis, followed by DNA binding and washing on a silica column. Important to note is that a few steps differed among both labs. SCK CEN included an additional vortexing step of 10 min after incubation in the water bath, they used larger volumes for elution and the purification method of both labs was different.

UGR (Lab 2) and SCK CEN used the method of Povedano-Priego *et al.* (2021) that includes pre-treatment with phosphate buffer and glass beads, chemical and enzymatic lysis using a cocktail containing polyvinylpyrrolidone (PVP), SDS, proteinase K, lysozyme and mechanical/thermal shocks, followed by DNA precipitation with agents including phenol and chloroform. Also here, some differences were observed between both labs with the most important being the washing steps after the DNA extraction with phenol:chloroform:isoamyl alcohol (25:24:1 v/v) and further purification and concentration of the DNA.

16S rRNA amplicon sequencing

All DNA samples were sent to SCK CEN where all the PCRs were performed, to minimize variability that could be introduced by that step. The V3-V4 region of the 16S rDNA was amplified with primers 341F (5'-CCTACGGGNGGCWGCAG-3') and 785R (5'-GGACTACHVGGGTATCTAATCC-3') using the Phusion High-Fidelity Polymerase (Thermofisher Scientific, Belgium). Primers contained an Illumina adapter overhang sequence: 5'-TCGTCGGCAGCGTCAGATGTGTATAAGAGACAG-3' for the forward primer and 5'-GTCTCGTGGGCTCGGAGATGTGTATAAGAGACAG-3' for the reverse primer. PCR conditions were as follows: 1 min at 98°C followed by 30 cycles of 10 s at 98°C, 30 s at 62°C and 1 min at 72°C followed by a final extension of 10 min at 72°C. Five ng was used as DNA template in all samples except when the concentration was too low, where 5 µl was used. To examine possible PCR bias, mock community standards consisting of DNA instead of intact cells were included. PCR results were evaluated via gel electrophoresis. PCR products from samples that were positive were purified with the Wizard® SV Gel and PCR Clean-Up System (Promega, The Netherlands) according to the manufacturers' protocol. Samples were sequenced on the Illumina MiSeq platform according to the manufacturer guidelines at BaseClear B.V (the Netherlands).

Bioinformatics and statistical analyses

First, primers were removed using cutadapt (Martin 2011). Subsequently, raw reads were processed according to the DADA2 pipeline with recommended settings (Callahan *et al.* 2016). Briefly, reads with ambiguous, poor-quality bases and more than two expected errors were discarded. The paired reads were merged, chimeras were identified and removed. Only amplicon sequence variants (ASV) with more than two reads were retained. Taxonomy was assigned to the ASVs using the naive Bayesian classifier

method implemented in DADA2 with the Silva taxonomic training dataset (version 132) as a reference (Callahan 2018).

Potential contaminant ASVs were identified through the "Decontam" (v.1.6.0) R package (Davis *et al.* 2018). Specifically, the "combined" method was used, where frequency and prevalence probabilities are combined with Fisher's method and used to identify contaminants. With a probability threshold of 0.5 we identified contaminant ASVs, and excluded them from subsequent analyses (ten ASVs).

The 16S rRNA amplicon sequencing data were further analysed in R version 4.3.0 with the R package phyloseq (McMurdie and Holmes 2013). Subsampling was performed based on the lowest number of reads obtained over the different samples amended with a mock community, i.e., a coverage of 8,403 reads. Rarefaction curves indicate that this level of subsampling adequately represented the bacterial diversity in the samples. The package chkMocks was used to compare the composition obtained in each condition with the theoretically expected composition (Sudarshan *et al.* 2023). The β-diversity was calculated by non-metric multidimensional scaling (NMDS) with Bray-Curtis distances with the command "ordinate." Afterwards, a distance matrix of these data was calculated with the command "distance." This distance matrix was used to perform a permutation test for homogeneity of multivariate dispersions using the command "betadisper" in the package vegan (Oksanen *et al.* 2020). Permutational Multivariate Analysis of Variance (PERMANOVA) using the "adonis" at 999 permutations and α = 0.05 were performed to test if there was a difference between the DNA extraction methods and if the bentonite had an effect on the outcome. Pairwise multilevel comparison was performed with the R package pairwiseAdonis with FDR (False Discovery Rate) correction to the *p*-values.

Results and Discussion

The most important differences between the methods and the labs was quantity of the total DNA that could be extracted from the samples and the purity of the DNA, which either facilitated or hindered PCR amplification.

Total DNA obtained

Each laboratory successfully obtained quantifiable DNA concentrations from all samples spiked with a mock community, except for Lab 1 when analyzing bentonite samples spiked with mock 2. However, results show that even in the absence of bentonite, DNA yields were lower than half of the expected amount. In the presence of bentonite, this discrepancy increased at least sevenfold (Figure 31). On the one hand, large differences were observed between the two laboratories that employed the kit-based extraction method for both conditions, with and without bentonite. Lab 3 obtained ten times more DNA from mock 1, and in the presence of bentonite and also for all samples spiked with mock 2, an 80-fold difference was observed in DNA extracted. The slight differences in the followed DNA extraction procedure could result in the observed variability. On the other hand, these differences were not observed when using the phenol-chloroform based method for mock-only sample extractions, but similarly high differences were observed in spiked bentonite samples where lab 3 achieved a notably higher total DNA yield than lab 2 (ca. 18 and 5 times more for samples spiked with mock 1 and mock 2, respectively). Notably, in lab 3 the presence of bentonite did not adversely affect the efficiency of DNA extraction when using the phenol-chloroform extraction method, but large variation among the replicates was observed (Figure 31). It is worth mentioning that the kit-based extraction method failed to yield any measurable amount of DNA from the sterile unspiked bentonite samples. Conversely, the phenol-chloroform-based method successfully extracted DNA from five out of six replicates of sterile unspiked samples.

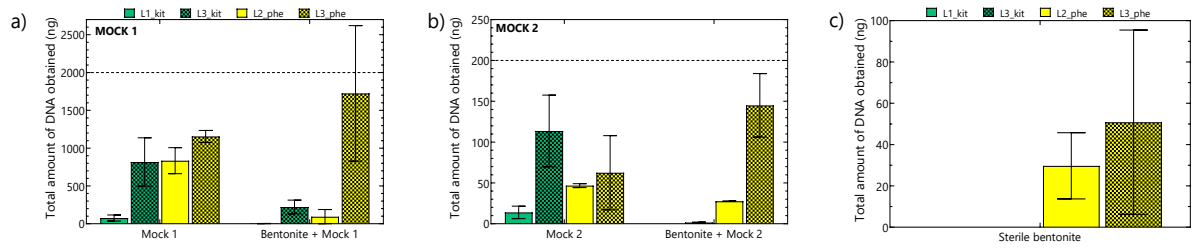

Figure 31: Total amount of DNA obtained for samples with a) Mock 1 or bentonite spiked with Mock 1 and b) Mock 2 or bentonite spiked with Mock 2 and c) sterile unspiked samples. The theoretical DNA yield expected in all samples following the procedure recommended by the manufacturer is given by a dotted line. Samples represent the average of three replicates except for L1_kit where two replicates were tested and L3_kit which includes four replicates. Kit based methods are shown in green, while phenol-chloroform based are shown in yellow.

16S rDNA amplicon sequencing

In total, we extracted DNA from 62 samples, including 48 samples spiked with a mock community, 12 sterile unspiked samples and two negative kit controls. Successful PCR was achieved for a total of 41 out of 48 samples spiked with a mock community, 6 of the 12 sterile bentonite samples and the 2 negative kit controls. However, for numerous samples, additional purifications were needed to obtain a successful PCR. All the samples, including PCR reactions performed on three replicates of the ZymoBIOMICS Microbial Community DNA Standard (Zymo Research Corporation, Irvine, USA), 2 NTC PCR controls, controls to assess the impact of additional phenol-chloroform extraction, drop dialysis and dilution were sent for 16S rDNA amplicon sequencing.

As a first step, possible contaminants were identified and removed from the dataset. After eliminating the ten ASV that were identified as true contaminants, most samples spiked with a mock community consisted of only the eight genera present in the mock. In the unspiked sterile bentonite samples, contaminants constituted more than 96% of the total reads, reaching over 99% in four out of six samples. Many spurious ASV were identified collectively representing only between 0.4% to 3.6% of the total relative abundance. Afterwards, we confirmed that we introduced minimal PCR bias and only minor variation across the different replicates by amplification and sequencing DNA mock community standards composed of DNA instead of intact cells.

In the analysis of samples spiked with Mock 1, both DNA extraction methods successfully captured all species, with minimal variation among replicates (Figure 32). However, higher variability was observed in samples extracted with the phenol-chloroform method (Figure 32). Notably, the variation in L2-processed samples without bentonite decreased after applying an additional phenol chloroform extraction according to the method of lab 3 (Figure 32). The presence of bentonite did not adversely affect the correlation with the theoretical composition. The samples spiked with Mock 2 also showed minor variations among the different replicates and with Spearman's correlation values above 0.6 (Figure 32). However, higher contaminant ASV abundance, especially in the presence of bentonite was observed. Important to note is that diluting the samples to mitigate the impact of PCR inhibitors could lead to a significant increase in the presence of contaminants (Figure 32).

Nonmetric multidimensional scaling confirmed limited variability among replicates, with better grouping in samples without bentonite. PERMANOVA analysis indicated a significant effect of DNA extraction method on both mock communities, but pairwise comparisons revealed no significant differences in microbial composition. The only distinction was between the DNA mock and phenol-chloroform-extracted samples spiked with Mock 1 and Mock 2. Bentonite had a significant effect on extraction methods, but pairwise comparisons mostly showed non-significant differences, except for Mock 1 kit-based extraction and Mock 2 phenol-chloroform extraction (Figure 33).

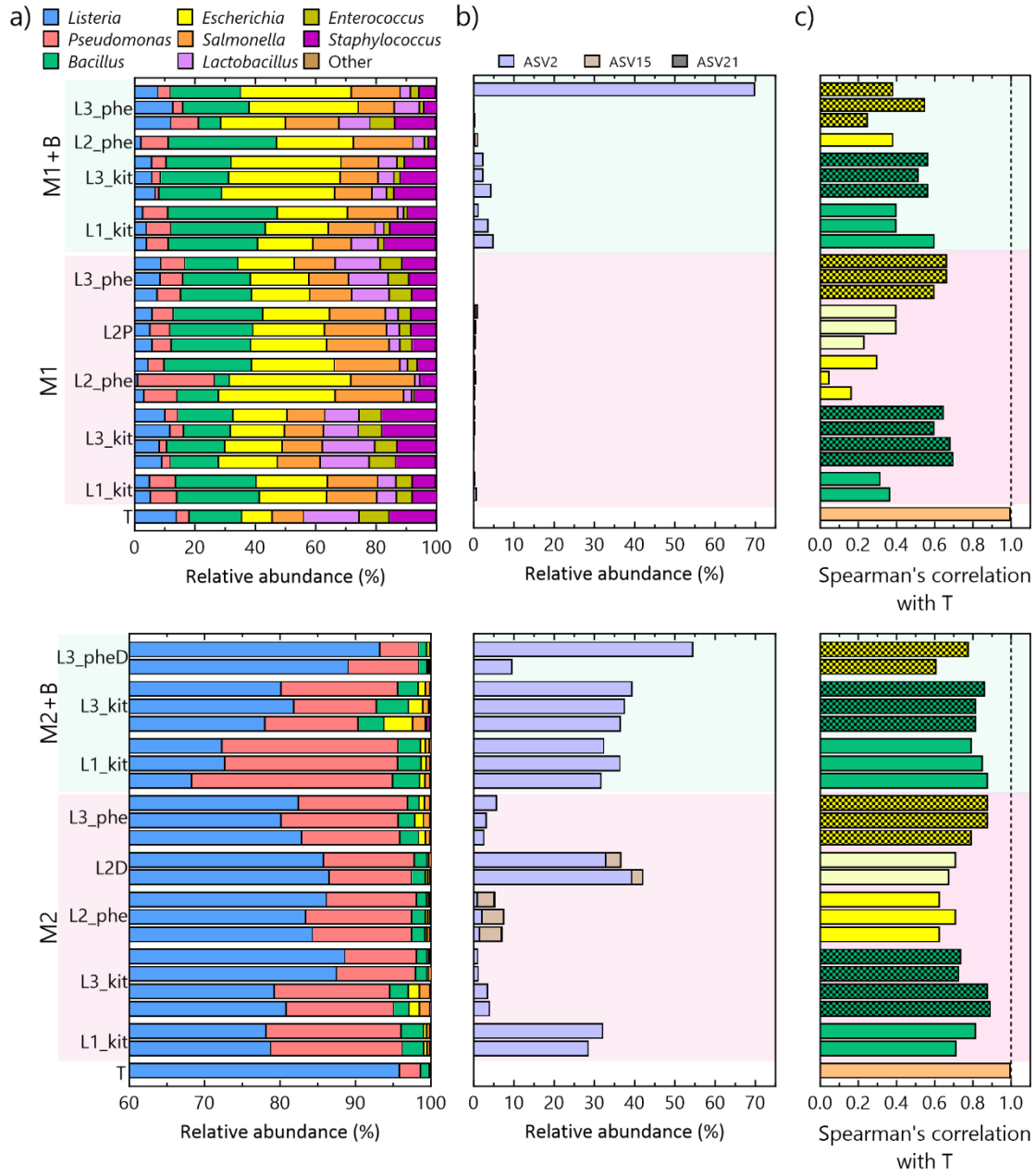

Figure 32: a) Bar plot showing the relative abundance of the genera present in samples spiked with Mock 1 or Mock 2 after removal of the contaminants; b) relative abundance of ASVs identified as contaminants in samples with Mock 1 and Mock 2. Only ASVs with a relative abundance > 0.1% are shown; c) Spearman's correlation coefficients compared to the theoretical distribution (T); L1 and L3a represent results of the kit-based extraction and are shown in green and dotted green; L2 and L3b are results from the phenol-chloroform extraction are presented in yellow and dotted yellow. L2P represent samples after an additional phenol chloroform extraction according to the method of lab 3 and samples that are 40-times diluted as PCR template are designated with L2D. Samples diluted before a successful PCR reaction was obtained are indicated with L3_PheD. Samples without bentonite are shown in pink and samples with bentonite are colloured light green.

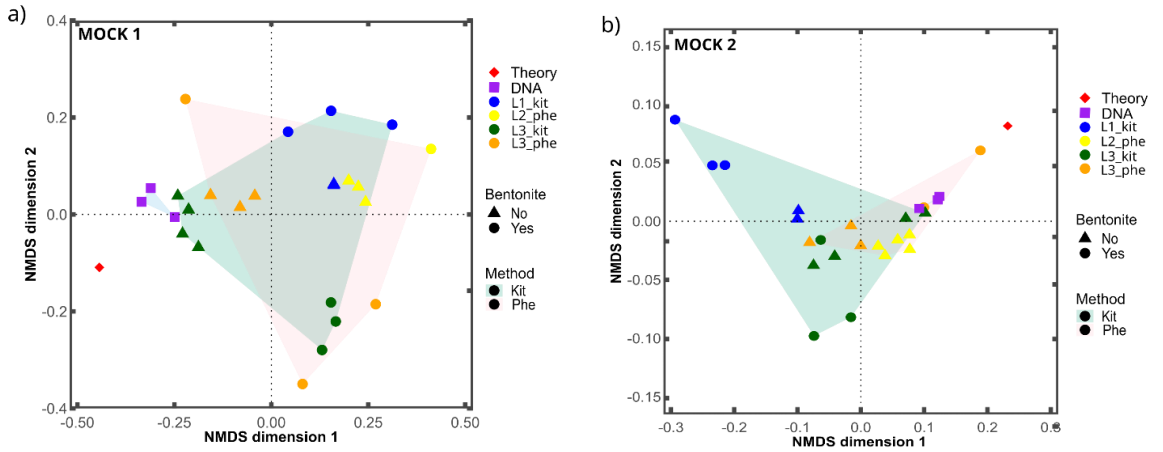

Figure 33: NMDS of ASV-based bacterial community composition in samples spiked with a) Mock 1 and b) Mock 2, using Bray-Curtis distances (stress = 0.13 and 0.02). Kit-based approaches performed by lab 1 are shown in blue, while those performed by lab 3 are shown in green, with a green convex hull encompassing the group. Phenol-Chloroform based methods carried out by lab 2 are depicted in yellow, and those performed by lab 3 are shown in orange, grouped with a pink convex hull. Samples without bentonite are represented as triangles, while samples with bentonite are shown as circles. The DNA mock is depicted as purple squares, and the expected composition is represented by a red diamond.

Overall, we conducted a comprehensive inter-laboratory comparison of two DNA extraction methods on bentonite clay. We showed that minor modifications to the extraction method could improve the extraction efficiency. Importantly, our findings indicate that the choice between the two methods is not critical, and each has advantages. The phenol-chloroform based method appears to be the optimal choice for bentonite samples, as it yields a higher amount of DNA. However, this method is more time-consuming and may be more susceptible to impurities in the final DNA sample and technical variations. On the other hand, if highly pure DNA is required, the kit-based method is recommended. However, pooling a large number of samples might be necessary to obtain sufficient DNA using this method. Lastly, our findings emphasize the importance of including appropriate controls when working with challenging samples, particularly those with low biomass.

3.3.2 Microbial consumption of hydrogen originating from the corrosion of carbon steel in compacted bentonite

Bentonite swelling pressure and the low water activity are expected to limit microbial presence and activity within the bentonite buffer. Nevertheless, previous laboratory and *in situ* experiments have shown the presence of sulphate reducing microorganisms in bentonite (Smart et al. 2017, Haynes et al. 2018, Engel et al. 2019). However, it remains unclear to what extent microbial activity can still occur at different bentonite dry densities and to what extent this can affect corrosion. Therefore, the purpose of our experiments was twofold:

- To investigate which bentonite dry density inhibits H_2 consumption originating from the anoxic corrosion of carbon steel by the indigenous community of the bentonite.
- To investigate the impact of the produced sulphides on the corrosion of carbon steel.

Materials and Methods

Experimental design

We opted to use in-house developed oedometers that are built with chemically and microbially inert contact materials such as titanium and titanium nitride and a very small surface of PTFE (Moors *et al.* 2016). We had three set-ups available (Figure 34); however, several tubings and parts (e.g. the pumps) needed to be replaced. In addition, we built three additional set-ups to increase the number of replicates that we could study. The oedometers and all materials were sterilized by steam, heat or 70% ethanol depending on the materials. Each consolidation cell has its own feed bottle to minimize the manipulations.

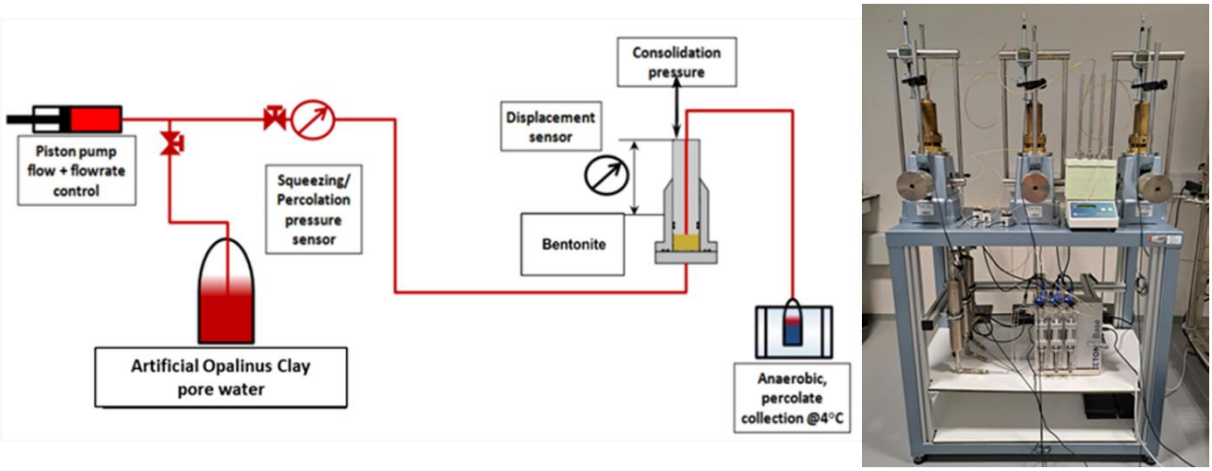

Figure 34: Experimental design of the oedometers.

Bentonite

Wyoming MX-80 bentonite was provided by the National Cooperative for the Disposal of Radioactive Waste (NAGRA). Bentonite blocks were crushed to powder. Sterile bentonite powder was obtained by exposing it to ^{60}Co gamma-irradiation with a dose rate of 6.4 kGy/h to a total dose of 57.6 kGy (SCK CEN BRIGITTE irradiation facility). Bentonite was stored in an anaerobic glovebox (99% Ar/1% H_2) until it was used.

Coupons

Cold rolled mild steel was used with a nominal chemical composition as given in Table 8.

Table 8: Chemical composition (wt.%) of the steel grade used in this study.

C	Mn	Si	P	S	N	Cu	Cr	Ni	Nb
0.0376	0.2068	0.0064	0.0095	0.0105	0.0027	0.0514	0.0304	0.0360	0.0002

As	Sn	Ti	B	V	Mo	Al
0.0045	0.0039	0.0009	0.0002	0.0003	0.0036	0.0353

Square samples were first cut from a 0.45 mm thick sheet that were afterwards further machined to the appropriate dimensions (18±0.1 × 18±0.1 mm). The samples were ground and polished (on both sides) to a P1200 grit finish.

Experimental setup

All manipulations were carried out in an anaerobic glovebox. The consolidation cells were filled with sterile or non-sterile MX-80 bentonite powder to obtain a dry density of 1.6 g/cm^3. Four coupons (on average 17.9 mm and 0.35 mm thick) were applied in each condition as such that they were completely mounted in the bentonite and there was no contact between the coupons and the consolidation cell (Figure 35). Once filled, a titanium outlet filter was mounted in a teflon sealing ring and squeezed straight vertical with the aid of a PVC squeeze adaptor into the top of the consolidation cell. When the filter was pushed inside the cell over a distance of a few centimetres, the PVC adaptor was removed and the TiN-coated piston is pushed inside the cell. When the piston and filter were in contact with the top layer of the bentonite, the venting hole was closed airtight to make sure that we had a completely closed system. The filled cell was transferred to the consolidation infrastructure outside the glove box.

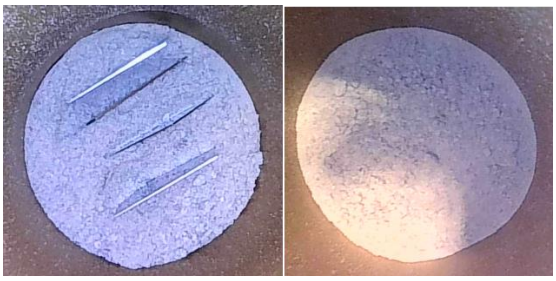

Figure 35: Picture taken with an endoscope camera of the distribution of the carbon steel coupons in the bentonite powder during the initiation of the experiments.

Afterwards, we started to consolidate the bentonite by applying consolidation pressure simultaneously with percolating sterile synthetic Opalinus Clay water with or without 1.5 bar of a H_2:CO_2 (80:20 v/v) mixture through the cells. The consolidation weight was gradually increased to 10 kg. Piston's motion and position were directly monitored. Percolation was controlled at a flow rate of 50 µl/h. Consolidation was performed until complete saturation of the bentonite, which was reached when we collected water in the septum bottle attached to the outlet of the consolidation cell. From that moment, the system was percolated for nine months after which we dismantled the cells. During the percolation, samples were collected in septum bottles at 4°C that were replaced every two months.

Initially, we started three abiotic cells without supplementation of hydrogen. Afterwards, we started the newly developed cells where we had one biotic sample without hydrogen and one biotic and one abiotic sample with hydrogen.

- Cell 1-3: sterile bentonite without hydrogen
- Cell 4: sterile bentonite + 1.5 bar hydrogen
- Cell 5: bentonite without hydrogen
- Cell 6: bentonite + 1.5 bar hydrogen

As only a limited amount of percolate could be collected, analysis was limited to:

- Hydrogen in the headspace was measured with a mini Ruedi gas analyser that works on the principle of mass spectrometry and only low amounts of gases are needed. It uses the standards composition and the total pressure and plots a calibration curve by subtracting the blank reading from the standards. The samples are then plotted onto this curve to obtain the partial pressures of the gases in the sample line. Afterwards, concentrations are determined based on ratios.
- ATP (total and internal) was determined with the microbial ATP kit HS of Biothema (Isogen Life Science, The Netherlands) according to the manufacturer's guidelines (Lundin 2000)
- Viable count was performed by plating 100 µl of each replicate was spread on R2A agar medium (Reasoner and Geldreich 1985). The presence of sulphate reducing bacteria (SRB) was scored by 1/10 dilution series in liquid Postgate medium (Postgate 1979).

Dismantling of the consolidation cells

After 244 days of percolation (419 days in total), the cells were transported to the anaerobic glovebox where they were dismantled. The bentonite plugs were pushed out of cells and sliced in three parts: one above the carbon steel coupons, one containing the coupons and one below the coupons (Figure 36). The coupons with some remaining bentonite were separated and prepared for analysis. The bentonite slices were divided into smaller sections to perform additional analysis (still ongoing).

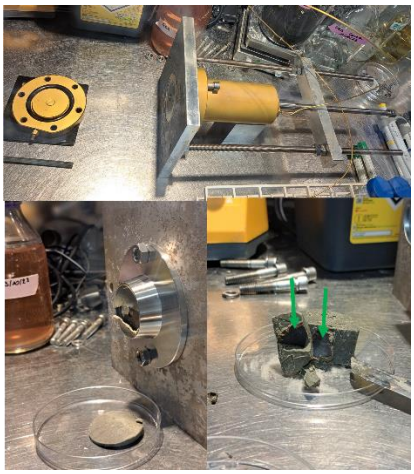

Figure 36: Pictures of the dismantling procedure. (top) consolidation cell; (bottom) bentonite slices that were collected. Carbon steel coupons in the saturated bentonite are indicated with a green arrow.

We determined the water content throughout the bentonite plug based on the wet weight and dry weight, the latter determined after incubation at 105°C for 3 days. In addition, bentonite slices were diluted 1/10 in PBS, placed on a horizontal shaker for 1 hour. Afterwards, plate counts were performed on R2A agar plates in aerobic and anaerobic conditions and diluted in liquid postgate medium to enable of SRB. In addition, swabs were taken from the inlet and outlet filter plates to perform similar analysis for microbial growth.

The other three cells are still running and can be dismantled Mid-June to have a similar percolation time in fully saturated conditions.

Results

The results that we have until now are rather limited as only three cells could be dismantled recently.

We monitored the height of the cells during the first 200 days. Figure 37 shows that cells 2 and 3 are almost identical while cell 1 is a bit lower in height. For all three cells, the height remains rather constant from day 40 onwards. From this moment onwards, the swelling is completed, and a swelling pressure is created. A bit more variation is observed for cells 4, 5 and 6 (Figure 37). This could partially be explained by the difference in infrastructure but for cell 4 (=sterilized bentonite + 1.5 bar H_2), there was a flow through problem after 1 week where a small part of the bentonite was lost. This could explain the shorter swelling time and why the swelling was not as high as the other cells.

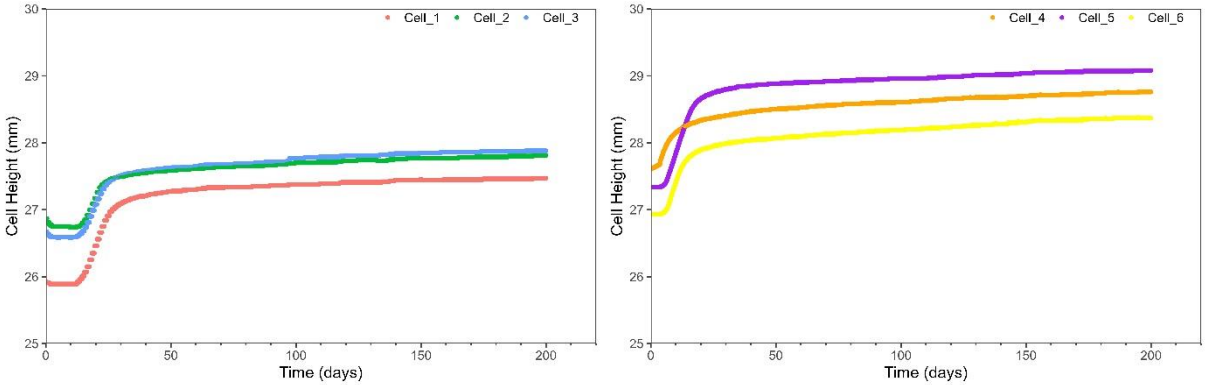

Figure 37: Changes in cell height of the different consolidation cells in function of time from the start of the hydration of the bentonite powder.

The hydraulic conductivity was determined and indicates that the cells evolved towards a constant system and ranges at the end of the experiment from 2.67 x 10^{-14} to 1.5 x 10^{-13} (Figure 38).

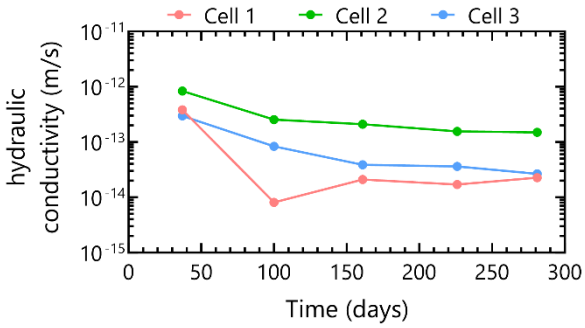

Figure 38: Evolution of the hydraulic conductivity during percolation. The first sample is two months after full saturated conditions were obtained.

Hydrogen measurements in the headspace of the percolate bottle indicate an increase of hydrogen in the first three consolidation cells (sterile bentonite without additional hydrogen). This increase was slower towards the end of the percolation (Figure 39). This suggests a faster corrosion in the beginning of the experiment, which evolves towards a slower process. There are only two data points available for the biotic conditions (cell 5 and cell 6), but hydrogen levels are ca. 5 times lower. Putatively, bacteria are still active in the consolidation cells and are consuming the hydrogen. However, currently it is not yet clear how long this microbial activity could persist during the percolation process. Moreover, we need to investigate if the microbial activity is occurring in the bentonite itself or in the filter plates. In addition, although we included an abiotic control supplemented with 1.5 bar H_2 (cell 4), this condition is probably contaminated as hydrogen levels were similar as in the biotic measurements.

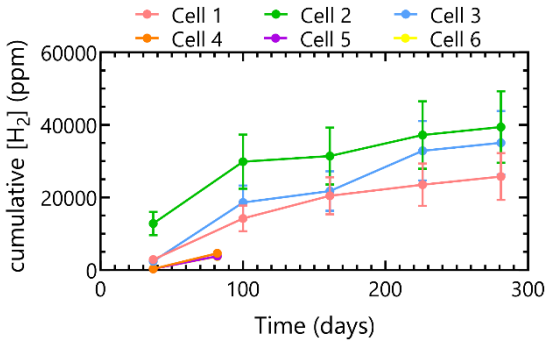

Figure 39: Cumulative hydrogen concentrations in the headspace of the percolate samples collected every two months. Values represent the result and measurement uncertainty. The measurement uncertainty is relatively high as it also includes the fact that septum bottles are not completely leak tight for hydrogen.

We attempted to monitor microbial presence and activity in the consolidation cells through the monitoring of microbial activity and – if we obtained enough water – viable cells. We assumed that bacteria would be pushed through the bentonite during the percolation and consequently be present in the percolate. However, no intracellular ATP was observed in the percolates. This suggests that cells are not mobile in the saturated compacted bentonite. Total ATP was also absent; however, ATP could be absorbed by the clay minerals (Graf and Lagaly 1980). Therefore, we will only be able to identify microbial presence and activity after dismantling of the consolidation cells. Nevertheless, as mentioned above, a flow-through problem occurred after 1 week of consolidation with cell 4, which supposed to be an abiotic condition. However, the water that we collected contained a low (but 10 times higher than all other measurements) amount of ATP (Figure 40). In addition, hydrogen levels were 10 times higher compared to the first measurement after saturation of the bentonite (Figure 40). This suggests that cell 4 is contaminated.

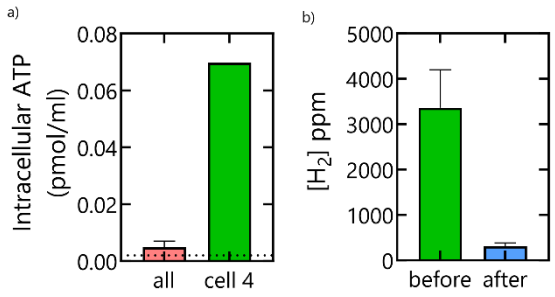

Figure 40: a) Intracellular ATP measured in percolates of all 6 cells (average and standard deviation of 17 samples) compared to intracellular ATP after 1 week of consolidation in cell 4, b) Hydrogen concentration in the headspace of the percolate samples collected after 1 week (green) compared to that measured after 37 days of percolating the saturated bentonite (blue). Values represent the result and measurement uncertainty.

The absence of aerobic heterotrophic bacteria in the bentonite was confirmed for cell 1 and cell 2 after dismantling of the abiotic consolidation cells without hydrogen. However, in 1 of the 6 samples taken from cell 3, small colonies were observed. These were located in the part where the coupons were mounted. The same sample was also positive for anaerobic heterotrophic bacteria (300 CFU/g), while these were not observed in cell 1 and 2. On the other hand, slices from the top and bottom part of the bentonite in cell 1 were positive for SRB. For cell 2, 2 slices at the top of the plug were positive and also for cell 3 one slice was positive for SRB. DNA extractions are currently being prepared to check which bacteria are present. Nevertheless, it seems that there was no bacterial activity in the consolidation cells as no hydrogen was consumed.

One of the slices was used to determine the water content, which ranged from 25-35% with some spread in the bentonite plugs itself (Figure 41).

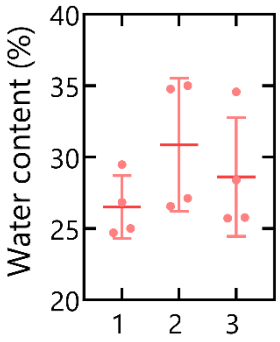

Figure 41: Scatter dot plot showing the water content measured in 4 slices spread in the saturated bentonite plugs. Mean and standard deviation are indicated as crossed lines.

However, the most important results, i.e. the effect on the carbon steel coupons and further results of the biotic samples are still pending.

4 Conclusions

4.1 Impact of irradiation on microbial activity

In relation to the studies carried out with FEBEX bentonite by UGR + CIEMAT, the effect of gamma radiation was studied under conditions of compaction and 100% saturation with artificial pore water. Natural FEBEX bentonite and bentonite artificially enriched with a sulphate-reducing bacterial (SRB) consortium prior to the experiment were included. The activity of SRB is relevant ot repository performance as these bacteria can influence copper corrosion. Obtained results demonstrated, that the effect of radiation on the natural bentonite microbial community depended on the total dose received (14 kGy or 28 kGy). In addition, the time at which the bacterial community receives the gamma radiation proved to be an important parameter. When the blocks were incubated for 6 months prior to receiving the 14 kGy dose and then incubated for another 6 months, the results hardly varied with respect to the non-irradiated controls. Thus, a prior adaptation and subsequent recovery period seems to be key to the survival of the indigenous microorganisms in bentonite. Interestingly, in the case of compacted bentonites enriched with a sulphate-reducing bacterial (SRB) consortium, survival of this group of bacteria was severely affected at both 14 kGy and 28 kGy doses. Based on these results, it can be expected, that the activity of this group of bacteria would be very low in the early stages of the DGR when radiation doses will be highest. The copper corrosion data aligns with the results of microbial diversity, as the copper coupons exhibiting the most significant corrosion were from the non-irradiated controls. The primary corrosion products included copper oxides and potential copper sulphides. These indications of copper sulphides were exclusively found in the coupons from the samples with the added SRB consortium. The results imply, that corrosion is mainly attributed to biotic causes. Concerning the irradiated sample with the SRB consortium, it was the only irradiated sample positive for the presence of viable SRBs, potentially justifying the presence of small, possible precipitates of copper sulphides in it. However, further investigations are necessary to confirm whether these are indeed copper sulphides and also to examine the survival of this SRB consortium at the gamma radiation doses studied in this work.

The second experiment performed by TUL + UJV focused on the impact of irradiation in combination with other repository-relevant stressors expected during the early phase on indigenous microorganisms in bentonite. Long exposure to elevated temperatures (90 °C and 150 °C) was found to significantly reduce the viability of bentonite microorganisms, with consistent effects observed in both BCV and MX-80 bentonites. Effect of irradiation (repository relevant dose rate of 0.4 Gy/h) or additional factors like bentonite state, and water availability was insignificant, but their particular effects could not be estimated due to the predominant effect of temperature. Our study further emphasized the critical role of exposure duration in understanding microbial responses to heat treatment. The potential for microbially induced corrosion of the canister during the initial hot phase of repository evolution is highly unlikely mostly due to the detrimental impact of high temperatures on microbial viability. Elevated temperatures might be, however, associated with increased abiotic corrosion rates, with irradiation potentially mitigating corrosion (see DL 15.7 (Bevas et al., 2024)).

Both experiments performed in Subtask 4.1 indicate, that the microbial activity around the canister, where highest temperatures and radiation doses are expected, will dramatically decrease microbial viability in bentonite, which can result in the evolution of a potentially abiotic zone in bentonite around the canister during the early repository stages. Formation and spatial distribution of this presumable zone will however depend on the temperature, radiation dose rate and water saturation conditions within the deep geological repository. Further long-term experiments at nearly-limiting temperatures in combination with mathematical modelling are recommended to refine predictions of microbial effects in the repository over time.

4.2 Impact of bentonite dry density on microbial activity

The work carried out in this section by EPFL has resulted in the design of a set-up for a new type of experiment to characterize the potential for microbial growth in compacted bentonite of various types and dry densities. This experimental design has bypassed many of the limitations previously encountered (e.g., growth outside bentonite) and can be applied to any bentonite.

In addition, it was shown that substantial growth takes place within MX-80 bentonite, without any electron donor amendment. This finding suggests the importance of endogenous electron donors, such as organic carbon and the likelihood of microbial growth during the saturation phase, prior to the onset of anoxic steel corrosion and the associated H_2 production at a low dry density of 1.2 g/cm^3.

The same diffusion reactor setup as at EPFL was also setup at HZDR with some small differences (e.g. different type of peristaltic pump). Due to several difficulties in setting up this system such as material procurement, corrosion of filters, and so on (see also above) we only managed to develop and establish a diffusion reactor setup during this time. Until the end of the project, experiments with Calcigel and the lowest dry density are still planned.

During the development of the diffusion reactor setup, batch microcosms with Calcigel bentonite incubated under different conditions and different incubation times were performed. The results showed that the sulphate concentration decreased the most in the microcosms containing hydrogen in the atmosphere, Calcigel bentonite and metal coupons. In addition, the hydrogen content in the atmosphere of these microcosms was also lower than that in the ones with sterilized bentonite. This leads to the conclusion that hydrogen as a potential electron donor and sulphate as an electron acceptor were consumed in these microcosms by the present microorganisms. Microbial diversity analysis also showed that sulphate-reducing bacteria from the genus *Desulfotomaculum* were enriched in these samples, indicating that Calcigel bentonite harbours sulphate reducing bacteria that are active under the applied conditions.

What is the consequence of this microbial activity on the corrosion of the metal coupons? The analysis of the surface of the coupons from these bentonite slurry microcosms showed that the alteration of the morphology was more intense at lower incubations times because a layer of Ca- containing minerals was later formed that seemed to protect the surface of the coupons. In addition, sulphide minerals were found on the surface, which indicate again the activity of sulphate reducing bacteria. In these microcosms were also obtained a high corrosion rate. A similar high corrosion rate was only observed in microcosms with hydrogen in the atmosphere and sterilized Calcigel bentonite. In these microcosms were also determined the highest hydrogen content in the atmosphere, which indicates an abiotic corrosion. Overall, the results show that the Calcigel bentonite is a good candidate to study the impact of dry density on microbial activity and corrosion because this bentonite has a low sulphate content and contains natural sulphate-reducing bacteria that can under suitable conditions contribute (production of sulphides) or prevent (consumption of formed hydrogen) the corrosion.

At SCK-CEN in-house developed oedometers to investigate which bentonite dry density inhibits H^2 consumption originating from the anoxic corrosion of carbon steel by the indigenous community of the bentonite and to investigate the impact of the produced sulfides on the corrosion of carbon steel. Three sets were available; however, several tubings and parts (e.g. the pumps) needed to be replaced. In addition, three sets were built to increase the number of replicates that could be studied. As coupons cold rolled mild steel was used (dimensions (18±0.1 × 18±0.1 mm), polished P1200 grit). Sterile or non-sterile MX-80 bentonite powder to obtain a dry density of 1.6 g/cm^3 was filled into the cells and four coupons (on average 17.9 mm and 0.35 mm thick) were added in each condition. The consolidation of the bentonite was performed by applying consolidation pressure simultaneously with percolating sterile synthetic Opalinus Clay water with or without 1.5 bar of a H_2:CO_2 (80:20 v/v) mixture through the cells. Initially, three abiotic cells without supplementation of hydrogen were set up. Afterwards, the newly developed cells were started with one biotic sample without hydrogen and one biotic and one abiotic sample with hydrogen. Three cells were dismantled after 244 days of percolation (419 days in total). So far only hydrogen measurements in the headspace of the percolate bottle are available and indicate an increase of hydrogen in the first three consolidation cells (sterile bentonite without additional hydrogen).

This increase was slower towards the end of the percolation. This suggests a faster corrosion in the beginning of the experiment, which evolves towards a slower process. There are only 2 data points available for the biotic conditions (cell 5 and cell 6), but hydrogen levels are ca. 5 times lower. Putatively, bacteria are still active in the consolidation cells and are consuming the hydrogen. It is only possible to identify microbial presence and activity after dismantling of the consolidation cells and these investigations are still ongoing.

4.3 Keynotes

The results obtained in Task 4 demonstrated, that the high initial temperatures and gamma radiation during the saturation phase have potential to exhaust most microbial activity in the bentonite zones long-term subjected to the temperatures of at least 90 °C. As a consequence of the suppression of microbial activity in the buffer, biofilm formation on the canister surface does not need to be considered. However, further microbiological studies combined with mathematical modelling of special temperature evolution in DGR are necessary to predict the size and spacious distribution as well as long-term persistence of such microbially depleted zones in the bentonite buffer around the metal canisters. When the saturation is reached, microbial activity will be further suppressed by compacted bentonite where the threshold dry density depends on the bentonite (their physical-chemical properties and the indigenous microbial communities). However, the diffusion reactor experiments and oedometer experiments investigating this within ConCorrD are still ongoing and no final conclusion can be made. But the current results indicate that the diffusion reactor and oedometer can be used as a standard method to investigate threshold densities for buffer candidates. It was shown by batch microcosm experiments that the Calcigel bentonite is a good candidate to study the impact of dry density on microbial activity and corrosion because this bentonite has a low sulphate content and contains natural sulphate-reducing bacteria that can under suitable conditions contribute (production of sulphides) or prevent (consumption of formed hydrogen) the corrosion.

It is expected, that the only form of microbial induced corrosion that needs to be considered is that due to the diffusion of aggressive metabolic by-products (invariably sulphide) to the canister surface from locations at which microbial activity is deemed to be possible. In accordance with this assumption, the compacted bentonite samples from UGR that were supplemented with SRB and IRB showed highest alteration of the metal surface (at 1.6 g/cm^3). This shows that introduced microorganisms can affect the corrosion even in bentonite compacted at a high dry density. The non-irradiated compacted bentonite samples without additional bacteria showed that the metal surface was covered with copper oxides and the coupons had a low corrosion rate (studied in detail in Task 3). Results from UGR/CIEMAT also showed that the used porewater (see also Task 3) and the way of compaction (first saturated and then compacted or first compacted and then saturated) can have an influence on the corrosion.

5 Outlook

The additional molecular-genetic analyses of the samples from the zero state and after 6m exposure from the UGR experiment will be analysed in cooperation with TUL till the end of the project. The result from TUL + UJV experiment are now being prepared for publication. The diffusion reactor setup is now developed and established at EPFL and HZDR. Similar experiments as shown here in Sections 3.1 and 3.2 should be run for higher dry densities to evaluate whether microbial growth would be greater (due to the higher concentration of TOC) or lower (due to the more limited space).

With this system, it is now possible to determine whether H_2 would further contribute to biomass production or whether, once saturated, bentonite does not support further growth.

Several experimental improvements are being considered. Running the experiment for longer is an obvious one. Additionally, instead of passing the water through the filter a single time, it would be useful to devise a system of water filtration that would allow recirculation of the water. Finally, H_2 could be added directly to the reactor containing compacted bentonite, at both ends, and rely on the dissolution of gypsum to supply sulphate. This experiment would bypass the need for a Phase 1 and thus, will result in the simultaneous use of organic carbon and H_2 as electron donors.

References

Aoki, K., Sugita, Y., Chijimatsu, M., Tazaki, K., 2010. Impacts of thermo-hydro-mechanical experiments on the microbial activity in compacted bentonite at the Kamaishi Mine, Northeast Japan. Appl. Clay Sci. 47, 147–154.

Aüllo, T., Ranchou-Peyruse, A., Ollivier, B., Magot, M. (2013). *Desulfotomaculum* spp. and related gram-positive sulfate-reducing bacteria in deep subsurface environments. Frontiers in Microbiology, 4(DEC), 58161. https://doi.org/10.3389/FMICB.2013.00362/BIBTEX

Bartak, D., Bedrníková, E., Kašpar, V., Říha, J., Hlaváčková, V., Večerník, P., Šachlová, Š., Černá, K., 2023. Survivability and proliferation of microorganisms in bentonite with implication to radioactive waste geological disposal: strong effect of temperature and negligible effect of pressure. World J. Microbiol. Biotechnol. 40, 41. https://doi.org/10.1007/s11274-023-03849-0

Bagnoud A., Chourey K., Hettich R. L., de Bruijn I. and Andersson A. F., Leupin O.X., Schwyn B., Bernier-Latmani R. (2016) Reconstructing a hydrogen-driven microbial metabolic network in Opalinus Clay rock, in Nature Communications, vol. 7, p. 12770.

Bell E., Lamminmäki T., Alneberg J., Andersson A., Qian C., Xiong W., Hettich R., Frutschi M., and Bernier-Latmani R. (2020) Active sulfur cycling in the terrestrial deep subsurface, in The ISME Journal.

Bengtsson A., Pedersen K. (2016) Microbial suphate-reducing activity over load pressure and density in water saturated Boom Clay. Applied Clay Science, 132-133, 542-551.

Bengtsson A., Pedersen K. (2017) Microbial sulphide-producing activity in water saturated Wyoming MX-80, Asha and Calcigel bentonites at wet densities from 1500 to 2000 kg m−3. Applied Clay Science 137, 203–212.

Bengtsson A., Blum, A., Hallbeck, B., Heed, C., Johansson, L., Stahlen, J., Pedersen, K. (2017a) Microbial sulphide-producing activity in water saturated Wyoming MX-80, Asha and Calcigel bentonites at wet densities from 1500 to 2000 kg m−3. Swedish Nuclear fuel and Waste Management Company, report TR-16-09.

Bevas C., Hesketh J., Rance A., Stevenson L.-A., Uthayakumaran S., Pateman B., Padovani C., Šachlová Š., Kašpar V., Dobrev D., Götz D., Kolomá K., Večerník P. (2024): Elucidation of the effect of radiation on the corrosion of canister materials. Final version as of 02/02/2024 of deliverable D15.7 of the HORIZON 2020 project EURAD. EC Grant agreement no: 847593.

Brown, A.R., Boothman, C., Pimblott, S.M., Lloyd, J.R., 2015. The impact of gamma radiation on sediment microbial processes. Appl. Environ. Microbiol. 4014–4025. https://doi.org/10.1128/AEM.00590-15

Burzan, N, Murad Lima, R., Frutschi, M., Janowczyk, A., Reddy, B., Rance, A., Diomidis, N., and R. Bernier-Latmani (2022) Growth and persistence of an aerobic microbial community in Wyoming bentonite MX-80 despite anoxic in situ conditions. Frontiers in Microbiology, v13, 858324.

Cai, P., Q. Huang, J. Zhu, D. Jiang, X. Zhou, X. Rong and W. Liang (2007). Effects of low-molecular-weight organic ligands and phosphate on DNA adsorption by soil colloids and minerals. Colloids Surf B Biointerfaces 54: 53-59

Callahan, B. J., McMurdie, P. J., Rosen, M. J., Han, A. W., Johnson, A. J. A., Holmes, S. P. (2016). DADA2: High-resolution sample inference from Illumina amplicon data. Nature Methods 13, 581–583.

Callahan, B. (2018). Silva taxonomic training data formatted for DADA2 (Silva version 132). Zenodo

Černá, K., Černoušek, T., Polívka, P., Ševců, A., Steinová, J. 2019. MIND Deliverable 2.15: Survival of microorganisms in bentonite subjected to different levels of irradiation and pressure.

Červinka, R., Vašíček, R., Večerník, P., Kašpar, V., 2018. Kompletní charakterizace bentonitu BCV 2017 (No. Technická zpráva číslo 419/2019). SÚRAO.

Chi Fru, E. and R. Athar (2008). In situ bacterial colonization of compacted bentonite under deep geological high-level radioactive waste repository conditions. Applied Microbiology and Biotechnology 79: 499-510

Claesson, M.J., Wang, Q., O'sullivan, O., Greene-Diniz, R., Cole, J.R., Ross, R.P., O'toole, P.W., 2010. Comparison of two next-generation sequencing technologies for resolving highly complex microbiota composition using tandem variable 16S rRNA gene regions. Nucleic Acids Res. 38, e200–e200.

Clifford, R.J., Milillo, M., Prestwood, J., Quintero, R., Zurawski, D.V., Kwak, Y.I., Waterman, P.E., Lesho, E.P., Mc Gann, P., 2012. Detection of bacterial 16S rRNA and identification of four clinically important bacteria by real-time PCR. PLoS ONE 7. https://doi.org/10.1371/journal.pone.0048558

Davis, N.M., Proctor, D.M., Holmes, S.P., Relman, D.A., Callahan, B.J., 2018. Simple statistical identification and removal of contaminant sequences in marker-gene and metagenomics data. Microbiome 6, 226. https://doi.org/10.1186/s40168-018-0605-2

Dowd, S.E., Callaway, T.R., Wolcott, R.D., Sun, Y., McKeehan, T., Hagevoort, R.G., Edrington, T.S., 2008. Evaluation of the bacterial diversity in the feces of cattle using 16S rDNA bacterial tag-encoded FLX amplicon pyrosequencing (bTEFAP). BMC Microbiol. 8, 125. https://doi.org/10.1186/1471-2180-8-125

Engel, K., Coyotzi, S., Vachon, M. A., McKelvie, J. R., Neufeld, J. D. (2019). Validating DNA extraction protocols for bentonite clay. MSphere, 4(5). https://doi.org/10.1128/msphere.00334-19

Fernandez, A.M., Rivas. P (2005). Pore water chemistry of saturated FEBEX bentonite compacted at different densities. Advances in Understanding Engineered Barriers. Alonso & Ledesma (eds). Taylor and Francis Group, London. Pp 505- 514 ISBN 04-1536-544-9 (2005).

Forman, L., Picek, M., Dobrev, D., Gondolli, J., Mendoza Miranda, Straka, M., Kouřil, M., Stoulil, J., Matal, O., Čermák, J., Král, J., Žaloudek, J., Vávra, M., Čupr, M., 2021. Závěrečná technická zpráva výzkumná část projektu: Výzkum a vývoj ukládacího obalového souboru pro hlubinné ukládání vyhořelého jaderného paliva do stadia realizace vzorku (Technická zpráva 544/2021). SÚRAO (in Czech).

Frostegård, A., S. Courtois, V. Ramisse, S. Clerc, D. Bernillon, F. Le Gall, et al. (1999). Quantification of bias related to the extraction of DNA directly from soils. Appl Environ Microbiol 65: 5409-5420

Gilmour, K.A., Davie, C.T., Gray, N., 2021. An indigenous iron-reducing microbial community from MX80 bentonite - A study in the framework of nuclear waste disposal. Appl. Clay Sci. 205, 106039. https://doi.org/10.1016/j.clay.2021.106039

Graf, G. and G. Lagaly (1980). Interaction of Clay-Minerals with Adenosine-5-Phosphates. Clays and Clay Minerals 28: 12-18

Haynes, H.M., Pearce, C.I., Boothman, C., Lloyd, J.R. (2018). Response of bentonite microbial communities to stresses relevant to geodisposal of radioactive waste. Chemical Geology 501, 58–67. https://doi.org/10.1016/j.chemgeo.2018.10.004.

Hlavackova, V., Shrestha, R., Hofmanova, E., Kejzlar, P., Riha, J., Bartak, D., Sevcu, A., Cerna, K., 2023. A protocol for the extraction of viable bacteria for identification of bacterial communities in bentonite. Appl. Clay Sci. 232, 106809. https://doi.org/10.1016/j.clay.2022.106809

Huertas, F., Fuentes-Santillana, J.L., Jullien, F., Rivas, P., Linares, J., Fariña, P., Ghoreychi, M., Jockwer, N., Kickmaier, W., Martínez, M.A., Samper, J., Alonso, E., Elorza, F.J. (2000). Full Scale Engineered Barriers Experiment for a Deep Geological Repository for High-level Radioactive Waste in Crystalline Host Rock. EC Final REPORT EUR 19147 (2000).

Laskowska, E., Kuczyńska-Wiśnik, D. (2020). New insight into the mechanisms protecting bacteria during desiccation. Curr. Genet. 66, 313-318. https://doi.org/10.1007/s00294-019-01036-z

Kašpar, V., Šachlová, Š., Hofmanová, E., Komárková, B., Havlová, V., Aparicio, C., Černá, K., Bartak, D., Hlaváčková, V., 2021. Geochemical, geotechnical, and microbiological changes in Mg/Ca bentonite after thermal loading at 150 °C. Minerals 11, 965. https://doi.org/10.3390/min11090965

Lundin, A. (2000). Use of firefly luciferase in ATP-related assays of biomass, enzymes, and metabolites. Methods Enzymol 305: 346-370

Maanoja, S., Palmroth , M., Salminen, L., Lehtinen, L., Kokko, M., Lakaniemi, A., Auvinen, H., Kiczka, M., Muuri, E., and J. Rintala. (2021) The effect of conpaction and microbial activity on the quantity and release rate of water-soluble organic matter from bentonites. Applied Clay Science, v211, 106192

Martin, M. (2011). Cutadapt removes adapter sequences from high-throughput sequencing reads. 2011 17: 3

Martinez-Moreno, M. F., Povedano-Priego, C., Morales-Hidalgo, M., Mumford, A. D., Ojeda, J. J., Jroundi, F., and Merroun, M. L. (2023). Impact of compacted bentonite microbial community on the clay mineralogy and copper canister corrosion: a multidisciplinary approach in view of a safe Deep Geological Repository of nuclear wastes. Journal of Hazardous Materials, 458, 131940.

Matamoros-Veloza, A., Barker, R., Vargas, S., Neville, S. (2020) Iron calcium carbonate instability: structural modification of siderite corrosion films. ACS Applied Materials & Interfaces 12, 49237−49244.

Matschiavelli, N., Kluge, S., Podlech, C., Standhaft, D., Grathoff, G., Ikeda-Ohno, A., Warr, L.N., Chukharkina, A., Arnold, T., Cherkouk, A. The Year-Long Development of Microorganisms in Uncompacted Bavarian Bentonite Slurries at 30 and 60 °C (2019) Environ. Sci. Technol., 53, 10514–10524.

McMurdie, P. J., & Holmes, S. (2013). Phyloseq: An R Package for Reproducible Interactive Analysis and Graphics of Microbiome Census Data. PLoS ONE, 8, e61217. https://doi.org/10.1371/journal.pone.0061217

Mijnendonckx, K., P. Monsieurs, K. Černá, V. Hlaváčková, J. Steinová, N. Burzan, et al. (2021). Chapter 4 - Molecular techniques for understanding microbial abundance and activity in clay barriers used for geodisposal. The Microbiology of Nuclear Waste Disposal. J. R. Lloyd and A. Cherkouk, Elsevier: 71-96

Moors, H., S. Smets, W. Verwimp and H. De Soete (2016). COSMOS: Concept, design and use of the experimental infrastructure, Studiecentrum voor Kernenergie

Motamedi, M., Karnland, O., Pedersen, K., 1996. Survival of sulfate reducing bacteria at different water activities in compacted bentonite. FEMS Microbiol. Lett. 141, 83–87. https://doi.org/10.1111/j.1574-6968.1996.tb08367.x

Nicholson, W.L., Munakata, N., Horneck, G., Melosh, H.J., Setlow, P., 2000. Resistance of Bacillus endospores to extreme terrestrial and extraterrestrial environments. Microbiol. Mol. Biol. Rev. 64, 548–572.

Oksanen, J., F. G. Blanchet, M. Friendly, R. Kindt, P. Legendre, D. McGlinn, et al. (2020). Vegan: community ecology package. from https://CRAN.R-project.org/package=vegan.

Pearson, F. J. (1998). Opalinus clay experimental water: A1 Type, Version 980318. Internal Technical Report TM-44-98-07.

Pitonzo, B. J., Amy, P. S., & Rudin, M. (1999). Effect of gamma radiation on native endolithic microorganisms from a radioactive waste deposit site. Radiation Research, 152(1), 64-70. https://doi.org/10.2307/3580050

Postgate, J. R. (1979). The sulfate-reducing bacteria, CUP Archive

Povedano-Priego, C., Jroundi, F., Lopez-Fernandez, M., Sánchez-Castro, I., Martin-Sánchez, I., Huertas, F.J., Merroun, M.L. (2019). Shifts in bentonite bacterial community and mineralogy in response

to uranium and glycerol-2-phosphate exposure. Science of The Total Environment 692, 219–232. https://doi.org/10.1016/j.scitotenv.2019.07.228

Povedano-Priego, C., Jroundi, F., Lopez-Fernandez, M., Shrestha, R., Spanek, R., Martín-Sánchez, I., Villar, M.V., Ševců, A., Dopson, M., Merroun, M.L., 2021. Deciphering indigenous bacteria in compacted bentonite through a novel and efficient DNA extraction method: Insights into biogeochemical processes within the Deep Geological Disposal of nuclear waste concept. Journal of Hazardous Materials 408, 124600. https://doi.org/10.1016/j.jhazmat.2020.124600

Povedano-Priego, C., Jroundi, F., Lopez-Fernandez, M., Morales-Hidalgo, M., Martin-Sánchez, I., Huertas, F. J., Dopson, M. & Merroun, M. L. (2022). Impact of anoxic conditions, uranium (VI) and organic phosphate substrate on the biogeochemical potential of the indigenous bacterial community of bentonite. Applied Clay Science, 216, 106331. https://doi.org/10.1016/j.clay.2021.106331

Povedano-Priego, C., Jroundi, F., Solari, P.L., Guerra-Tschuschke, I., Abad-Ortega, M. del M., Link, A., Vilchez-Vargas, R., Merroun, M.L., 2023. Unlocking the bentonite microbial diversity and its implications in selenium bioreduction and biotransformation: Advances in deep geological repositories. Journal of Hazardous Materials 445, 130557. https://doi.org/10.1016/j.jhazmat.2022.130557

Reasoner, D. J. and E. E. Geldreich (1985). A new medium for the enumeration and subculture of bacteria from potable water. Applied and environmental microbiology 49: 1-7

Quast, C., Pruesse, E., Yilmaz, P., Gerken, J., Schweer, T., Yarza, P., Peplies, J., Glöckner, F. O. (2013). The SILVA ribosomal RNA gene database project: Improved data processing and web-based tools. Nucleic Acids Research 41, D590–D596. https://doi.org/10.1093/nar/gks1219

Schneeberger, R. *et al.* (2023) HotBENT Project - Bentonite materials requirements and production. Nagra Report NAB 22-007.

Smart NR, Reddy B, Rance AP, et al. The anaerobic corrosion of carbon steel in compacted bentonite exposed to natural Opalinus Clay porewater containing native microbial populations. *Corrosion Engineering, Science and Technology*. 2017;52(1_suppl):101-112. doi:10.1080/1478422X.2017.1315233

Stroes-Gascoyne, S., Lucht, L.M., Borsa, J., Delaney, T.L., Haveman, S.A., Hamon, C.J., 1995. Radiation Resistance of the Natural Microbial Population in Buffer Materials. MRS Online Proc. Libr. Arch. 353. https://doi.org/10.1557/PROC-353-345

Stroes-Gascoyne, S., West, J.M., 1997. Microbial studies in the Canadian nuclear fuel waste management program. FEMS Microbiol. Rev. 20, 573–590. https://doi.org/10.1111/j.1574-6976.1997.tb00339.x

Stroes-Gascoyne, S. (2010) Microbial Occurrence in Bentonite-Based Buffer, Backfill and Sealing Materials from Large-Scale Experiments at AECL's Underground Research Laboratory, Appl. Clay Sci., 47 (1), 36–42

Stroes-Gascoyne, S., West, J.M., 1997. Microbial studies in the Canadian nuclear fuel waste management program. FEMS Microbiology Reviews 20, 573–590. https://doi.org/10.1111/j.1574-6976.1997.tb00339.x

Sudarshan, A. S., K. Jolanda and F. Susana (2023). A tool to assess the mock community samples in 16S rRNA gene-based microbiota profiling studies. Microbiome Research Reports 2: 14

Taborowski, T., A. Bengtsson, A. Chukharkina, A. Blom, K. Pedersen (2019) Bacterial presence and activity in compacted bentonites. MIND Deliverable D2.4, v2

Tamisier, M., Musat, F., Richnow, H.-H., Vogt, C., Schmidt, M. (2023) Onthe corrosion of ductile cast iron by sulfate reducing bacteria — implications for long-term nuclear waste repositories. Frontiers in Geochemistry 1:1244283.

van Gerwen, S. J. C., Rombouts, F. M., Riet, K. van't, Zwietering, M. H. (1999). A Data Analysis of the Irradiation Parameter D10 for Bacteria and Spores under Various Conditions. J. Food Prot. 62, 1024–1032.

Van Loon, L., Soler, J.M., and M.H. Bradbury (2003) Diffusion of HTO, 36Cl− and 125I− in Opalinus Clay samples from Mont Terri: Effect of confining pressure. Journal of Contaminant Hydrology, v. 61, 1-4, p73-83.

Walters, W., Hyde, E. R., Berg-Lyons, D., Ackermann, G., Humphrey, G., Parada, A., Gilbert, J.A., Jansson, J.K., Caporaso, J.G., Fuhrman, J.A., Apprill, A., Knight, R. (2016). Improved bacterial 16S rRNA gene (V4 and V4-5) and fungal internal transcribed spacer marker gene primers for microbial community surveys. MSystems, 1(1). https://doi.org/10.1128/msystems.00009-15